An-Najah National University
Faculty of Graduate Studies

Preparation and Enhancement of CdS/ZnS Thin Films for Photovoltaic Purposes

By
Maysa Tayseer Mohammad Atatrih

Supervisors
Dr. Musa El-Hasan
Professor Hikmat S. Hilal

Submitted in Partial Fulfillment of the Requirement for the Degree of Master of Physics, Faculty of Graduate Studies, at An-Najah National University, Nablus, Palestine.

2010

Preparation and Enhancement of CdS/ZnS Thin Films for Photovoltaic Purposes

By
Maysa Tayseer Mohammad Atatrih

This thesis was defended successfully on 4/3/2010 and approved by:

Committee Members	**Signature**
1. Dr. Musa El-Hasan / Supervisor	..………………
2. Prof. Hikmat Hilal / Co-Supervisor	………….…..…
3. Assis. Prof. Dr. Atef Qassrawi / External Examiner	……………
4. Dr. Iyad Sad El-Deen / Internal Examiner	.....……………

Biographical Sketch

Maysa T. M. Atatrih was born on January 14, 1982 in Jinen, Palestine. In 2000 she graduated from Ya'bad Secondary School (Ya'bad, Jinen-Palestine). In 2004 she graduated from An-Najah National University (Nablus-Palestine) with the degree of Bachelor of Science in Physics. In 2005 she enrolled in the Graduate School at An-Najah Ntional University, and she has been engaged in research under the supervision of Professor Hikmat S. Hilal and Dr. Musa El-Hasan.

Dedication

To my son Fayeq……………..

Acknowledgments

The author wishes to express her sincere appreciation to her supervisors Professor Hikmat S. Hilal and Dr. Musa El-Hasan for their guidance, help and encouragement throughout research work and writing up.

Thanks are extended to Dr. Ahed Zuod for help with SEM, spectra, PL and XRD measurements. Donation of free FTO/glass samples, by Dr. Guy Campet of ICMCB, University of Bordeaux, France.

Thanks to the teaching and technical staff in the laboratories in the Department of Chemistry at An-Najah N. University. Research equipment donated by the French-Palestinian University Cooperaton program is acknowledged.

Last, but in no way least, I would like to thank my family especially my parents and my husband Fares for their support during my educational.

Maysa T. Atatri

Nablus–An-Najah N. University

Decemper – 2010 A.C. -1430 H.

الإقرار

أنا الموقع أدناه، مقدم الرسالة التي تحمل العنوان:

Preparation and Enhancement of CdS/ZnS Thin Films for Photovoltaic Purposes

تحضير الأفلام الرقيقة من سبائك (CdS/ZnS) تم تحسين فعاليتها في التحولات الفوتوكهروكيمياوية

أقر بأن ما اشتملت عليه هذه الرسالة إنما هو نتاج جهدي الخاص،باســـتثناء مـــا تمـــت الإشارة إليه حيثما ورد، و أن هذه الرسالة ككل، أو أي جزء منها لم يقدم من قبل لنيل أي درجة أو لقب علمي أو بحثي لدى أي مؤسسة تعليمية أو بحثية أخرى.

Declaration

The work provided in this thesis, unless otherwise referenced, is the researcher's own work, and has not been submitted elsewhere for any other degree or qualification.

Student's name: اسم الطالب:

Signature: التوقيع:

Date: التاريخ:

Table of Contents

List of Tables

List of Figures

**Preparation and Enhancement of CdS/ZnS Thin Films for
Photovoltaic Purposes
By
Maysa Tayseer Mohammad Atatrih
Supervisors
Dr. Musa El-Hasan
Professor Hikmat S. Hilal**

Abstract

Polycrystalline CdS/ZnS thin films were prepared by chemical bath deposition (CBD) technique on fluorine-doped tin oxide (FTO) coated glass substrates. Enhancement of deposited CdS/ZnS thin film characteristics at solid/liquid interface in photoelectrochemical (PEC) systems was investigated. Deposited CdS/ZnS thin films were exposed to different treatment methods and different experimental conditions. The films were heated to desired temperatures (300 C, 400 C) under air. Cooling of heated films to room temperature was achieved by either slow cooling or quenching. Etching of film surface was conducted using dilute HCl solution. The effect of such treatment on the film photoelectrochemical characteristics was measured by monitoring different parameters, such as: open-circuit voltage (V_{oc}), short-circuit current density (J_{sc}), dark current density-potential (J-V) plots, photo J-V plots, conversion efficiency (η), fill factor (FF), Scanning electron microscopy (SEM), X-ray diffraction, together with electronic absorption and photoluminescence (PL) emission spectra.

The characteristics of CdS/ZnS thin films in PEC systems were enhanced by controlling different experimental conditions, controlling

preheating temperatures and controlling cooling rates. The dark- and photo-current densities vs. potential plots were improved by annealing. Cell efficiency, fill factor, short-circuit current densities (J_{sc}) and SEM results were enhanced for the annealed CdS/ZnS films. The best annealing temperature for CdS/ZnS films was found to be 300 C at which the photo J-V plots and cell efficincy were improved significantly.

Slowly cooled electrodes from temperature 300 C, gave better dark and photo current density vs. potential plots with higher efficiency than their quenched counterparts. SEM measurements were consistent with these findings, and showed better surfaces for slowly cooled CdS/ZnS thin film electrodes. Maximum values of conversion efficiencies were obtained by slow cooling of preheated CdS/ZnS electrodes cooled from temperature 300 C compared to that of electrodes cooled from 400 C.

The effect of coating the CdS/ZnS electrodes with MnP/polysiloxane was also studied. The (J_{sc}) values of coated CdS/ZnS films (with certain Zn ratios) were significantly enhanced. The MnP/polysiloxane coating introduces a charge-transfer mediator species that enhances current and electrode stability.

Chapter 1

Fundamentals and Historical Background

1.1 Photoelectrochemical Cells vs. Photovoltaic Cells

Both photovoltaic (PV) and photoelectrochemical (PEC) cells are based on using semiconductor materials in solar energy conversion into electricity. Materials that have an energy gap (E_g) of ~ 0.7- 3 eV are called semiconductors. Table (1.1) shows the energy band gaps for some semiconductors. At T=0 K, all electrons are in the valence band. Thus semiconductors are non conductors at very low temperatures [1].

Table (1.1): Energy Band Gap Values for Some Semiconductors [1]

Crystal	E_g (eV) at 0 K	E_g (eV) at 300 K
Si	1.17	1.14
Ge	0.744	0.67
InP	1.42	1.35
GaP	2.32	2.26
GaA s	1.52	1.43
CdS	2.582	2.42
CdTe	1.607	1.45
ZnO	3.436	3.2
ZnS	3.91	3.6

When n-type SC electrode is brought in contact with an electrolytic solution, Figure (1.1), the (e^- - h^+) pairs will be generated within the depletion layer and generated electric field will drive photogenerated holes toward the interface. The electrons will be driven toward the interior (bulk) of the electrode. By joining a SC electrode with a suitable counter electrode a PEC cell is constructed [2].
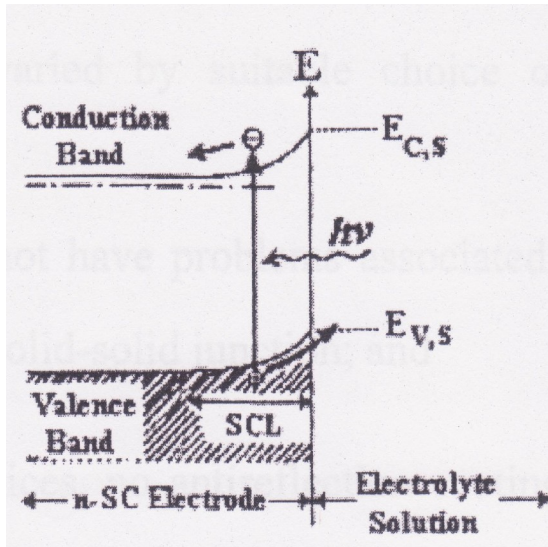
Figure (1.1): Energy level diagram for SC/electrolyte interface showing band bending and the creation of an electron-hole pair in n-type SC upon absorption of a photon with wavelength equal or shorter than threshold wavelength. $E_{c,s}$ and $E_{V,s}$ mark the surface energies of the conduction and valence edges respectively (reproduced from ref. [3]).

In PEC systems, a semiconductor-electrolyte junctions are used as the active layer instead of the solid-state p-n junctions in photovoltaic. In both cases, a space charge region is formed where contact formation compensates for the electrochemical potential differences of electrons on both sides of the contact.

Potentially, there are several advantages for PEC cells, in solar energy conversion, over conventional PV devices [2]:

(a) PEC devices can be fabricated and modified with considerable ease. Contrary to PV devices, only solid-liquid junctions are demanded in PEC. The band bending characteristics of the SC can be conveniently varied by suitable choice of electrolyte and cell variables.

(b) PEC cells do not have problems associated with different thermal expansions of p-n junctions.

(c) PEC devices can store energy in the form of either conventional fuel or electricity.

(d) Unlike PV devices, no antireflection coatings are required in PEC cells.

(e) PEC much less expensive than PV cells.

However, absorption of light by the electrolyte solutions, reflection losses from the cell and the stability of the electrode limit the energy conversion efficiencies in PEC devices in many cases and are shortcomings of PEC systems [4].

1.2 Fundamentals of PEC Cells

The PEC systems are based on the formation of a SC/electrolyte junction when a SC electrode is immersed in a suitable electrolyte solution. For the SC electrode, the Fermi level (E_F) is determined by chemical potential of majority carriers (electrons in n-type SC, and holes in p-type SC). For electrolyte solution, the redox couples and their concentrations determine the initial chemical potential [5].

In n-type SC/electrolyte junction, before equilibrium the E_F will remain above E_{redox}. Electrons will therefore flow down from SC to E_{redox}, Figure (1.3a). As a result, E_F will be lowered. The electron flow will continue until the equilibrium is established, Figure (1.3b). At equilibrium E_F and E_{redox} will match up. This produces a positive depletion region or space charge layer (SCL) in the SC because of chemical reduction process which will produce an electric field in the depletion layer. As a result,

conduction and valence band edges are bent, and a potential barrier is established against further electron transfer into the electrolyte, Figure (1.3), [6].
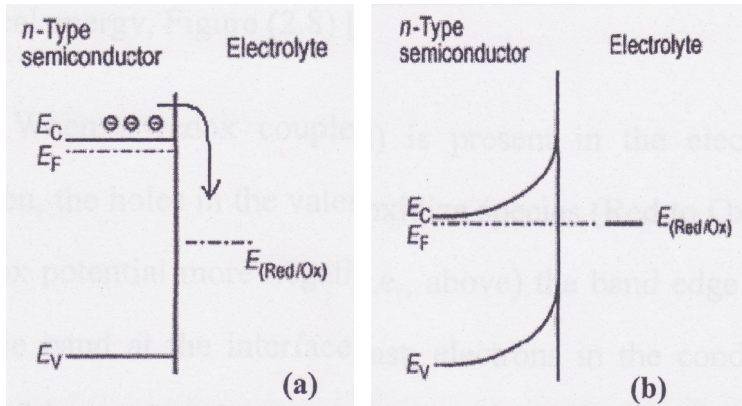
Figure (1.2): n-type SC/electrolyte junction in the dark (a) before equilibrium, (b) at equilibrium. E = electron potential; E_c = lower conduction band edge; EV = upper valence band edge; E_F = Fermi level; $E_{Red/Ox}$ = standard potentials.

Using these principles two types of PEC cells can be built. (1) Regenerative PEC cells are used to convert light energy into electrical energy, and (2) Photoelectrolytic PEC cells are used to store chemical energy, Figure (1.4) [7].
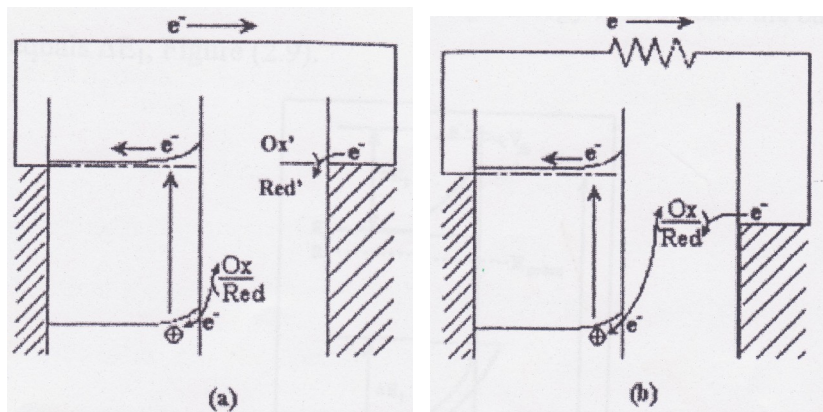
Figure (1.3): Operational principles for the two types of PEC cells: a) photoelectrolytic energy storage cell and b) regenerative photovoltaic cell (copied from ref. [8]).

1.2.1 How Dark Current Occurs in PEC Cells

In n-SC/liquid junctions, the dark current results from electron transfer from the Conduction Band to the electrolyte redox couple (cathodic current flow). At equilibrium, the band bending creates an energy barrier for the electrons to overcome before they transfer. For any given SC and electrolyte, there exists a unique potential for which the potential drop between the surface and the bulk of the electrode is zero (no SCL). This potential is called the *flat band potential* (V_{fb}), with no band bending. Thus, for dark current to occur, the n-type SC must be negatively biased to provide the electrons with enough energy (ΔE) to overcome the barrier.

1.2.2 How Photocurrent Occurs in PEC Cells

When light absorption generates a population of excited holes and electrons, the majority carrier concentration changes relatively little and the minority carrier concentration is greatly enhanced. Hence photo-effects are greatest when minority carriers dominate the electrode response. This occurs when the electrode is biased to form a depletion layer and the photo-generated minority carriers transfer towards the electrode/electrolyte interface [9].

The SC exhibits a threshold response to photon energy dictated by the band gap energy. The photo-effects switch on as the wavelength of incident light (λ) becomes shorter than the threshold wavelength (λ_g). With longer wavelength, electrode is insensitive to light. A useful relation between the threshold wavelength (λ_g) and the band gap energy E_g [10] is:

$$=1240/E_g \qquad (1) \qquad \lambda_g$$

Where (λ_g) has units of nanometers, and E_g units of electron-volts (eV).

1.2.3 Stability Enhancement of SC in PEC Systems

SC stability can be enhanced by different methods:

a) Protective Layers

The unstable SC is prevented from direct contact with the electrolyte and the photo-generated carrier can tunnel through the thin protective layers. Different techniques of protective layer are reported such as:

(i) Thin layer of metallic coating on the surface stabilizes the electrode. Consequently the deVice will be transformed into a buried SC-metal Schottky barrier [11]. The strategy is to shield SC coming into direct contact with the electrolyte. However, it is obvious that the hole transfer or tunneling through the metallic layer is not effective as for the case of direct contact, especially if Schottky barrier exists.

(ii) Coating semiconductors with a wide band gap material (like TiO_2, ITO or SnO_2) which is relatively more stable [12-13]. This strategy is also not effective for the same reasons in (i).

(iii) Electrode stabilization was achieved using electro-active species attached to the electrode surface. The photo-generated holes first oxidize the molecules attached to the surface which in turn oxidizes the reduced species of the electrolyte [14].

(iv) Encouraging results of stabilization have been obtained by growing thin polymer films on the SC electrode [15-16].

b) Chemical and Photochemical Etching

Chemical and photochemical etching of many SC electrodes has been found to reactivate them. It is found that different enchants change differently the stability and efficiency of some SC electrodes [17-18]. Short time etching yields better results [19]. Removal of surface impurities and change in surface morphology are apparently responsible for stability and efficiency enhancements.

c) Redox Couple and Solvent Variation

The variation in the nature of redox couple and solvent can profitably be used in stabilizing SC electrode. Examples of stabilization are described below:

(i) A fast redox couple is added to the electrolyte which can provide an alternative path to minority carrier capture. Rapid carrier transfer effectively competes with corrosion [20].

(ii) Non-aqueous electrolytes containing the appropriate redox couple sometimes creates less damage to SC electrodes than aqueous electrolytes. The anodic decomposition potentials have been observed to a more positive value in non-aqueous solutions [21].

(iii) Addition of NaCl and LiCl salts in the aqueous electrolyte seems to stabilize CdS and CdSe electrodes [21]. This increases the overall kinetics of hole collection from the CdS and CdSe electrodes.

(iv) Some simple techniques like stirring or relative ratio of redox species can be used to suppress corrosion.

(v) Various reducing agent species in the electrolyte would give different stabilities [22].

d) Annealing of Semiconductors

Annealing of semiconductors was found to increase the efficiency of the PEC cells. This is due to the fact that there is an increase in the grain size and removal of frozen-in defects in the SC. Consequently, there is an increase in minority carrier diffusion to electrolyte solution in PEC solar cell. Surface enhancement in SC can be obtained by annealing of SC [23].

1.3 Semiconductor Materials for PEC Cells

One of the most challenging aspects of the solar cell research is that of finding a stable absorber material with needed properties at acceptable cost. The following basic requirements should be fulfilled [24]:

a) The band gap of the material should be such that maximum part of solar spectrum is used. Most of the visible part of solar energy reaching the earth's surfaces is centered in the range 1.0-3.0eV (1240- 413nm).

b) The efficiency of the cell, which depends on absorption coefficient, band gap, diffusion length, conductivity, recombination, surface states, etc, should be high.

c) The electrode must be stable against corrosion when placed in the specific redox electrolyte. Low band gap semiconductors are generally easily corroded.

1.4 SC Thin Film Deposition Techniques

There are many dozens of deposition technologies for material formation [25-29]. Since the concern here is with SC thin-film deposition methods for forming layers in the thickness range of a few nanometers to about ten micrometers, the task of classifying the technologies is made simpler by limiting the number of technologies to be considered.

Basically, SC thin film deposition technologies are either purely physical (such as evaporative methods) or purely chemical (such as gas and liquid-phase chemical processes). A considerable number of processes that are based on glow discharges and reactive sputtering combine both physical and chemical processes; such overlapping processes can be categorized as physical-chemical methods [29]. In our study, we will focus on one type of preparation as shown below.

1.5 Chemical Bath Deposition (CBD)

CBD is a process in which a film of the SC is plated spontaneously onto a substrate dipped in a bath of appropriate composition.

In order to prepare CdS/ZnS films by CBD method, a chemical bath containing a cadmium salt and zinc salt (e.g., $CdCl_2$, $ZnCl_2$, CdSO4 or $Cd(CH_3COO)$ as Cd/Zn sources, thiourea $(CS(NH_2)_2)$ as a sulfur source and ammonia water (NH_4OH) as a buffer, in suitable proportions is used. The bath temperature is controlled and the substrate (glass, Ti, ITO, FTO, etc) is immersed in it with continuous stirring [30-34].

1.6 What is This Work All About?

As mentioned earlier, different thin film deposition methods and different SC enhancement techniques have been reported in literature. In this work, we study the effect of change the CdS/ZnS molar ratio, effect of metalloporphyrin modification and effect of annealing and cooling rate of polycrystalline SC thin films, deposited by using CBD method, on their PEC characteristics for the first time. Polycrystalline CdS/ZnS thin films will be prepared by CBD method under different experimental conditions to find the best electrode. The prepared samples will be treated by heating to different temperatures and by cooling at different rates, will be studied.

Chapter 2
Introduction

Thin-film photovoltaic technologies are being developed to reduce the cost of photovoltaic (PV) systems. The rationale for this is that thin-film modules are expected to be cheaper to manufacture to reduce material costs, energy costs, handling costs and capital costs. The idea of thin films dates back to the inception of photovoltaics. It is an idea aimed at achieving truly low-cost photovoltaics appropriate for mass production [35].

a) Amorphous Silicon (a-Si)

Amorphous silicon is the non-crystalline form of silicon. It can be deposited in thin films at low temperatures, as low as 75 C. Technology has made good progress. Now it appears that commercial, multijunction a-Si modules could be in the 7%–9% efficiency range [36-39].

b) Cadmium Telluride (CdTe)

The advantage of CdTe is easiest of films to fabricate, this kind of cell used of a thin n-CdS layer to form the junction with p-CdTe. This CdS layer must be thin enough to allow high energy light to reach the junction. The ability to achieve high current and high voltage with thin CdS is the main research problem in CdTe technology [35, 40, and 41].

2.1 Earlier Studies

The chemical bath deposition is a simple and suitable method for obtaining smooth, uniform, high reflecting and strong adherent CdS/ZnS

thin films [42]. The resistivities of the CdS/ZnS films increases as [Zn] value increase, and higher band-gap CdS/ZnS films can be obtained by increasing the relative Zn/Cd ratio in the CBD [43].

Annealing of semiconductor surfaces plays an important role in crystallization process of the SC crystals. It enhances the crystals homogeneity, quality, performance and reliability. Annealing also reduces defects, and lowers surface roughness [44-53]. Cooling rate of heated SC electrodes also has an obvious effect on the quality of the crystals through improving their parameters [54-58]. Etching removes recombination centers at the surface and at grain boundaries, reduces surface impurity and changes surface morphology [22].

2.2 Objectives

The main goal of this work is to enhance the characteristics of polycrystalline cadmium zinc sulfide ($Cd_{1-x}Zn_xS$) thin film electrodes, at the solid/liquid interface in photoelectronchemical (PEC) systems. $Cd_{1-x}Zn_xS$ thin films will be grown using chemical bath deposition (CBD) on fluorine-doped tin oxide (FTO) coated glass substrates. Different techniques will be used to enhance characteristics of thin films, including: (1) studying the effect of annealing and cooling rates of CdS/ZnS, (2) studying the effect of CdS/ZnS molar ratio in order to have the highest efficient photocatalytic system, (3) investigating the effect of metalloporphyrin modification on the CdS/ZnS thin film electrodes.

Enhancements of prepared polycrystalline CdS/ZnS thin film characteristics have been investigated by measuring performance parameters including, open-circuit voltage (V_{oc}), short-circuit current (I_{sc}), dark current density-potential (J-V) plots, photo J-V plots.

Zinc and cadmium sulfides are compound semiconductors with a wide range of potential applications. These materials have many similarities; both exist in cubic or hexagonal forms and are wide and direct band gap semiconductors. The CBD process uses a controlled chemical reaction to effect the deposition of a thin film by precipitation.

Thin films are deposited using various techniques such as: electrodeposition, ultrasonical colloid chemistry deposition (UCCD), vacuum eVaporation, sputtering, spraying, molecular-beem epitaxy, laser-induced, electroless plating and CBD. The CBD technique is not the most efficient polycrystalline thin film deposition technique; but it appears to be relatively simple, inexpensive and convenient for large area deposition of polycrystallione thin films. CBD technique has been intentionally employed in this work, so as to see if our modification techniques are competent or not. If found satisfactory, the modification techniques may then be recommended for SC electrodes deposited by other techniques.

The deposition of CdS by CBD is straitghforward and involves an alkaline solution of a cadmium salt, a complexant and a chalcogen source, often thiourea or thioacetamide. In contrast ZnS is more difficult to deposit. $Cd_{1-x}Zn_xS$ alloy compounds have attracted technological interest because

the energy gap can be tuned and lattice parameters can be varied. In recent years the replacement of CdS with its ternary alloy

$Cd_{1-x}Zn_xS$ has been attempted to improve the (Cd, Zn) S/Cu (In, Ga) Se_2 solar cell performance, this has resulted in a higher efficiency of 16.9%. Moreover, the replacements of CdS with the higher energy gap ternary $Cd_{1-x}Zn_xS$ has also led to a decrease in window absorption loss, and has resulted in an increase in the short circuit current in solar cell.

2.3 Hypothesis

The combined CdS/ZnS thin films will function as converters of light to electricity. A synergistic effect may enhance the efficiencies of both species. It is assumed that molar ratios of the system may affect efficiency.

Heating pre-prepared thin films of CdS/ZnS would give crystallites with larger sizes and better sintering, which would give higher carrier mobility across the thin film matrix. Thus the film resistance would be lowered by heating. So it is anticipated to have better photovoltaic characteristics for annealed films. The quenched thin films are assumed to have more cracks (imperfections). Slow cooling is expected to give better chances for heated films (likely to have many imperfections) to go back to more ideal ordering.

In earlier works, the effect of annealing and cooling rates of single crystalline n-Si and n-GaAs wafers has been investigated. It has been found

that, n-Si and n-GaAs electrode efficiency can be easily enhanced by controlling preheating temperatures and rates of cooling. Annealing of single n-Si and n-GaAs surfaces improves the surface quality by minimizing defects and improving crystal characteristics. Also, slow cooling of these SC improves crystal properties. If the heated crystal is slowly cooled, the crystal will be able to gain its original order. If quenched, the crystal will retain its imperfection. Imperfection will be exhibited in many ways, such as the ill-defined band-edge structure, and the distorted crystal surface. To our knowledge, such technique has not been investigated as a tool to enhance the characteristics of $Cd_{1-x}Zn_xS$ thin films. Therefore; we intend to formulate a convenient method to enhance the surface structure of $Cd_{1-x}Zn_xS$ thin films for the purpose of enhancing their PEC properties.

In this work, we expect to enhance the characteristics of $Cd_{1-x}Zn_xS$ thin films prepared by CBD method in PEC systems by controlling film thickness, change the CdS/ZnS molar ratio, effect of metalloporphyrin modification, preheating temperatures and rates of cooling.

Chapter 3
Experimental Work

3.1 Materials

3.1.1 Chemicals and Solvents

$ZnCl_2$, $CdCl_2$, thiourea (CS $(NH_2)_2$), NH_3, hydrazine hydrate, HCl, ethanol, $LiClO_4$, $K_3Fe(CN)_6$ and $K_4Fe(CN)_6$ were purchased from Aldrich. Tetra(-4-pyridal) porphyrinatomanganese complex (MnP), polysiloxane was obtained from earlier preparations in this Department. The electronic absorption spectra showed the presence of both $Mn^{2+}P$ and $Mn^{3+}P$ at the same time Figure (3.1). polysiloxane from RTV, and highly conductive FTO glass samples were donated by Professor. Guy Campet of ICMCB, University of Bordeaux, France.
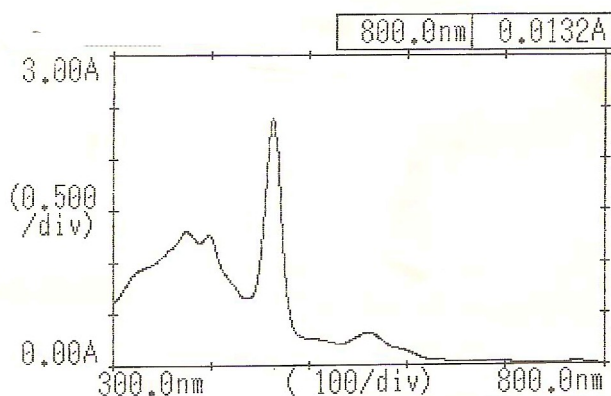
Figure (3.1): Absorption spectrum of metalloporphyrin

3.1.2 Preparation of CdS/ZnS Films

CdS/ZnS films have been grown by CBD on FTO/glass substrates, as shown in the literature [59-62]. Into the beaker was added 50ml of stirred deionized water at 70°C, ammonia (1.4M), hydrazine (2.25M),

thiourea (0.14M), $CdCl_2$ and $ZnCl_2$ with concentrations between 0 and 0.1M where ($[CdCl_2]+[ZnCl_2]=0.1M$) as desired. The deposition took place on cleaned FTO/ glass substrate. The FTO/ glass substrates were cleaned with ethanol and etched in a 10% HCl solution just before depositions. The FTO/ glass slids were placed in the 50 ml closed beaker. This was placed in a water bath at a constant temperature of 70°C. $CdCl_2$ and $ZnCl_2$ were added first to the $NH_3/NH_2\text{-}NH_2$ solution under stirring followed by the addition of thiorea [67].

The deposition process is based on controlled precipitation of zinc or cadimum sulfide in the reaction bath. The solubility products of metal sulphides are very small and therefore pericipetation control has to be made by controlling the concentrations of free Zn^{2+} and Cd^{2+} in the bath. This can be achieved by using suitable complexing agents which release small concentrations of ions according to the complex ion dissociation and equilibrium constant. In this work the complexing agent used was ammonia.the dissociation equilibriums of the mentioned complex ions and thier corresponding equilibrium constant are:

$$Cd(NH_3)_4{}^{2+} \rightarrow Cd^{2+} + 4NH_3 \qquad\qquad (1)$$

$$Zn(NH_3)_4{}^{2+} \rightarrow Zn^{2+} + 4NH_3 \qquad\qquad (2)$$

The solubility products and the complex ion dissociation constants indecate that the CdS precipitation is easier and faster than that of ZnS. Hydrazine has been added to the reaction bath, as was done to promote the

ZnS incorporation within the film. Thiourea has been used as the S^{2-} source. Thiourea hydrolyses in alkaline media through:

$$SC(NH_2)_2 + OH^- \rightarrow SH^- + CH_2N_2 + H_2O \qquad (3)$$

In this medium the HS^- is in equilibrium with water according to:

$$HS^- + OH^- \rightarrow S^{2-} + H_2O \qquad (4)$$

This reaction sequence indicates that it is posible to obtain only an extremly small S^{2-} concentration by having large excess of OH^- in the bath [63]. Using the previously mentioned conditions, we obtaind deposits which are homogeneous and colours varying from orange-yellowish to white-yellowish depending on the bath composition. The deposition time was 45 min. After each deposition, the coated substrate was cleand with distilled water and dried in nitrogen atmosphere and stored in a clean place [43, 49].

3.1.3 Etching Process

The prepared CdS/ZnS electrodes were etched by treatment with dilute HCl (10% v/v) solution. The electrode was immersed in the dilute HCl solution for about 5 seconds and then rinsed with distilled water [63]. The above procedure was repeated two or three times to obtain a shiny film surface. The electrode was then rinsed with distilled water and methanol, and dried with nitrogen.

3.1.4 Annealing Process

Annealing was conducted using a thermostated horizontal tube furnace. The prepared CdS film substrates to be annealed were inserted in a long Pyrex cylinder. The heat was raised to the desired temperature (300°C or 400°C), under air and was left for 30 min before cooling. The system was left to cool, in the desired method quenching or slow cooling.

3.1.5 Cooling Process

Quenching Process

The annealing system was left to cool under continuous flow of air from the desired temperature to room temperature within 3 min, from the desired temperature. This was achived by removing the cylinder from the furnace immediatly after switching off the heater, and allowing the system to rapidly cool in air.

Slow Cooling Process

After the substrates were annealed to the desired temperature, the temperature was in steps of 50°C, and annealing system was left for 20 min interval at each cooling step. When the cooling time interval between variou temperature cooling steps above 30 min, the furnace was shut down, and left to cool to room temperature. The time intervals of slow cooling process were varid from between 3-5 hour, depending on the annealing temperature.

3.1.6 Electrode Modification with MnP/polysiloxane

The MnP/polysiloxane stock solution was prepared by adding the MnP solution to the polysiloxane solution in a 1:4 (v/v) ratio, respectively. Then 0.1 ml of the MnP/polysiloxane stock solution, containing 4.0×10^{-5}g polysiloxane and 2.0×10^{-4}g MnP, the electrode dropped in the solution for 3 min, and then leave the modified electrode to dry under nitrogen gas.

The modified electrode was further annealed, after fabrication, at 125°C for 30 min under nitrogen. The system was then left to cool at room temperature under N_2 [15].

3.2 Equipment

3.2.1 PEC Cell Description

The prepared CdS/ZnS film electrode was incorporated as a working electrode into a three-electrode one-compartment photoelectrochemical cell, with a platinum counter electrode and a reference saturated calomel electrode.

The redox couple used in this study was: $LiClO_4$ (0.01 M), K_4Fe $(CN)_6$ (0.05 M), $K_3Fe(CN)_6$ (0.05 M) as a redox couple in distilled water. The solution was stirred at the beginning, and was stopped as the PEC experiment started. High purity (99.999 %) nitrogen gas was bubbled through the solution for at least 5 min before each experiment, and was kept to flow above the solution during the experiment to minimize contamination with air. The measurements of current- voltage data were

performed using a computer controlled Princeton Applied Research (PAR) Model 263A Potentiostat/Galvanostat. The measured current (I) was converted into current density (J), by dividing the current I by the area of the illuminated electrode.

3.2.2 Light Source

Illumination was carried out using a 50 Watt Xenon lamp equipped with housing and a concentration lens. The lamp has a high stability and an intense coverage of wide spectral range, from about 450 to 800 nm [64]. The Xenon lamp was placed at a defined distance from the working electrode. The intensity of light used in the experiment is equal 0.972 W/m^2.

3.3 Measurements

3.3.1 Current Density-Potential Plots

Current density voltage (J-V) plots were measured using a PC controlled potentiostat at room temperature under nitrogen atmosphere. The dark experiments were performed, by covering the system with a black thick cloth. On the other hand, 50 W Xenon lamp was used in the photocurrent measurements.

3.3.2 Spectra

Absorption spectrophotometry:

A shimadzu UV_1601 spectrophotometer , equipped with thermal printer model DPV-411-040 , Type 20BE, was used for electronic

absorption spectra ; measurements .The spectrophotometer was used to measure remaining contaminant concentrations during photo – degradation experiments, it was also used to measure solid spectra for different catalyst systems.

3.3.3 Photoluminescence

Fluorescence Spectrometry:

A Perkin-Elmer LS 50 Luminescence spectrophotometer was used to measure emission fluorescence spectra for different catalyst systems as solid films. Emission spectra were also measured for a number of reagents. Emission spectra were used to measure semiconductor catalyst band gap. The ware length of the photoluminescence peak was taken to be the wave length of the band gap for the quantum wells.

3.3.4 Scanning Electron Microscopy (SEM)

SEM is useful to directly study the surface of solid objects. By scanning with an electron beam that is generated and focused by the operation of the microscope. SEM uses electrons instead of light to form an image. A beam of electrons is produces at the top of the microscope by heating of a metallic filament. The electron beam follows a vertical path through the column of the microscope. It makes its way through electromagnetic lenses which focus and direct the beam down towards the sample. Once it hits the sample, other electrons are ejected from the sample. Detectors collect the secondary or backscattered electrons, and

convert them into a signal that is sent to a viewing screen to produce an image.

3.3.5 X-ray Diffraction (XRD)

XRD patterns were measured for CdS/ZnS thin film. The measurements were carried out in the ICMCB laboratories, Bordeax University, using a Philips XRD X'PERT PRO diffractometer with Cu Kα ($\lambda = 1.5418$) as a source.

Chapter 4
Results and Discussion

4.1 General Remarks

In this work, $Cd_{1-x}Zn_xS$ semiconductor thin films have been prepared using chemical bath deposition technique (CBD). Deposited $Cd_{1-x}Zn_xS$ thin films were exposed to different experimental conditions and different treatment techniques. The effects of different experimantal conditions on the photoelectrochemical (PEC) cell performance such as: repeated depositions, changing the CdS/ZnS molar ratio, metalloporphyrin modification of the CdS/ZnS thin film were investigated. The prepared thin films have been treated by heating and cooling. The films were heated to a desired temperature (300°C and 400°C) under air. Cooling of pre-heated films to room temperature has been done using two different methods, slow cooling and quenching.

An ideal dark J-V plot illustrated in Figure (4.1a), can be defined as: a smooth plot in which the current density remains zero for a given potential, and suddenly it drops negative at onset potential (V_{onset}). An ideal photo J-V plot displayed in Figure (4.1b), can be defined as: a smooth plot in which the fill factor approaches 100%.
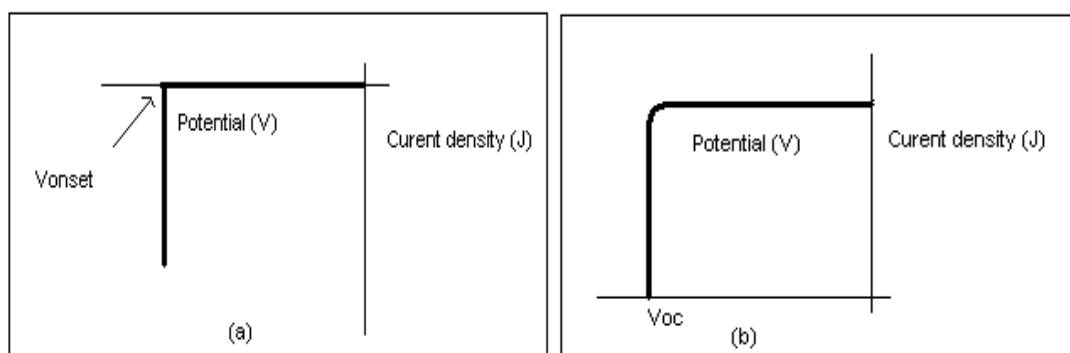
Figure (4.1): Ideal dark J-V plot b) Ideal photo J-V plot for semiconductor

Cooling rate of a pre- heated metal crystal may affects the crystal properties. As for example, it is reported that quenching of pre-heated aluminum rods prevents their contraction to original volume [65]. The metastable spheres, in the heated crystal, may not return to original stable positions with quenching due to kinetic restriction. Alternatively, slow cooling could kinetically allow the return of metastable spheres to original positions. Therefore, it can assumed that slow cooling improves crystallinity, by allowing removal of imperfections.

Annealing of single SC wafers was reported to enhance their characteristics, such as crystal structure, surface and doping distribution. Slow cooling has also been reported to enhance SC characteristics [23, 66-71]. Slowly cooled crystals may retain their original order. On the other hand, quenched crystals would retain imperfection. Such imperfections may be exhibited in many ways, such as ill-defined band-edge structures, distorted crystal surfaces and increased surface states. This will consequently affect the dark current and photo current plots [22].

Moreover, chemical and photochemical etching of many semi conductor (SC) electrodes reactivates them. It is found that different etchings change differently the stability and efficiency of some SC electrodes [17-19]. Removal of surface impurity and change in surface morphology are apparently responsible for stabilization.

Since cooling rate technique has not been widely used as a tool to enhance the PEC characteristics of CdS/ZnS thin film [72]. We hereby

utilized such ideas to improve the PEC characteristics of CdS/ZnS thin film SC electrodes.

4.2 Effect of Experimental Preparation Conditions on CdS/ZnS Cell Efficiency

In this work, we investigated the influence of different experimental conditions on PEC cell performance as, change the CdS/ZnS molar ratio, metalloporphyrin modification, repeated depositions, annealing and cooling rates. In other words, CdS/ZnS cell efficiency is observed to be affected by different parameters such as, multiple depositions, bath concentration and rate of cooling. We found that CdS/ZnS films prepared from a bath of molar ratios Cd/Zn 0.10:0.00, Cd/Zn 0.09:0.01, Cd/Zn 0.08:0.02, Cd/Zn 0.07:0.03 have better photo J-V plots than films prepared from a bath of Cd/Zn 0.06:0.04, Cd/Zn 0.05:0.05, Cd/Zn 0.04:0.06, Cd/Zn 0.03:0.07, Cd/Zn 0.02:0.08, Cd/Zn 0.01:0.09, Cd/Zn 0.00:0.10. This is presumably due to the increasing Zn concentration in the solution. Which is observed to attenuated the electrical parameters [43].

With multiple depositions, the best film performance has been obtained with three-deposition films.

The effect of number of depositions on $Cd_{1-x}Zn_xS$ cell efficiency has been studied. The one, two and four deposition steps gave no PEC result. Figure (4.2), shows absorption spectrum of CdS/ZnS prepared by CBD, four deposition steps were done at Cd/Zn 0.06:0.04 with slowly cooling

from 300 C. The figure reflects, the absorption spectra for the samples being prepared at different Cd/Zn ratios. As it is evident from the figure, the four deposition steps prepared at Cd/Zn ratio of 0.06:0.04, revealed a very week spectrum with rather broaden line in the wave length region of 200-800 nm. This is an indication failure in film construction.

Figure (4.2) displays the effect of Zn concentration of the absorption spectra. Increasing Zn ratio does not show a systemic behavior in the absorbance values. However, at the absorption edge there is an apparent shift in the spectra.

To give better understanding to the observed absorbance, we have analyzed the spectra in accordance to the energy bang theory in solid.

The experimentally determined absorbance is related to the absorption coefficient through the relation (A = $\Box$d with d being the film thickness). The direct energy gap is determined from the relation,

$$(\alpha E)^2 = E - E_g .$$
(4.1)
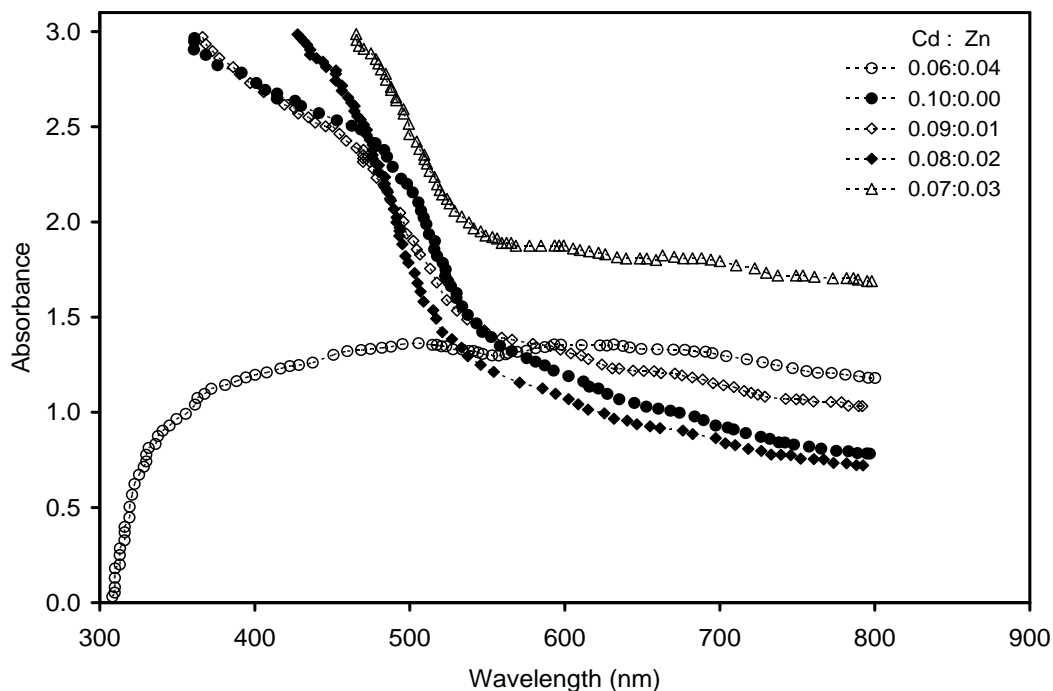
Figure (4.2): Absorption spectrum of CdS/ZnS prepared by CBD with slow cooling from 300 C.

Figure 4.3 displays the absorption coefficient as function of incident photon energy in the energy region of 2.2-2.7 eV where the absorbance appeared to be very strong. The intercept of the figure, reveal the direct allowed transition energy band gap of the material (E_g). As it is clear from the E-axis, the energy band gap for the pure CdS is 2.21 eV and for Cd:Zn ratio of 0.09:0.01 is 2.25 eV. Figure 4.4 displays the other ratios of Cd:Zn. The energy band gap is 2.35 for 0.08:0.02 ratio and 2.19 eV for 0.07:0.03 ratio. From the calculated data of energy band gap, there is a systematic increase from 2.21 to 2.25 and 2.35 eV as the Zn concentration increased from 0 to 0.01 and 0.02, respectively. Further increase in the Zn concentration reduces the energy gap to 2.19 eV. The increase in the energy gap with increasing Zn concentration may be attributed to many

reasons like structural modifications and energy band alignment with increasing Zn atom Zn percentages.
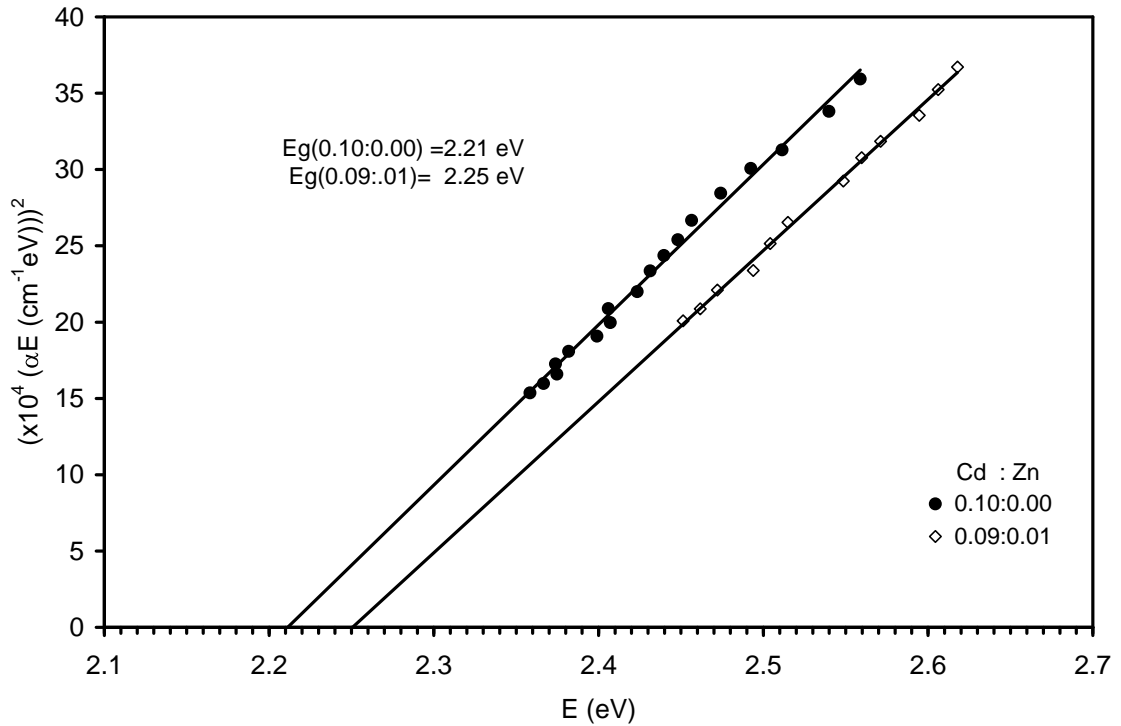
Figure (4.3) the $(\alpha E)^2 - E$ **dependence for slow cooling from 300** ^0C **at Cd: Zn ratio of 0.10:0.00 and 0.09:0.01.**
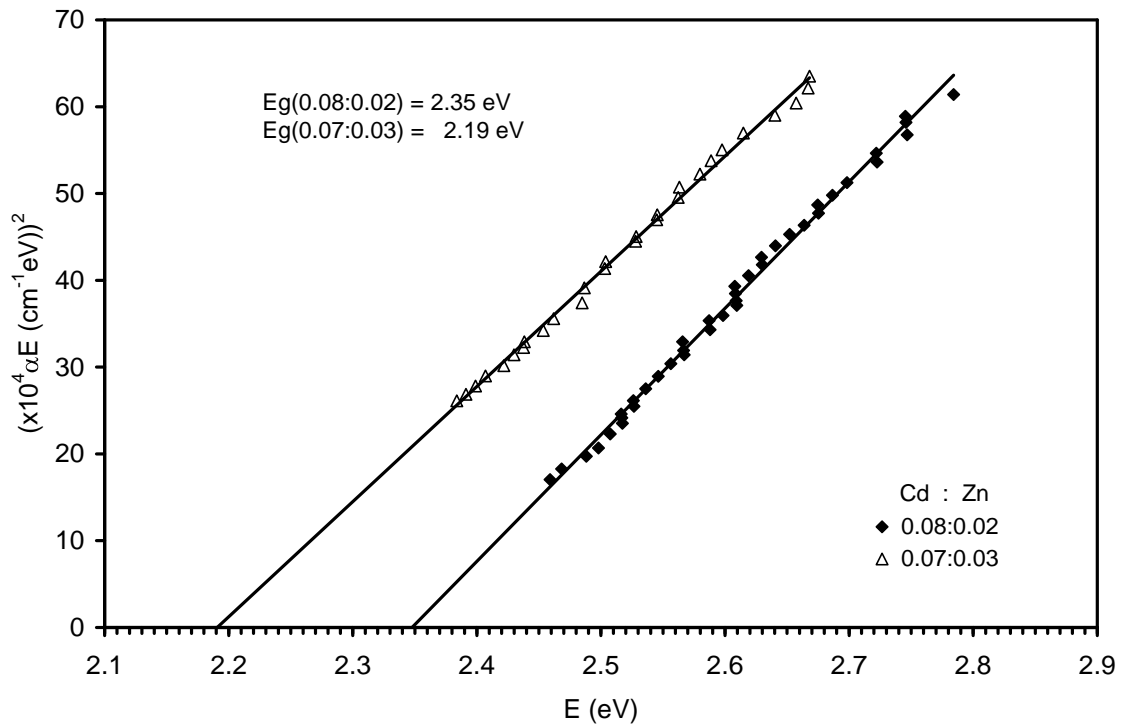
Figure (4.4) the $(\alpha E)^2 - E$ **dependence for slow cooling from 300** ^0C **at Cd: Zn ratio of 0.08:0.02 and 0.07:0.03.**

4.3   Effect of Annealing on CdS/ZnS Thin Film Electrodes

In general, pre-heated multideposited CdS/ZnS film samples give results photo J-V plots, where as untreated samples gave no PEC results, for all different CdS/ZnS ratios. As explained earlier, better photo J-V plots mean higher J_{sc} value and more negative V_{oc}.

The photo J-V plot displayed in Figure (4.5), was observed for CdS/ZnS thin film electrode which we slowly cooled from 300°C and was found to be better than that from 400°C, with molar ratio Cd/Zn 0.10:0.00. Moreover, we note enhancement in absorbance spectrum of thin films, for the same rate of cool, the energy gap for the film was 2.35 eV.

The CdS/ZnS thin film electrodes prepared by three-time deposition were pre-heated, to different temperatures, and then cooled (slowly or quenched) to room temperature. Heating and cooling procedures were conducted under air. The dark J-V plots of the electrodes were affected by both annealing temperature and cooling rate.

For the molar ratio Cd/Zn 0.10:0.00, the slow cooling from 300°C reveals higher dark current density than that of slow cooling from 400°C, as indicated in Figure (4.6). This is consistent with photo-current vs. potential plot results in Figure (4.5).
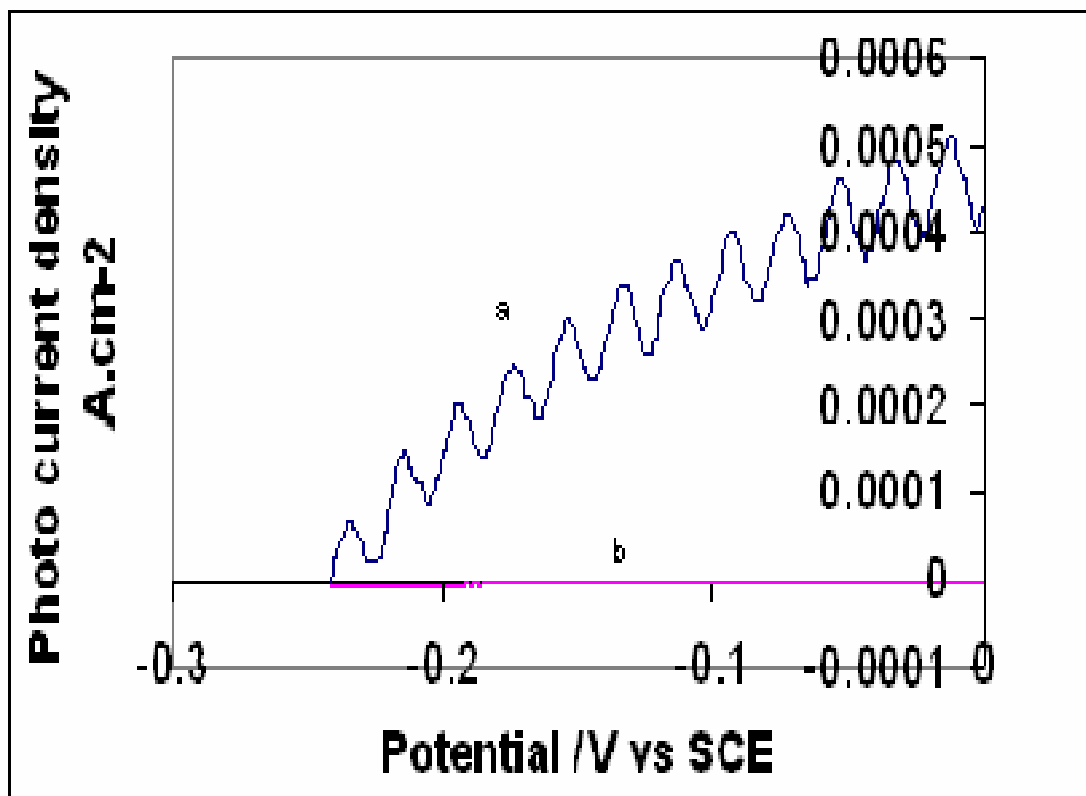
 Figure (4.5): Photo current J-V plots for slowly cooled CdS/ZnS electrodes at [Zn] =0.00 [Cd] =0.10 from a) 300 C b) 400 C. All measurements were conducted in aqueous LiClO$_4$/K$_4$Fe(CN)$_6$/K$_3$Fe(CN)$_6$ at 25 C.
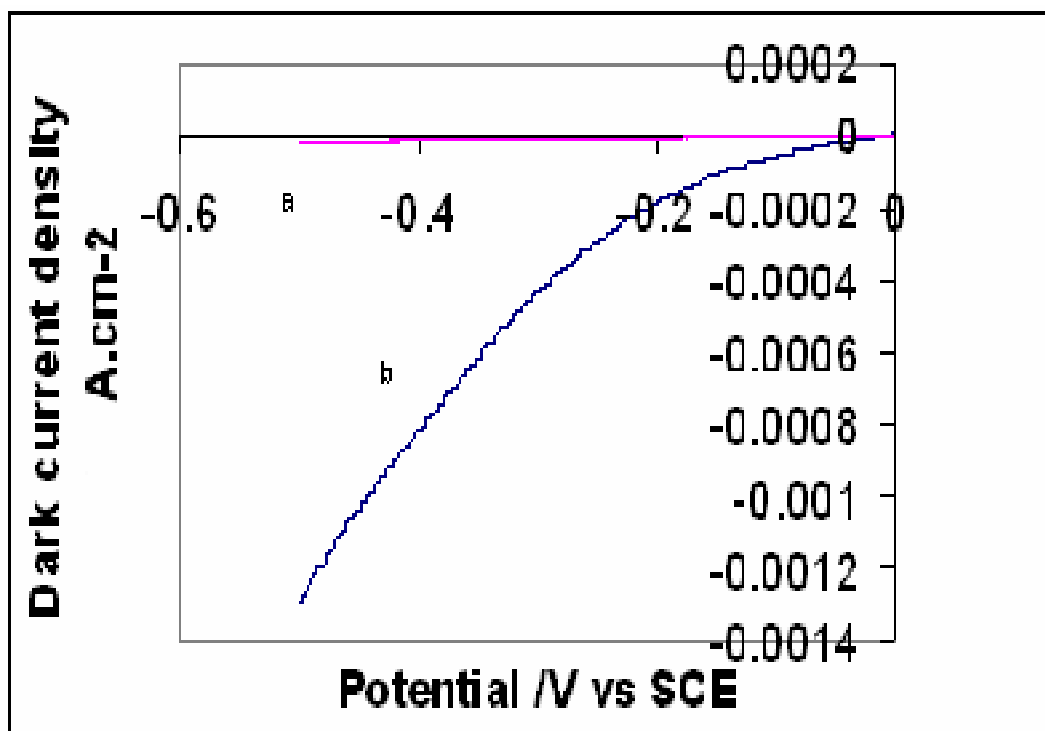
 Figure (4.6): Dark current J-V plots for slowly cooled CdS/ZnS electrodes at Cd/Zn 0.10:0.00 from a) 400 C b) 300 C. All measurements were conducted in aqueous LiClO$_4$/K$_4$Fe(CN)$_6$/K$_3$Fe(CN)$_6$ at 25 C.

For molar ratio Cd/Zn 0.09:0.01, slow cooled thin film electrodes from 300 C to room temperature, the energy band gap was 2.25 eV as observed from absorption spectra show in Figure (4.3). Photo J-V plot for electrodes slowly cooled from 300°C are better than J-V plots for slowly cooled electrodes from 400°C to room temperature, as shown in Figure (4.7). This result is consistent with balance with dark J-V plot results of slowly cooled CdS/ZnS thin film electrodes from 300°C and 400°C, Figure (4.8). The Figure shows that slow cooling from 300°C gives slightly higher dark current density than slow cooling from 400°C.
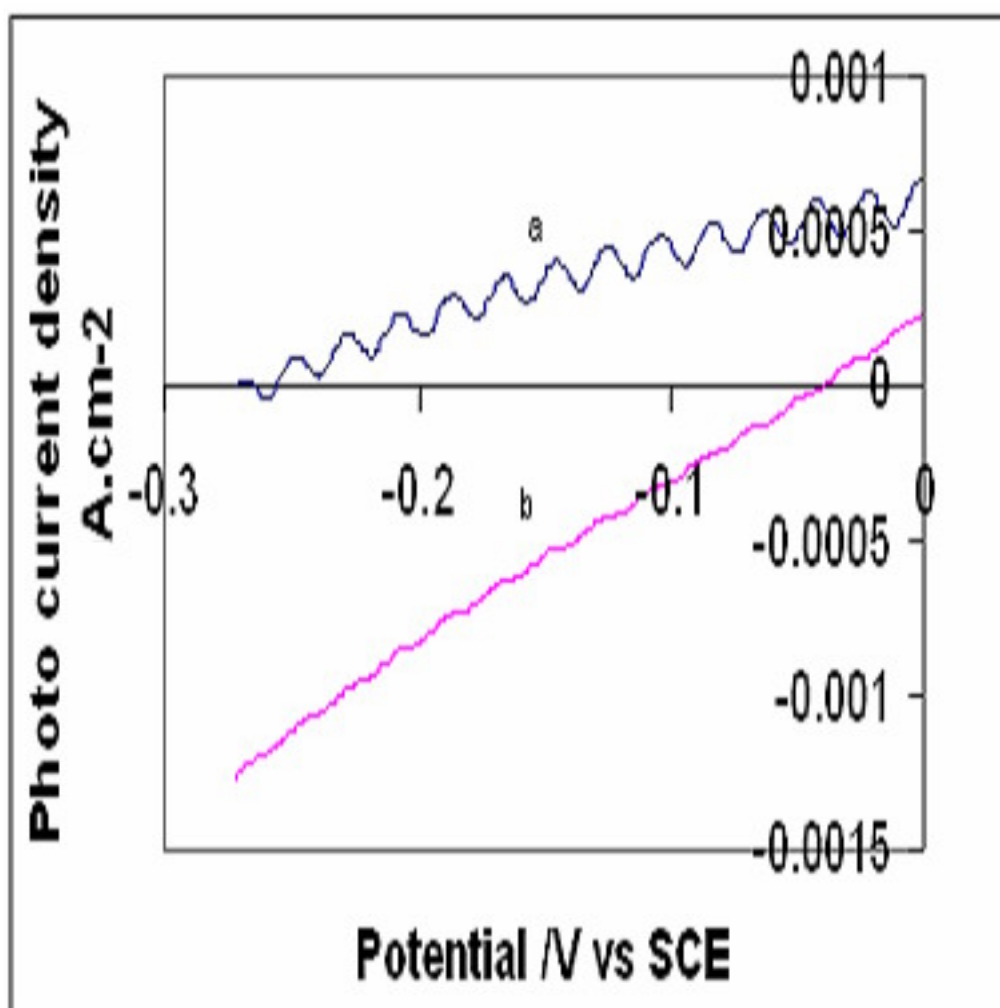
Figure (4.7): Photo current J-V plots for slowly cooled CdS/ZnS electrodes at Cd/Zn 0.09:0.01 from a) 300 C b) 400 C. All measurements were conducted in aqueous LiClO₄/K₄Fe(CN)₆/K₃Fe(CN)₆ at 25 C.
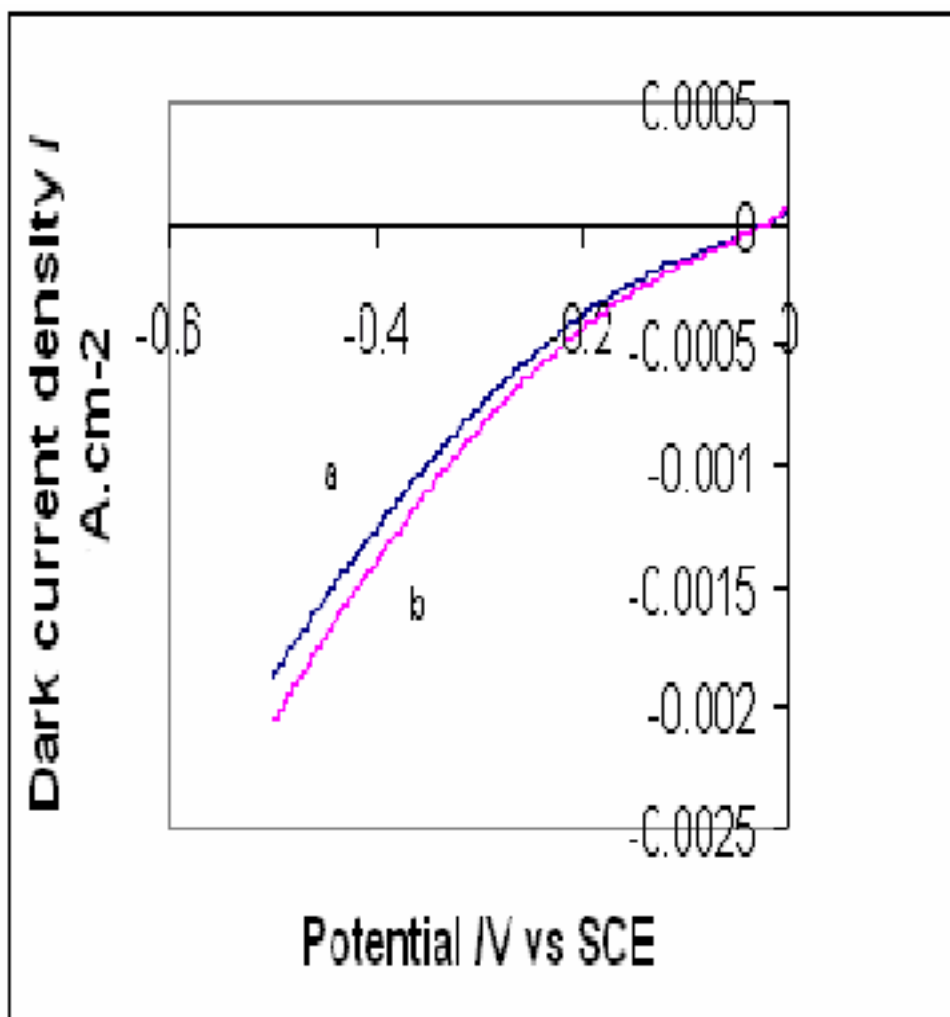
Figure (4.8): Dark current J-V plots for slowly cooled CdS/ZnS electrodes at Cd/Zn 0.09:0.01 from a) 300 C b) 400 C. All measurements were conducted in aqueous LiClO$_4$/K$_4$Fe(CN)$_6$/K$_3$Fe(CN)$_6$ at 25 C.

For molar ratio Cd/Zn 0.08:0.02, three deposition steps, the photo current J-V plots for slowly cooled electrodes from 300 C is better than J-V plots for slowly cooled electrode from 400°C as shown in Figure (4.9). The energy gap of the film calculated from absorption spectra, Figure (4.4) was 2.35 eV. Figure (4.11), shows the dark J-V plots of slowly cooled CdS/ZnS thin film electrodes from 300°C and 400°C, The figure shows that, thin film slow cooling from 300°C gives higher dark current density than from 400°C.
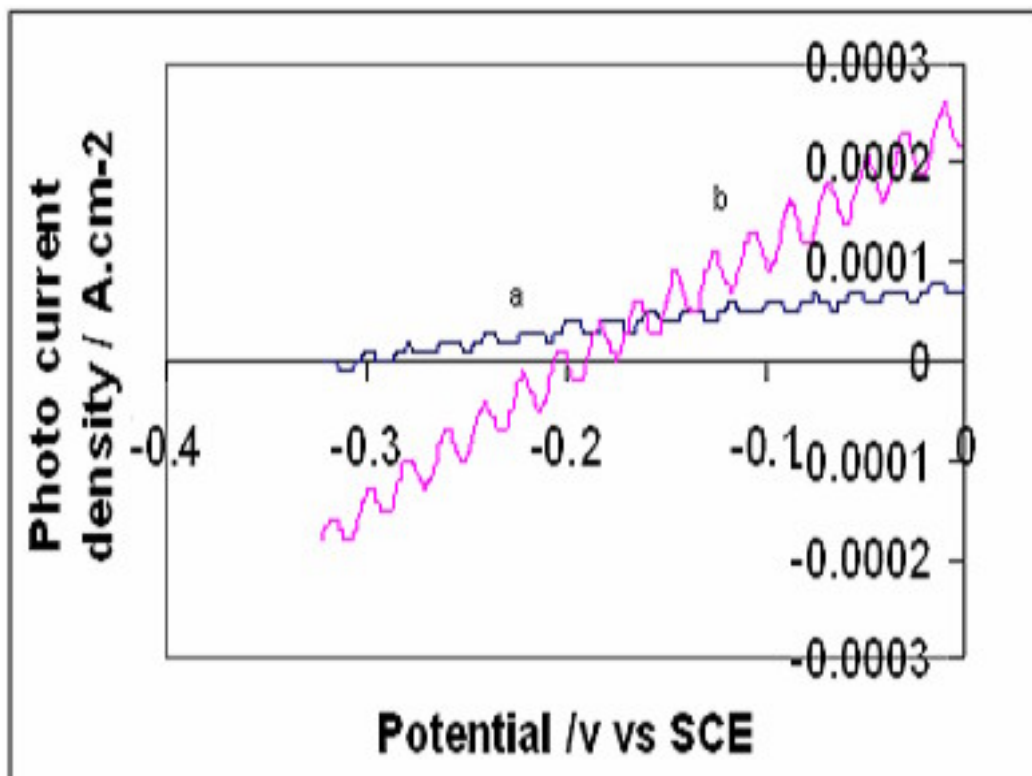
Figure (4.9): Photo current J-V plots for slowly cooled CdS/ZnS electrodes at Cd/Zn 0.08:0.02 from a) 300 C b) 400 C. All measurements were conducted in aqueous LiClO$_4$/K$_4$Fe(CN)$_6$/K$_3$Fe(CN)$_6$ at 25 C.
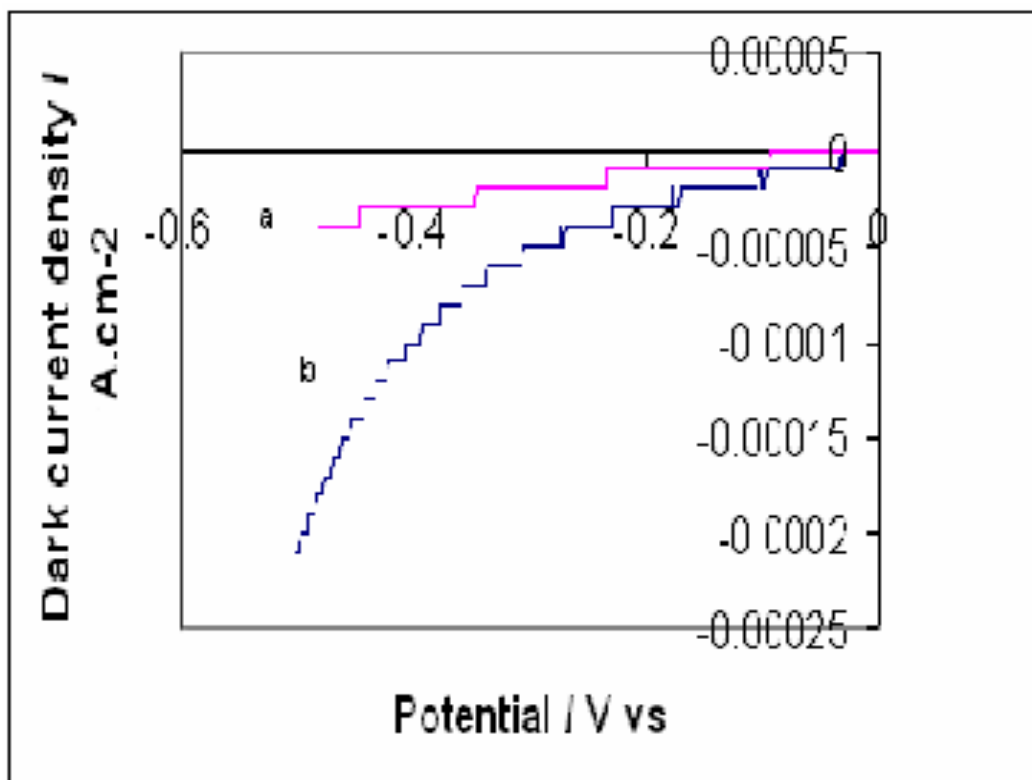
Figure (4.10): Dark current J-V plots for slowly cooled CdS/ZnS electrodes at Cd/Zn 0.08:0.02 from a) 400 C b) 300 C. All measurements were conducted in aqueous LiClO$_4$/K$_4$Fe(CN)$_6$/K$_3$Fe(CN)$_6$ at 25 C.

For molar ratio CdS/ZnS 0.07:0.03 electrode three deposition step, the energy gap of the thin film electrode prepared by CBD, slow cooling from 300 C was 2.19 eV. This result was obtained from Figure (4.4), which shows the optical absorption spectra of CdS/ZnS thin film electrode.

The photo current J-V plots for slowly cooled electrodes, from 300 C is better than J-V plots for slow cooled from 400°C, Figure (4.11). This result is consistent with dark J-V plots shown in Figure (4.12). The Figure shows that, slow cooling from 300°C gives higher dark current density than slow cooling from 400°C.
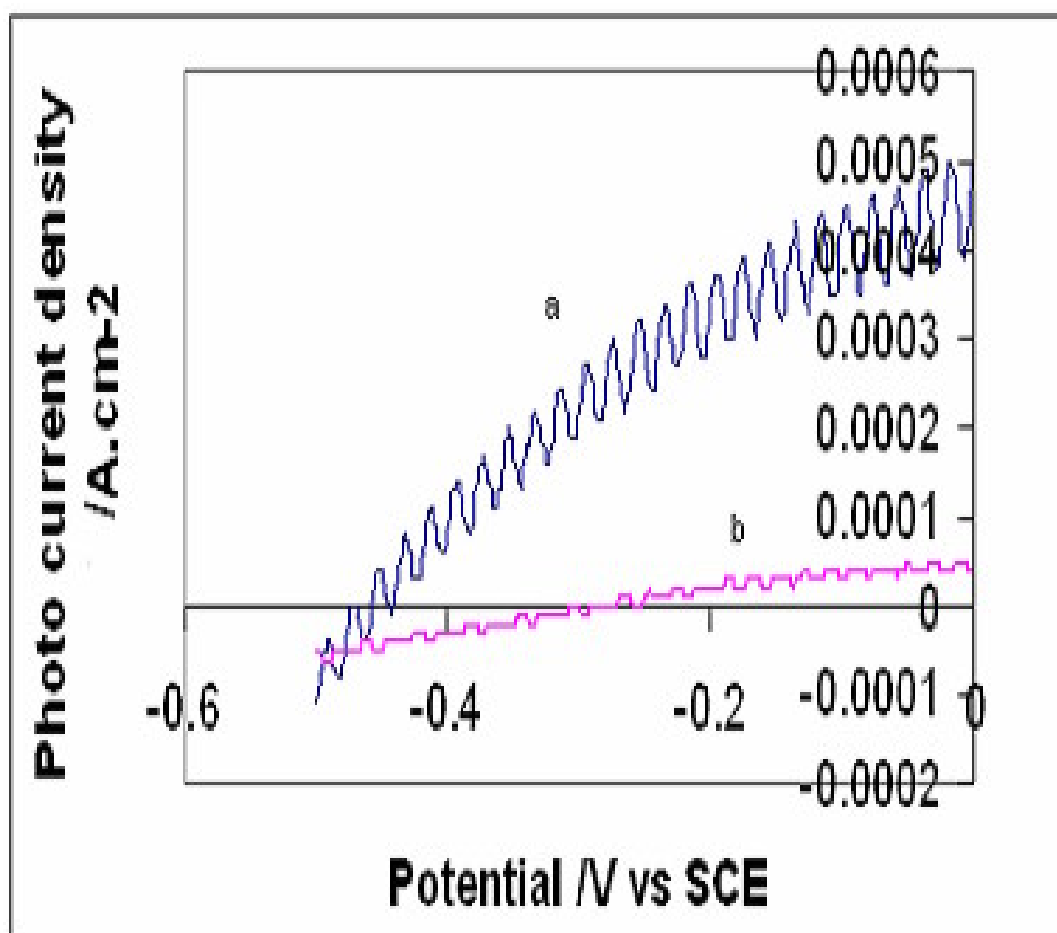
Figure (4.11): Photo current J-V plots for slowly cooled CdS/ZnS electrodes at Cd/Zn 0.07:0.03 from a) 300 C b) 400 C. All measurements were conducted in aqueous LiClO$_4$/K$_4$Fe(CN)$_6$/K$_3$Fe(CN)$_6$ at 25 C.
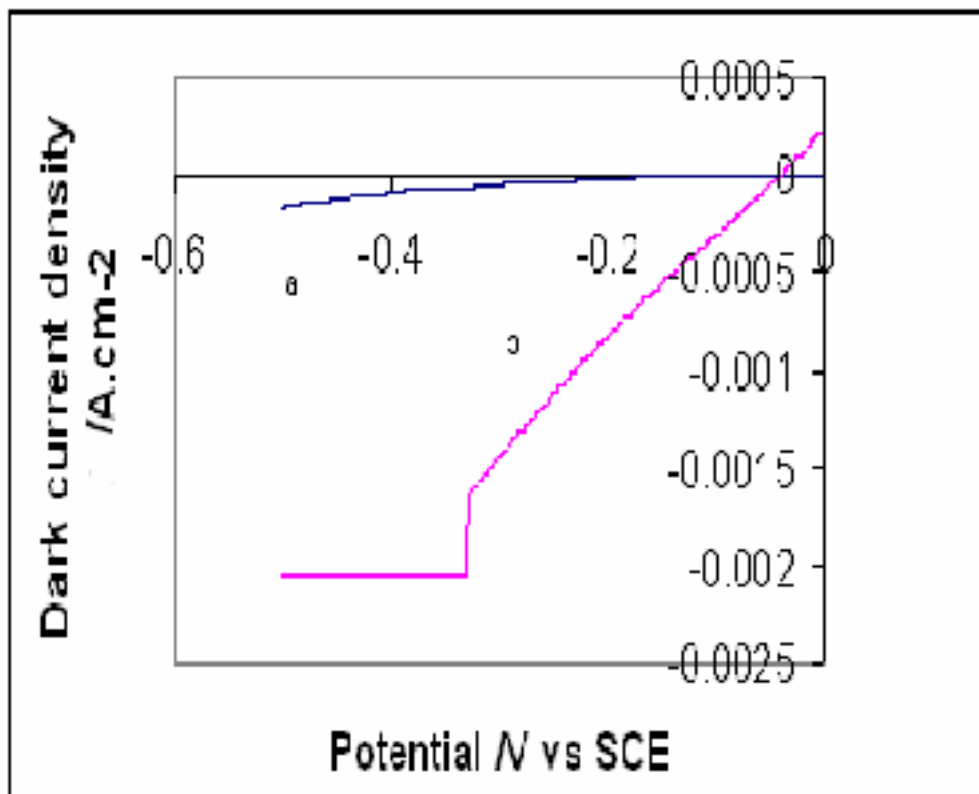
Figure (4.12): Dark current J-V plots for slowly cooled CdS/ZnS electrodes at Cd/Zn 0.07:0.03 from a) 300 C b) 400 C. All measurements were conducted in aqueous LiClO$_4$/K$_4$Fe(CN)$_6$/K$_3$Fe(CN)$_6$ at 25 C.

CdS/ZnS thin films grown by CBD technique are generally polycrystalline, composed of metastable cubic and stable hexagonal phases. Thermal annealing may lead to phase transition and thereby may change the band gap [44-53]. Similar results are observed in Figure (4.17).

Different annealing temperatures may affect the PEC cell performance. It is found that the best PEC cell performance is obtained when the CdS/ZnS film electrode is annealed at 300 C under air atmosphere for slow cooling when the concentration of zinc and cadmium Cd/Zn 0.07:0.03.

In this work, we intended to enhance efficiency of CdS/ZnS thin films in light-to-electricity conversion using economic and feasible

techniques. Annealing is one technique to improve crystal structure, and consequently cell efficiency. SEM, XRD, and PL results support this logic.

In this study, we studied J-V characteristics in the dark, for annealed CdS/ZnS film. No values of J-V plots have been observed for the naked CdS/ZnS film electrode. This is due to the film growth in the system atom-by-atom growth of well crystallized CdS film initially takes place due to the higher chemical stability of CdS than ZnS. As the concentration of Cd^{+2} becomes lower, the precipitation of ZnS begins in the solution. The cluster-by-cluster growth of the ZnS outer layer thus follows. The ZnS clusters can infiltrate the gaps in the CdS inner layer [2]. The effect of 400 C annealing is not significantly pronounced for different ratios of Cd and Zn, Figures (4.4-4.14). On the other hand, for samples annealed at 300 C the effect is more pronounced, the dark J-V plots were improved by annealing at 300 C. Quenched samples at 300 C gave better dark J-V plots than slowly cooled samples with different ratios of Cd and Zn.

The observed annealing effect on the dark J-V plots of CdS/ZnS films can be explained as follows: enhancement in dark J-V plots is presumably due to increased grain size and enhanced film structure by annealing. Consequently the carrier mobility is enhanced across the crystallite. Annealing may also induce higher thin uniformity by allowing CdS and ZnS to randomly diffuse into quasi-bilayer film. Moreover, annealing presumably increases sintering between crystallites [22]. Thus the grain boundary resistive effect will be lowered. Therefore, intra-and

inter-particle carrier mobility will be enhanced. Furthermore heat treatment increases the adherence of the films to their substrates. Thus annealed films will have lower overall resistance compared to that of untreated films [44-53]. Moreover, annealing leads to phase transition from the metastable cubic phase of CdS/ZnS to the more stable hexagonal phase with much improved crystalline quality. Annealing always favors films with more stable phases. We also assume that the untreated crystallites contain relatively high disorders in the forms of either dislocations or point defects during random growth. Annealing would thus eliminate such disorders yielding more order crystallites. Furthermore, annealing may help remove foreign impurities from the thin films. Combined together, these effects are expected to be responsible for the enhancement of the characteristics of CdS/ZnS thin film electrodes. Heated CdS/ZnS films exhibit lower surface roughness, higher cross linking and larger grain size than untreated counterparts. Convincing evidence to this discussion comes from measured absorption spectra in Figures (4.2, 4.3 and 4.4).

4.4 Effect of Cooling Rate

The photoluminescence (PL) spectra of pure CdS films, slowly cooled from 300 C showed emission band peaking at 570 nm. The film quenched from 300 C, showed emission band peaking at 570 nm with lower intensity. Non-annealed film showed no PL spectra, the energy gap calculated was 2.21 eV.
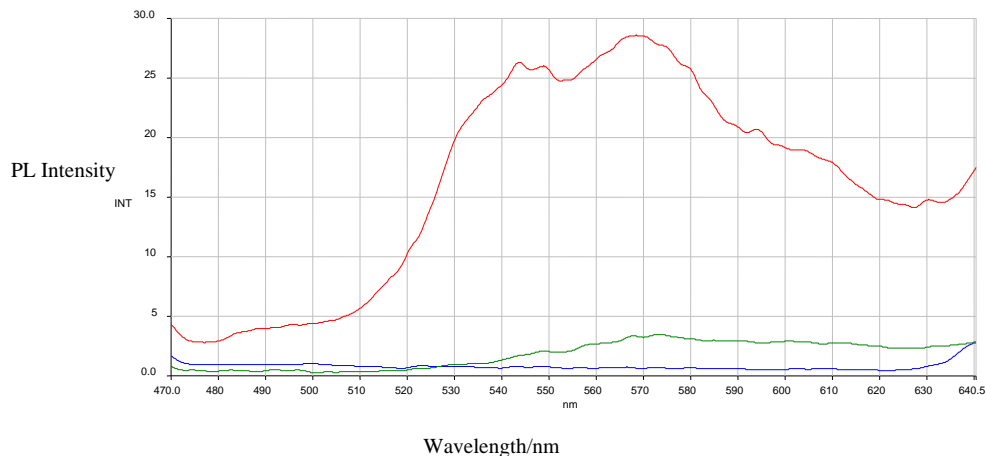
Figure (4.13): PL spectra of CdS thin films excited by λ_{exc}=220 nm at 27 C, three deposition prepared by CBD a) red lion slow cooling from 300 C b) green lion quenching from 300 C c) blue lion non-heating.

The photoluminescence (PL) spectra displayed in Fig. (4.13) reveals four distinct peaks being located at 542 nm, 549 nm, 579 nm and 594 nm. The maximum observed peak was at 579 nm, and it is assumed to represent the energy band gap of the material. In fact, determining the band gap requires the absorption spectra analysis through obtaining the absorption coefficient $\alpha = A/d$, where d is the film thickness.

The absorption coefficient is related to the energy gap through the relation $(\alpha E)^{1/n} = E - E_g$. For ($\alpha > 1000$ cm $^{-1}$) here n =2 for indirect allowed transitions band gap and n = 1/2 for direct allowed transition band gap. E_g is the intercept of the linear plot at the E- axis.

The study of CdS/ZnS electrode surface quality was studied in parallel to electrode PEC characteristics study. Scanning Electron Microscopy (SEM) was used to study the electrode surface quality. While investigating effects of different preparations and treatments on PEC characteristics, effects of such treatment on electrode surface quality (SEM micrographs) were also studied.

Pre-heated CdS/ZnS thin films, show higher quality surfaces than untreated counterparts. This was evident in both quenching and slow cooling processes.

The SEM surface quality results for the untreated CdS/ZnS thin film electrode, Figure (4.14) are rough, with small grain sizes and many islands and aggregates. SEM indicates that CdS/ZnS film surfaces, slowly cooled from 300 C, have smoother surfaces and larger grain size than untreated ones, (Fig.4.15). The grain size was enhanced by treatment. Moreover, quenching of pre-heated samples reduces the surface roughness and increases the grain size, compared to untreated and slowly cooled ones, (Fig.4.16).

SEM results for samples, slowly cooled and quenched, from 300 C are shown in Figures (4.15, 4.16). The quenched sample shows better surface quality than the slowly cooled counterpart, also this sample show large aggregate particles and more homogenous surface. Therefore, SEM results indicate that quenched surface give better CdS/ZnS film surface. Figure (4.15) shows that the CdS/ZnS surface, slowly cooled from 300 C, small aggregate particles more than in quenched sample of CdS/ZnS. SEM results, observed so far, are consistent with J-V plots shown earlier. In each case, the CdS/ZnS thin film electrodes were enhanced by heating. Furthermore, the slowly cooled sample for Cd/Zn 0.08:0.02 showed better J-V plots than their quenched counterparts.
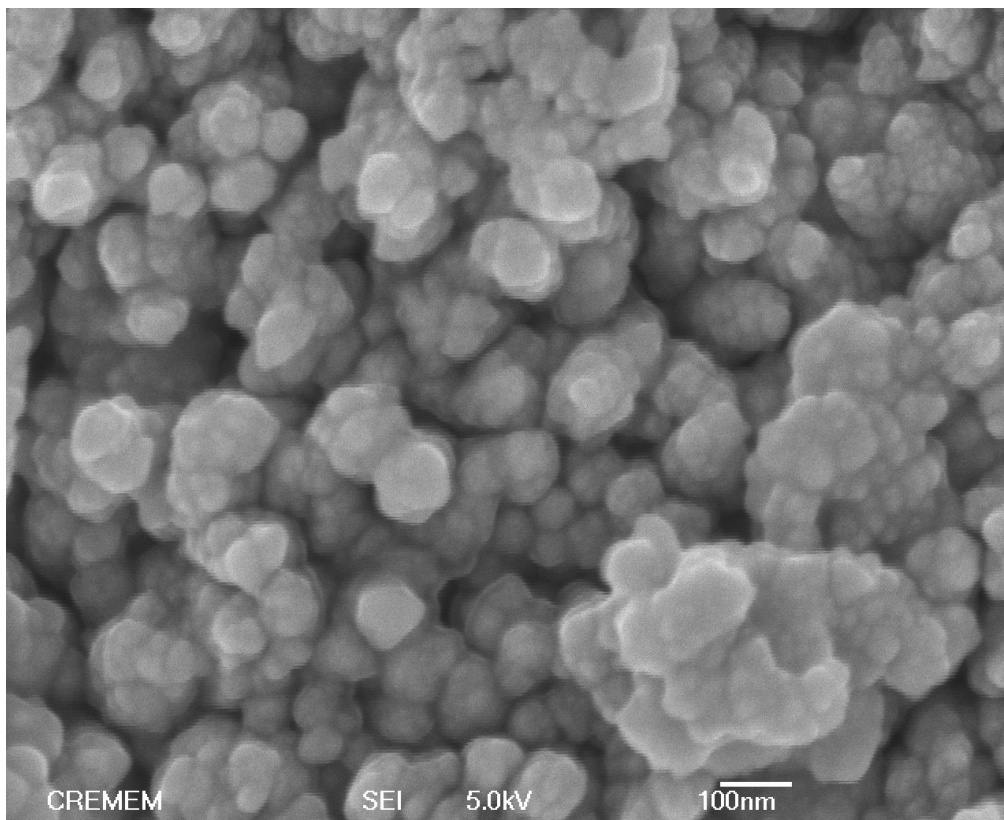
Figure (4.14a): **SEM micrographs of nonannealed CdS/ZnS film prepared from three deposition steps Cd/Zn 0.08:0.02, showing size of particles in nm.**
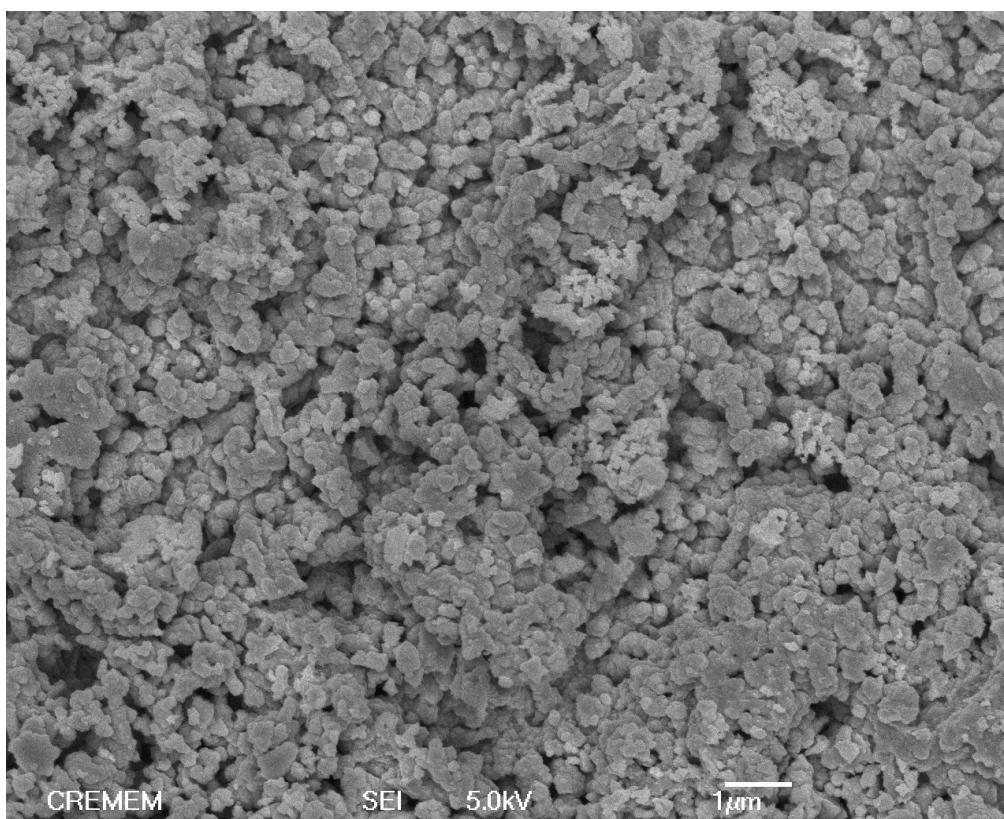
Figure (4.14b): **SEM micrographs of nonannealed CdS/ZnS film prepared from three deposition steps Cd/Zn 0.08:0.02, showing size of particles in μm**
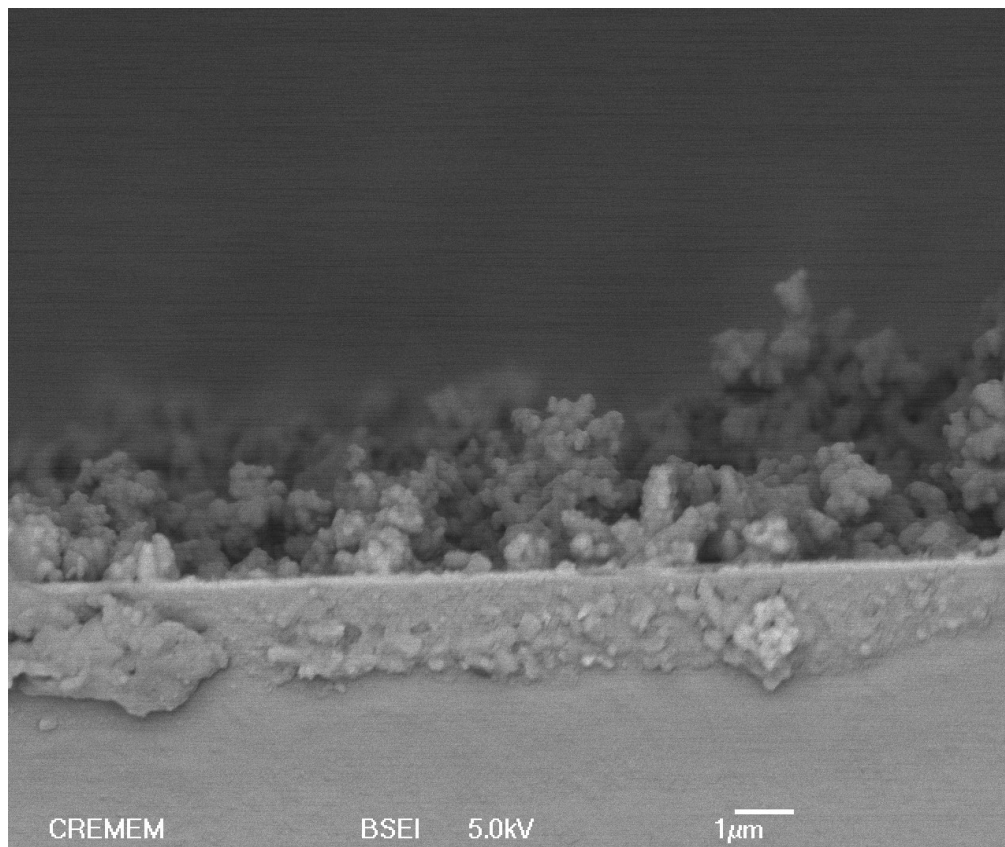
Figure (4.14c): SEM micrographs of nonannealed CdS/ZnS film prepared from three deposition steps Cd/Zn 0.08:0.02, showing side photo of the film in μm, to measure the film thickness. Film thickness was ～2 μm.
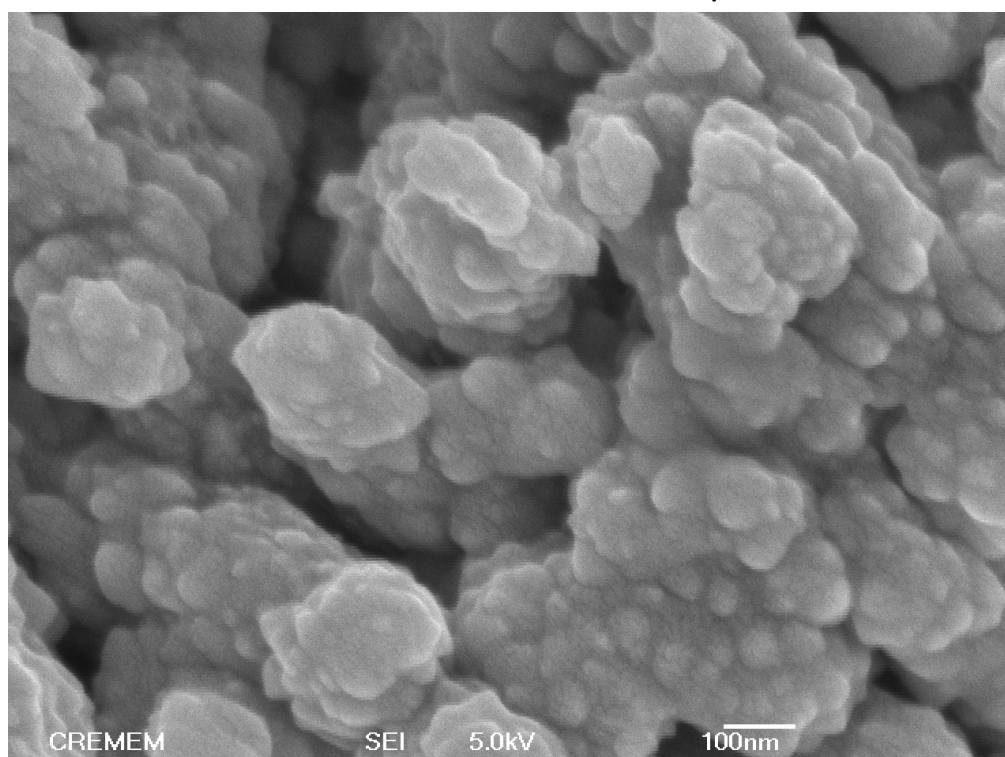
Figure (4.15a): SEM micrographs of slowly cooled from 300 C, CdS/ZnS film prepared from three deposition steps Cd/Zn 0.08:0.02, showing size of particles in nm.
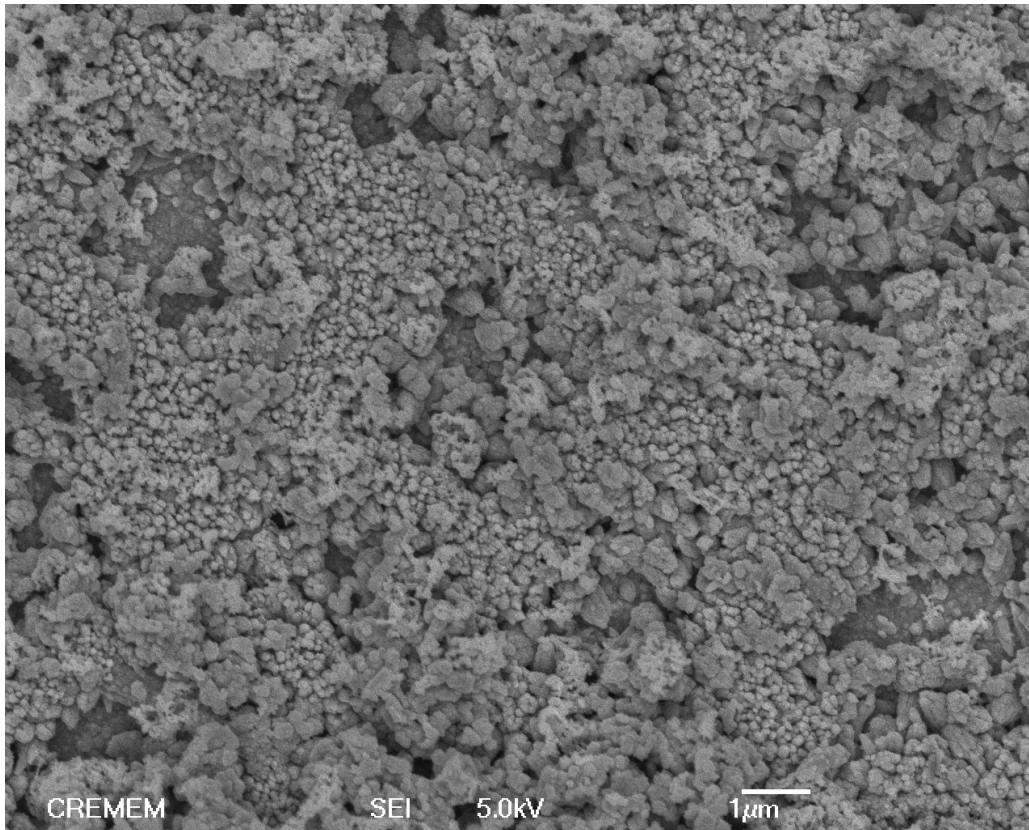
Figure (4.15b): SEM micrographs of slowly cooled from 300 C, CdS/ZnS film prepared from three deposition steps Cd/Zn 0.08:0.02, showing size of particles in µm. Size of particles was ∼200 nm
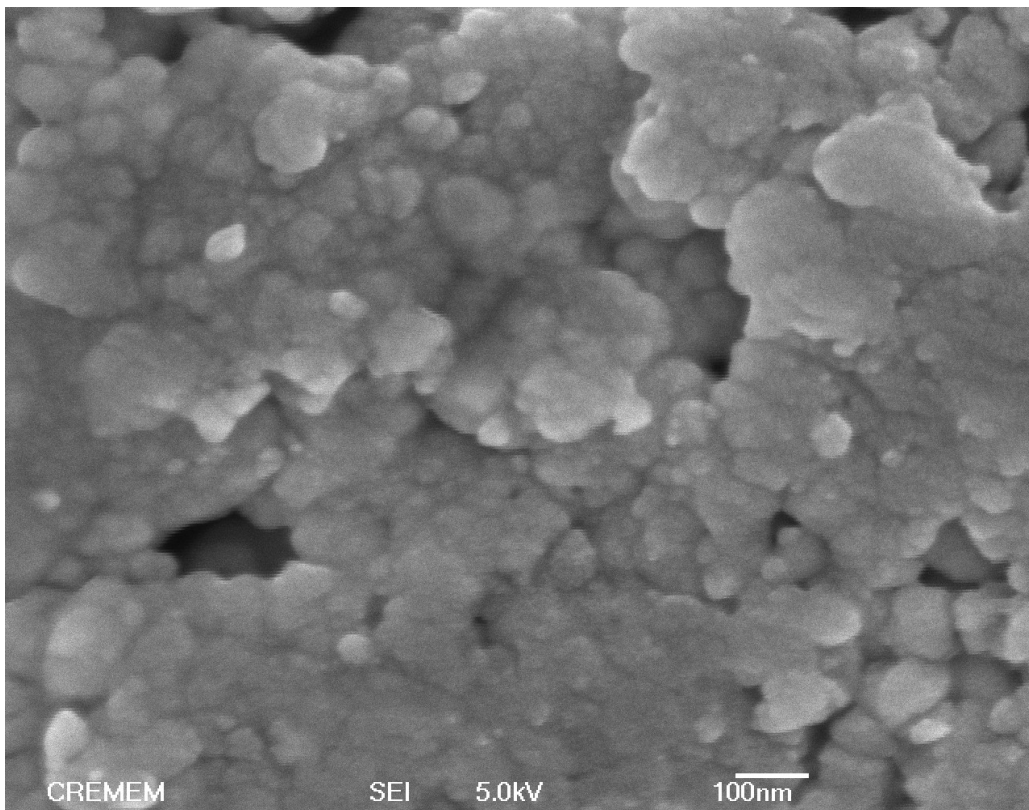
Figure (4.16a): SEM micrographs of quenched from 300 C CdS/ZnS film prepared from three deposition steps Cd/Zn 0.08:0.02, showing size of particles in nm
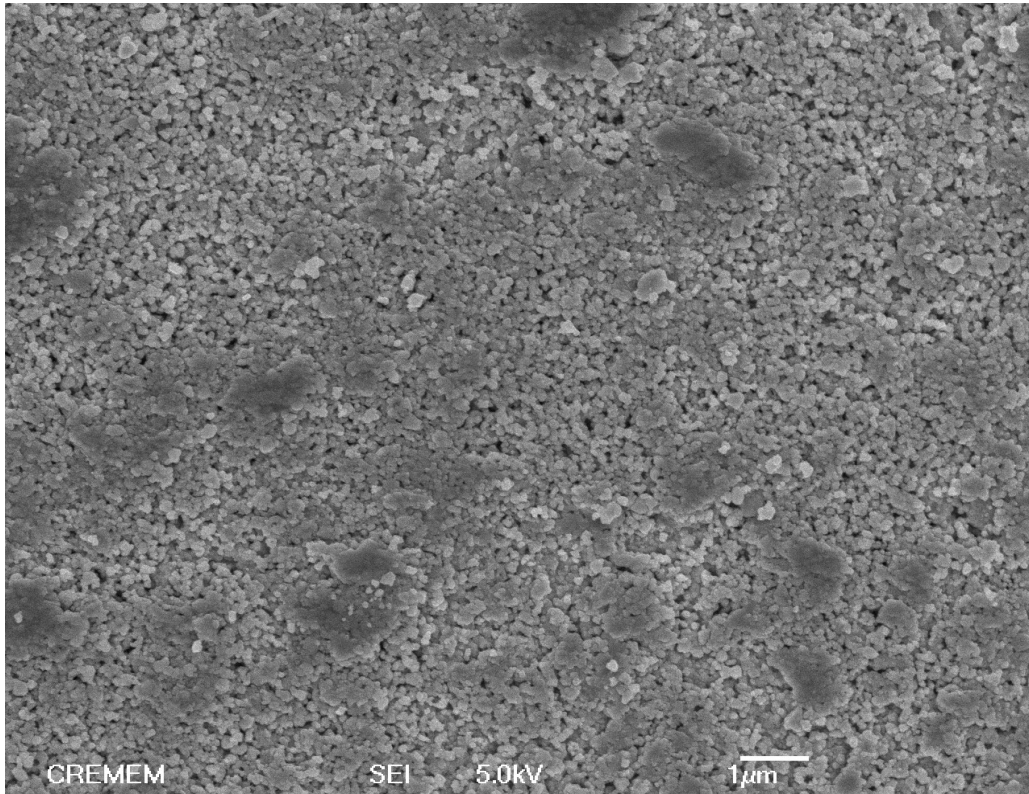
Figure (4.16b): SEM micrographs of quenched from 300 C CdS/ZnS film prepared from three deposition steps Cd/Zn 0.08:0.02, showing size of particles in µm.
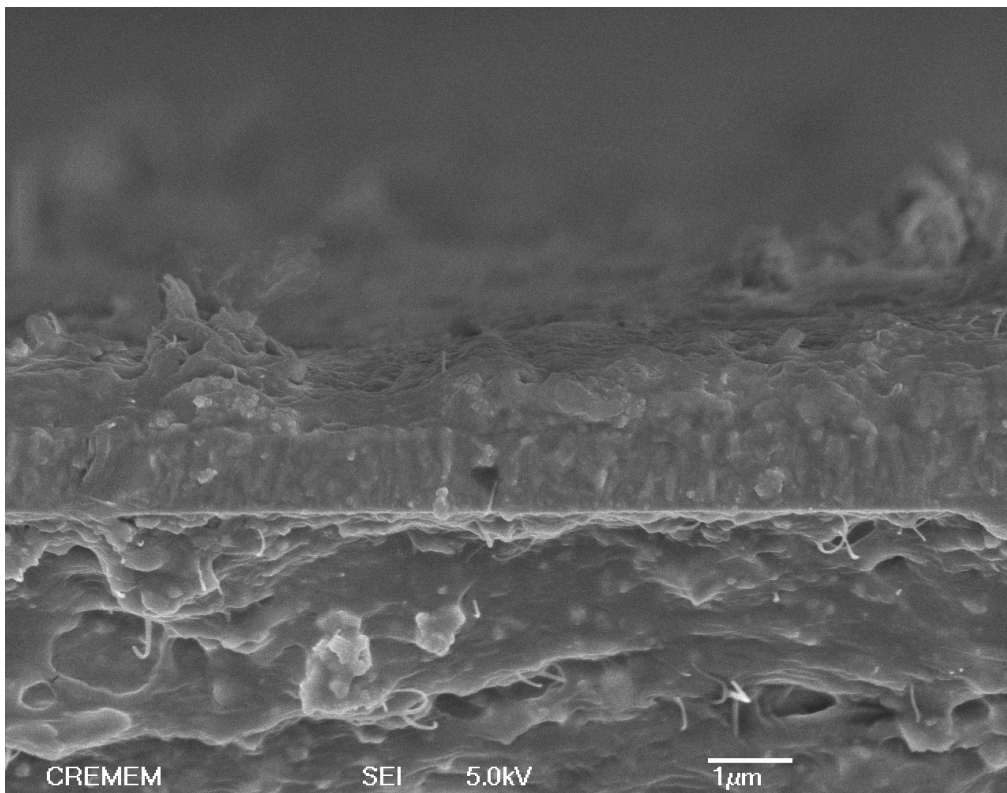
Figure (4.16c): SEM micrographs of quenched from 300 C CdS/ZnS film prepared from three deposition steps Cd/Zn 0.08:0.02, showing side photo of the film in µm. Film thickness was ∼1 µm

The XRD patterns of triply deposited CdS/ZnS films with Cd/Zn 0.08:0.02, are shown in Fig.(4.29). Unheated and slow cooled films from 300 C have the cubic and hexagonal structures. The structure change to cubic when the film was quenched from 300 C. Table (4.1), shows the size of particles from measurements at. The average particle size for non-annealed Cd/Zn 0.08:0.02 film is equal 14 nm. the average particle size for Cd/Zn 0.08:0.02 slowly cooled film is 21.8 nm, and the average particle size of a quenched Cd/Zn 0.08:0.02 quenched film is 16.5 nm. Films with Cd/Zn 0.07:0.03 quenched from 300 C showed 35.25 nm particle sizes.

Table (4.1): XRD calculated particle size for CdS/ZnS films after different treatments

[Zn]	[Cd]	Rate of cooling	2θ	d (nm)
		From 300 C		**Size of particle**
1) 0.02	0.08	quenching	26.5	14.5
			44	12
			54	15.5
2) 0.02	0.08	slow cooling	36	30
			48	20.5
			26.5	15
3) 0.02	0.08	non-heating	44	14
			28	14
			26.5	21
			25	17
4) 0.03	0.07	quenching	26.5	15
			44	11
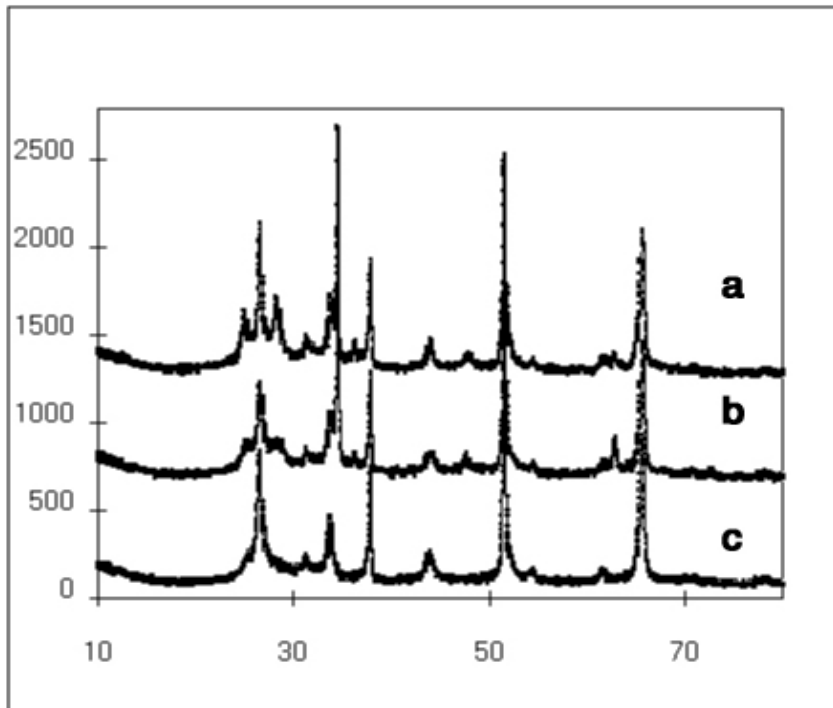
Figure (4.17): XRD patterns for triply deposited CdS/ZnS (Cd/Zn 0.08:0.02) films (a) non-heated (b) slow cooling from 300°C (c) quenched from 300°C.

Table (4.2): XRD powder data results. (analyses of Fig. (4.17)).

2θ	intensity	index
25.14	1590	(100H)
26.60	2145	(002H)
28.46	1678	(101H)
31.48	1467	(110H)
34.40	2113	(210 C- CdS)
36.34	1438	(200H)
37.90	1950	(201H)
44.18	1437	(203H)
48.50	1357	(006H)
51.59	2534	(112H)
54.92	1329	(222 C-CdS)
62.10	1346	(303H)
63.24	1351	(400 C- CdS)
65.68	2100	(215H)
71.66	1290	(312H)
79.08	1282	(109H)

(H) Hexagonal structure

(C) mean Cubic structure

For more information see Appendix A.

The study of photo current J-V plots for slowly cooled and quenched CdS/ZnS electrodes Cd/Zn 0.08:0.02 from 300 C, shows that the slow cooled electrode is better than the quenched as shown in Figure (4.22). The result is consistent dark J-V plots, Figure (4.23). The Figure shows that slow cooling gives higher dark current density than quenching.
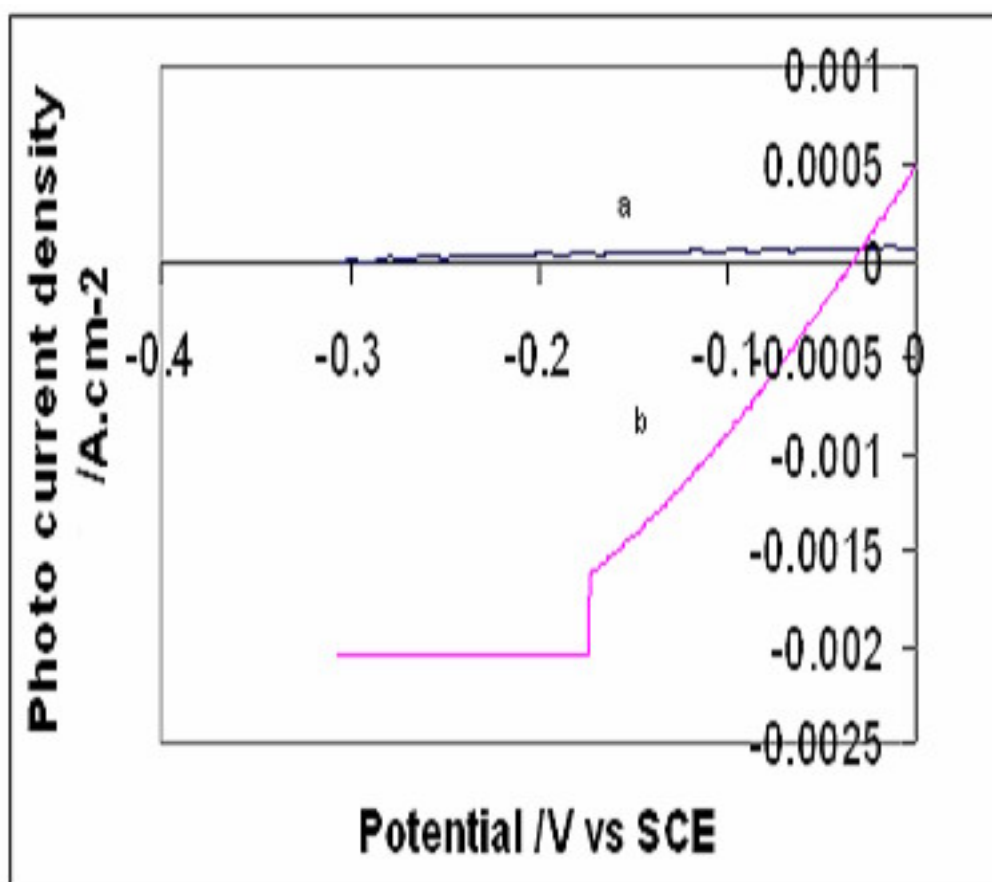
 Figure (4.18): Photo current J-V plots for a) slowly cooled CdS/ZnS electrodes at Cd/Zn 0.08:0.02 from 300 C b) quenched CdS/ZnS electrode at Cd/Zn 0.08:0.02 from 300 C. All measurements were conducted in aqueous LiClO$_4$/K$_4$Fe(CN)$_6$/K$_3$Fe(CN)$_6$ at 25 C.
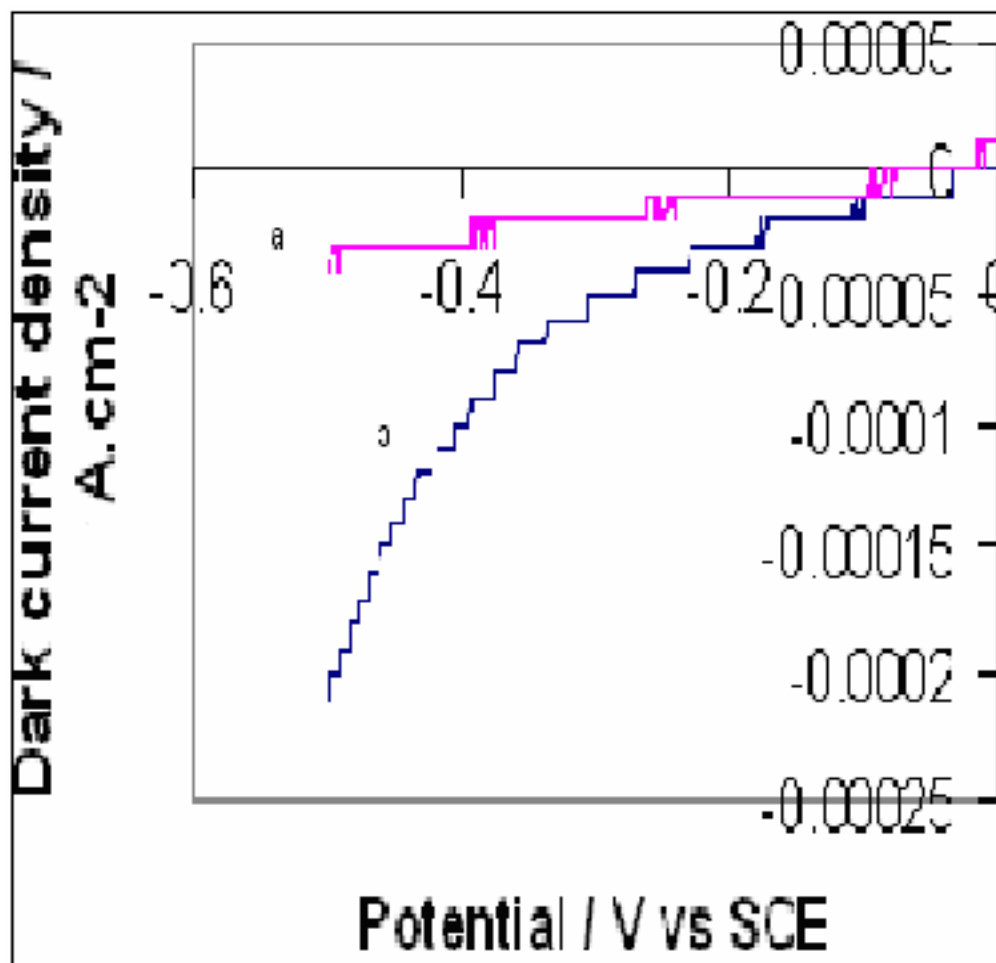
Figure (4.19): Dark current J-V plots for a) quenched, and b) slowly cooled CdS/ZnS electrodes, Cd/Zn 0.08:0.02 from 300 C. All measurements were conducted in aqueous LiClO$_4$/K$_4$Fe(CN)$_6$/K$_3$Fe(CN)$_6$ at 25 C.

Figure (4.20), shows photo current J-V plots for slowly cooled and quenched of CdS/ZnS electrodes with Cd/Zn 0.07:0.03 from 300 C. The figure shows that slowly cooled CdS/ZnS thin film electrode is slightly better than the quenched electrode. On the other hand, quenching gives higher dark current density for slowly cooled electrode, as shown in Figure (4.21). The energy gap for the quenched film is 2.23 eV, as calculated from the optical absorption spectra .
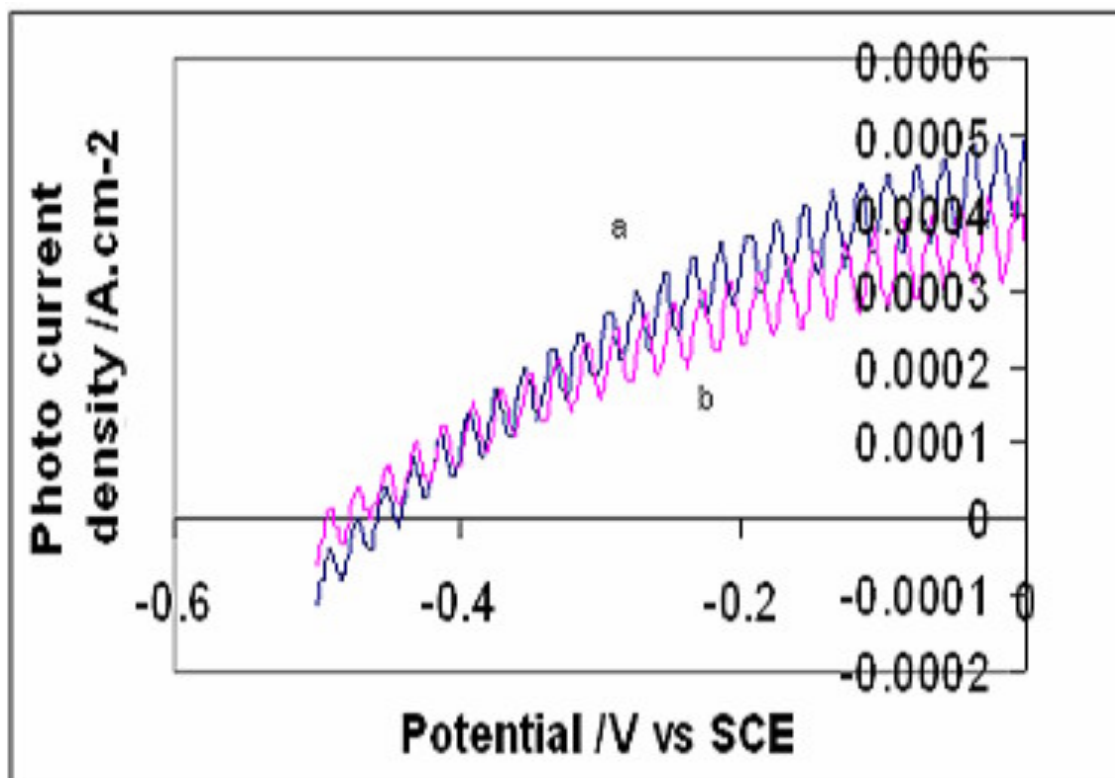
Figure (4.20): Photo current J-V plots for a) slowly cooled CdS/ZnS electrodes at Cd/Zn 0.07:0.03 from 300 C b) quenched CdS/ZnS electrode at Cd/Zn 0.07:0.03 from 300 C. All measurements were conducted in aqueous LiClO$_4$/K$_4$Fe(CN)$_6$/K$_3$Fe(CN)$_6$ at 25 C.
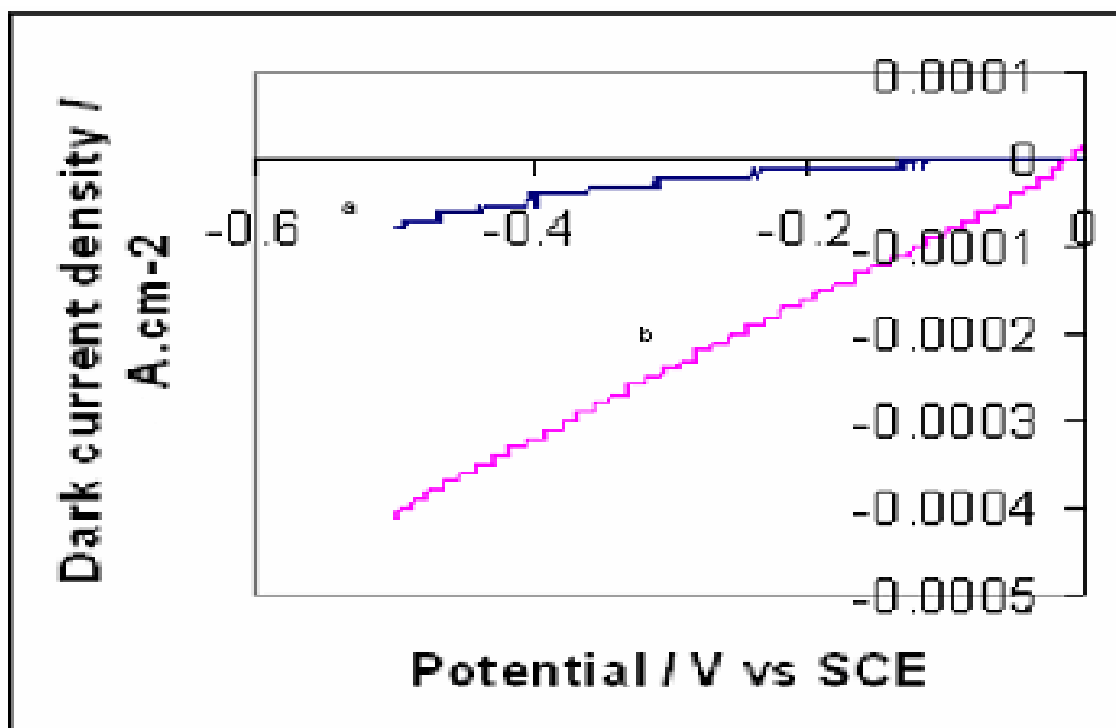
Figure (4.21): Dark current J-V plots for a) quenched, and b) slowly cooled CdS/ZnS electrodes, Cd/Zn 0.07:0.03, from 300 C. All measurements were conducted in aqueous LiClO$_4$/K$_4$Fe(CN)$_6$/K$_3$Fe(CN)$_6$ at 25 C.
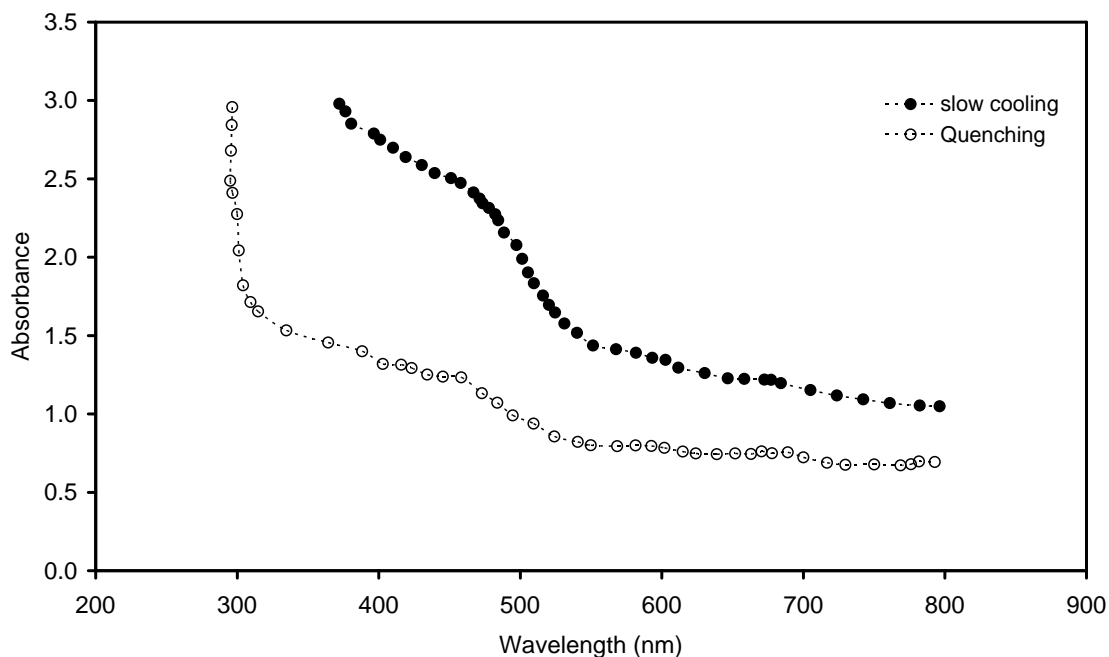
Figure (4.22) The absorbance sprectra for the slowly heated and quenched samples prepared at Cd:Zn ratio of 0.07:0.03.

Figure (4.22) displays the variation of absorbance with cooling technique. As it is clear, there is a particular difference between the slowly cooled and quenched absorbance. The slowly cooled sample reflected higher absorbance with sharp decay as compared to the quenched sample.

Following the same procedure we have previously described, the energy band gap which is presented in Figure (4.23) was found to be 2.21 for the slow cooling and 2.23 eV for the quenching. The difference between both gaps is very slight indicating no gap change by changing the method. The only apparent difference is the absorption level.
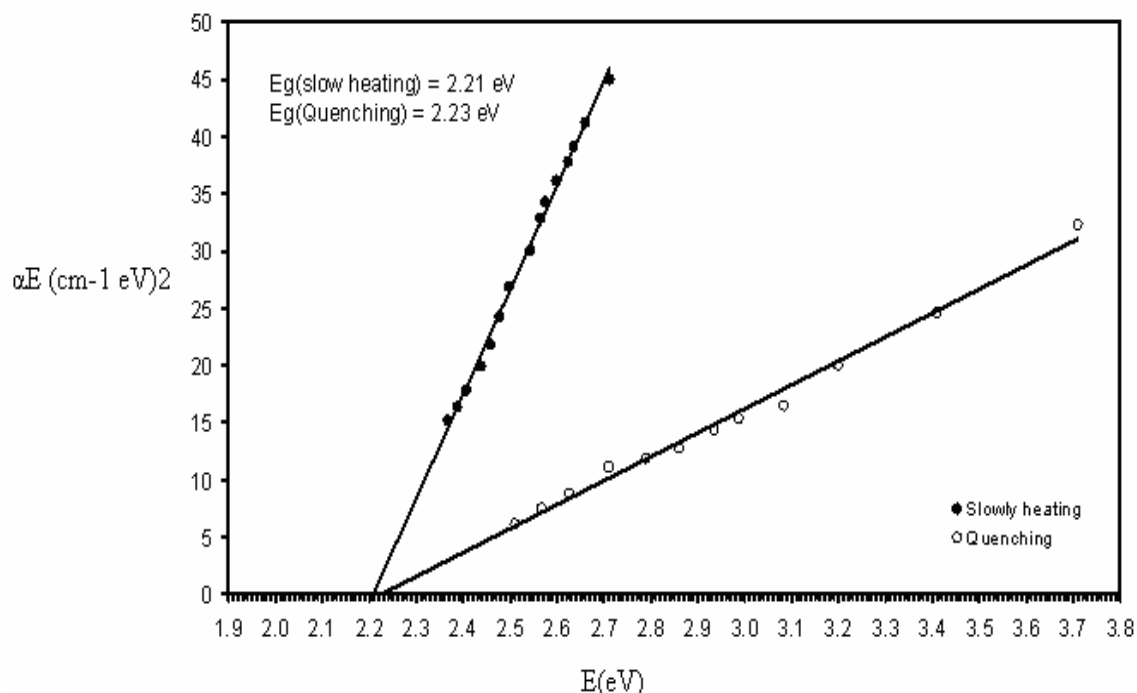
Figure (4.23) the $(\alpha E)^2 - E$ **dependence for slow cooling and quenching from 300** ^0C **at Cd: Zn ratio of 0.07:0.03.**

Cooling rate of pre-heated SC affects its structural quality by improving its parameters. Examples of such parameters are: growth thickness, composition uniformity and luminescence properties. The dislocation density and concentration of structural defects also depend on cooling rate of SC crystal [22].

The heat treatment of CdS/ZnS platelets leads to changes in the native defect concentration and distribution. Such changes depend on both annealing temperature and cooling rate. The uniform film growth of single crystal Si from Cu-Si solution, with constant temperature gradient distribution, at the cooling rate of 0.1 C/s and 0.05 C/s (low cooling rate), was possible [54]. It was found that the formation efficiency of large and loosely bound impurity complexes is very sensitive to the cooling rate and they would successfully form only when the cooling rate is carefully tuned.

Slow cooling of pre-heated monocrystalline SC samples improved their crystallinity by decreasing imperfections, including dislocation density and structural defect concentration [54-58]. Slow cooling also improves composition uniformity and luminescence properties .In this work, it has been found that slow cooling of CdS/ZnS thin film electrodes, when the molar ratio of Cd/Zn (0.07:0.03 and 0.09:0.01), shows better dark J-V plots than heated at 400 C, Figures (4.5, 4.7, 4.9). Slow cooling of CdS/ZnS thin film electrodes, heated at 400 Cwith (Cd/Zn 0.08:0.02 and 0.09:0.01), shows better dark J-V plots than those heated at 300 C, Figures (4.6, 4.8). The improvement of the dark J-V plots, of slowly cooled samples, can be explained.

Annealing thin film electrode sample provides atoms with enough energy to overcome the energy barrier and to move from stable positions to metastable new positions. Therefore heating itself increases structural defect density in the crystal. On cooling, metastable atoms try to move back to their stable positions [65]. Quenched electrodes will partly keep the atoms in their new metastable positions after annealing. Quenching will deprive the metastable atoms from any pathways to return to their stable positions. The defect density in quenched samples will therefore be greater than their slowly cooled counterparts. Slow cooling allows metastable atoms to return to stable positions, and consequently decreases imperfections. Moreover, slow cooling helps remove surface states by improving crystallinity at the surface. Slowly cooled electrodes are thus expected to give better dark J-V plots than quenched counterparts, and this is what we have observed from the results that we obtained in this work.

Photo J-V plots, Figures (4.28, 4.30), show that the slowly cooled CdS/ZnS film electrodes from temperatures 300 C have better photo J-V plots than their quenched counterparts. This result is consistent with the absorption spectra and PL spectra.

4.5 Effect of Modification with MnP/polysiloxane

Photo and dark J-V plots measured for CdS/ZnS film electrodes were improved by MnP/polysiloxan-modification, compared to polysiloxane-modified and non-modified electrodes; this was observed for CdS/ZnS films with different compositions.

However, the photo current J-V plots for naked CdS/ZnS thin film electrodes with Cd/Zn 0.09:0.01 is better than J-V plots for covered electrodes, as shown in Figure (4.24).
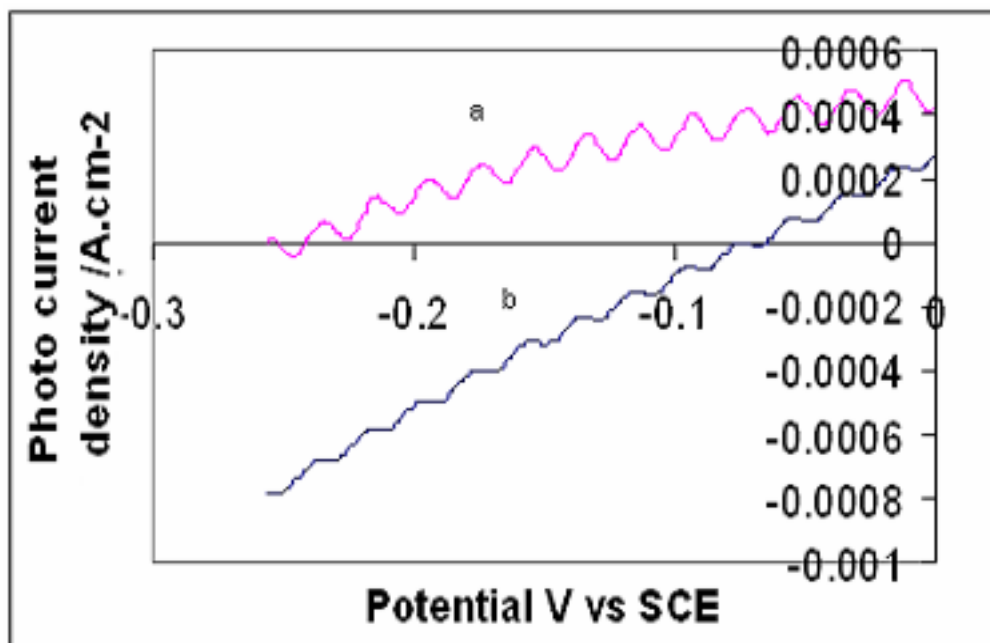
Figure (4.24): Photo current J-V plots for slowly cooled CdS/ZnS film electrodes (with Cd/Zn 0.09:0.01) from 300 C a) naked electrode b) modified with MnP/Polysiloxane. All measurements were conducted in aqueous LiClO$_4$/K$_4$Fe(CN)$_6$/K$_3$Fe(CN)$_6$ at 25 C.

The CdS/ZnS thin film electrodes prepared by three-time depositions were pre-heated to 300 C, and then cooled slowly to room temperature. After that the electrodes covered with MnP/polysiloxane. The naked electrodes showed better dark J-V plots than MnP/polysiloxane modified electrodes at different molar ratio CdS/ZnS, (Fig. 25, 28 and 30).

Figure (4.25), shows Dark current J-V plots for slowly cooled CdS/ZnS electrodes with Cd/Zn 0.09:0.01 from 300 C, to determine the effect of electrode modification with Mn/polysiloxane. The Figure shows that the naked electrode gives higher dark current density than the modified electrode. This result is consistent with photo J-V plot results. Photo J-V plots for naked electrode is better than photo J-V plots for modified electrodes, with Cd/Zn 0.09:0.01, as shown in Figure (4.26).

With Cd/Zn 0.08:0.02 ratio, different results were observed. Photo J-V plots, for modified electrode is better than naked electrode as shown in Figure (4.27). This result is consistent with the dark J-V plots, Figure (4.28).

Figure (4.29), shows photo current J-V plots for CdS/ZnS thin film electrodes which covered with MnP/Polysiloxane and non-covered CdS/ZnS thin film electrodes at Cd/Zn 0.07:0.03, we note from the figure CdS/ZnS thin film electrode J-V plots for non-covered with MnP/Polysiloxane is better than J-V plots for covered electrodes. This result is parallel with the result that we obtained in dark J-V plots, Figure (4.30), shows Dark current J-V plots for slowly cooled CdS/ZnS electrodes

at Cd/Zn 0.07:0.03 from 300 C, to determine the effect of cover electrodes with Mn/polysiloxane, we note from the figure that the non-coverage the electrode with Mn/polysiloxane gives higher dark current density from the cover electrode.
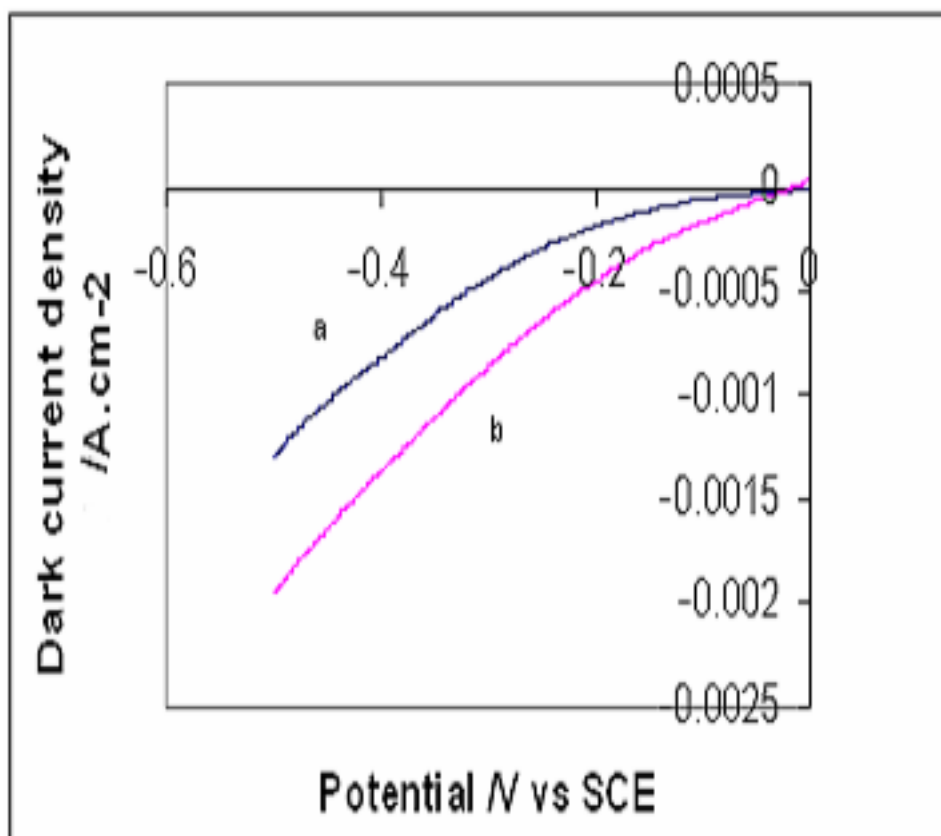
Figure (4.25): Dark current J-V plots for slowly cooled CdS/ZnS electrodes at Cd/Zn 0.09:0.01 from 300 C a) is not modified with Mn/polysiloxane b) modified with MnP/polysiloxane. All measurements were conducted in aqueous LiClO$_4$/K$_4$Fe(CN)$_6$/K$_3$Fe(CN)$_6$ at 25 C.
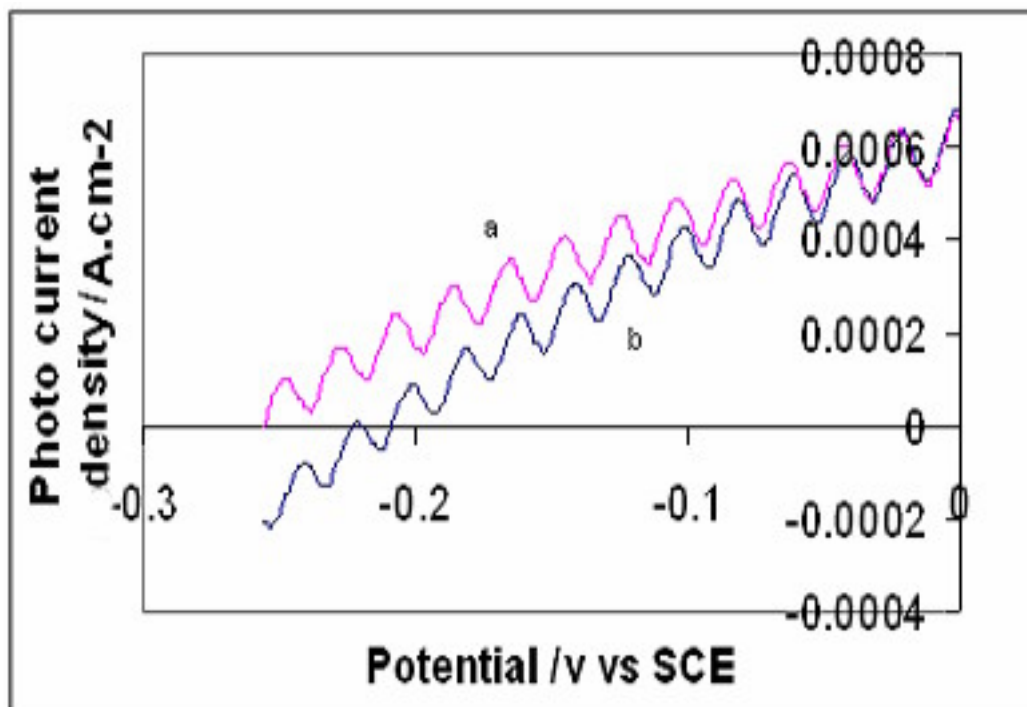
Figure (4.26): Photo current J-V plots for slowly cooled CdS/ZnS electrodes at Cd/Zn 0.09:0.01 from 300 C a) have not been modified with MnP/Polysiloxane b) modified with MnP/Polysiloxane. All measurements were conducted in aqueous LiClO$_4$/K$_4$Fe(CN)$_6$/K$_3$Fe(CN)$_6$ at 25 C.
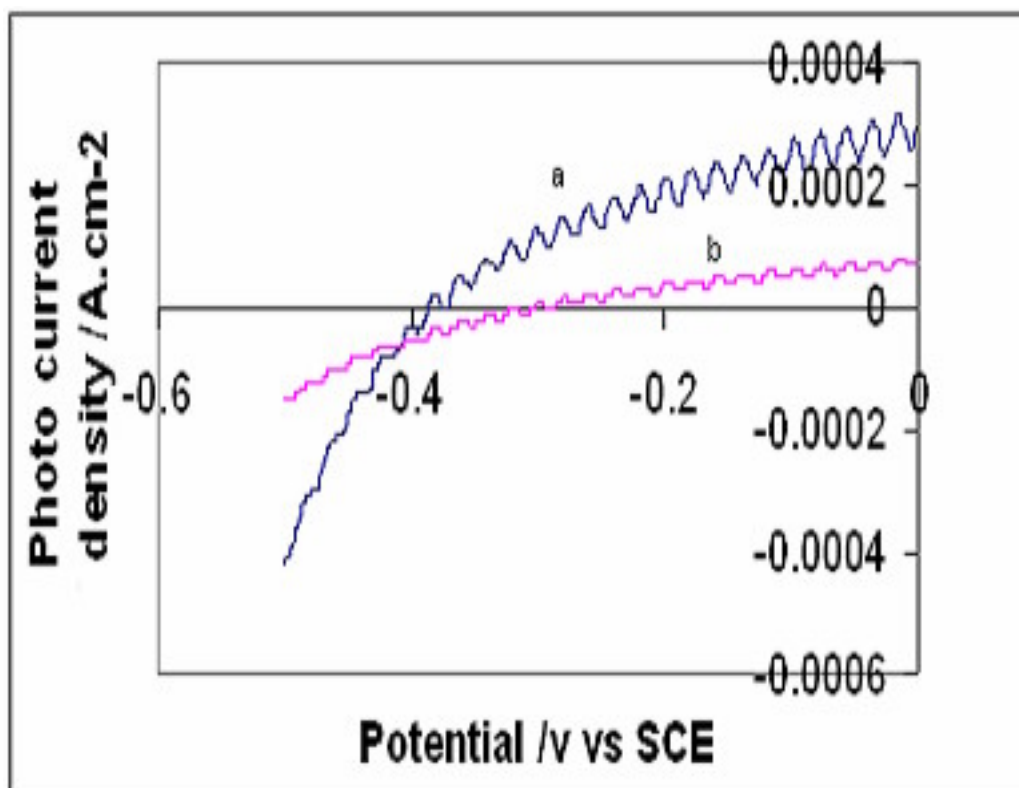
Figure (4.27): Photo current J-V plots for slowly cooled CdS/ZnS electrodes at Cd/Zn 0.08:0.02 from 300 C a) modified with MnP/Polysiloxane b) have not been modified with MnP/Polysiloxane. All measurements were conducted in aqueous LiClO$_4$/K$_4$Fe(CN)$_6$/K$_3$Fe(CN)$_6$ at 25 C.
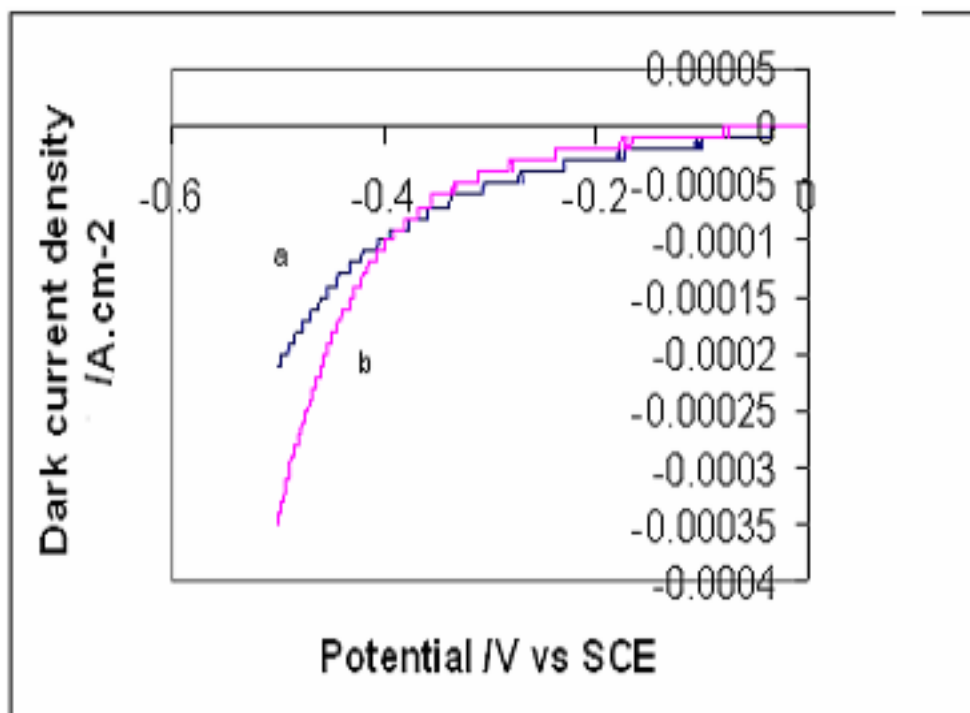
Figure (4.28): Dark current J-V plots for slowly cooled CdS/ZnS electrodes at Cd/Zn 0.08:0.02 from 300 C a) is not modified with Mn/polysiloxane b) modified with MnP/polysiloxane. All measurements were conducted in aqueous LiClO$_4$/K$_4$Fe(CN)$_6$/K$_3$Fe(CN)$_6$ at 25 C.
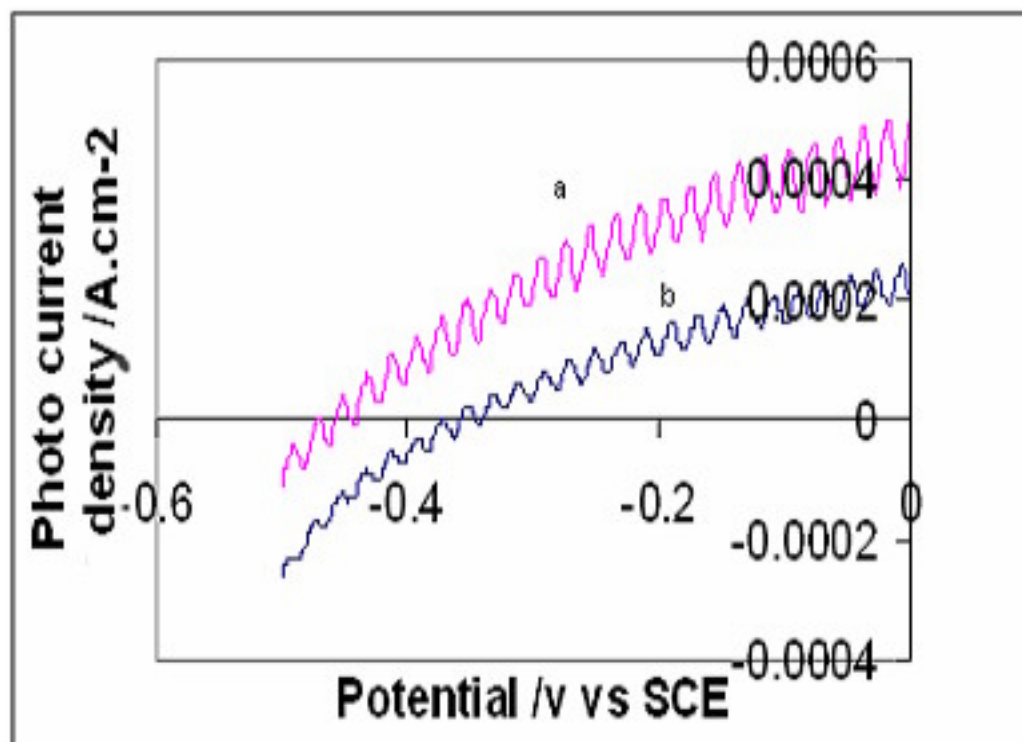
Figure (4.29): Photo current J-V plots for slowly cooled CdS/ZnS electrodes at Cd/Zn 0.07:0.03 from 300 C a) have not been modified with MnP/Polysiloxane b) modified with MnP/Polysiloxane. All measurements were conducted in aqueous LiClO$_4$/K$_4$Fe(CN)$_6$/K$_3$Fe(CN)$_6$ at 25 C.
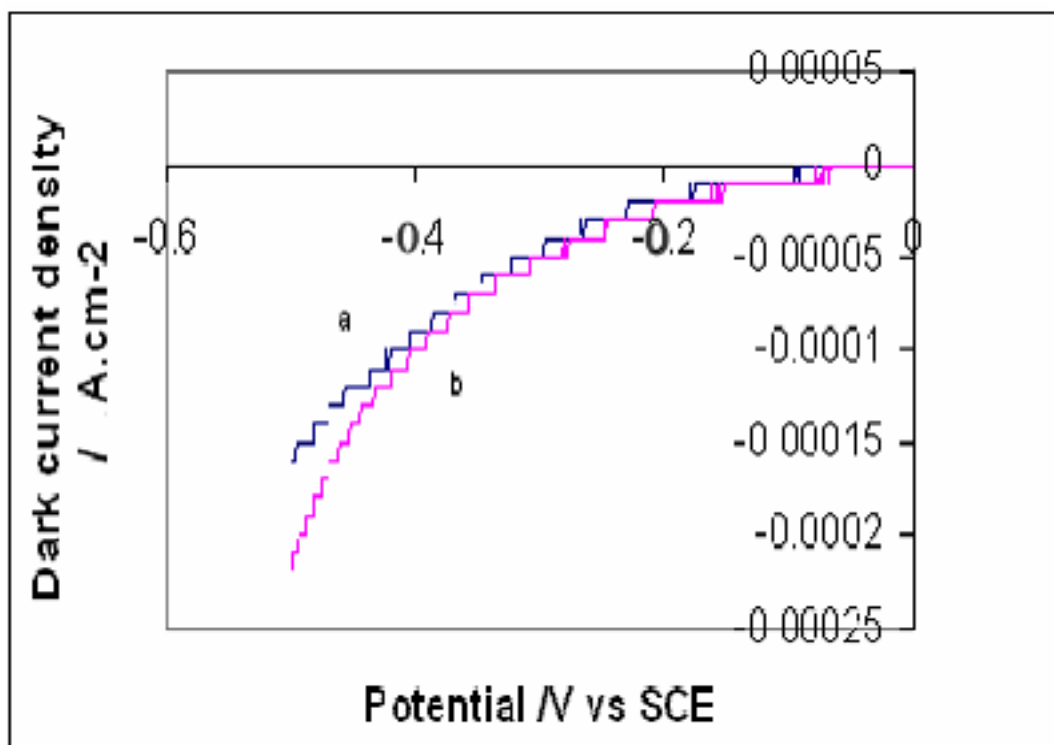
Figure (4.30): Dark current J-V plots for slowly cooled CdS/ZnS electrodes at Cd/Zn 0.07:0.03 from 300 C a) is not modified with Mn/polysiloxane b) modified with MnP/polysiloxane. All measurements were conducted in aqueous LiClO$_4$/K$_4$Fe(CN)$_6$/K$_3$Fe(CN)$_6$ at 25 C.

4.6 Effect of concentration

The effect of concentration on photo and dark J-V plots, photoluminescence (PL), absorbance spectra, and cooling rate have been studied.

Figure (4.31, a-d), shows photoluminescence (PL) spectra of CdS/ZnS thin films slow cooling from 300 C. The Cd/Zn 0.1:0.00 displayed in Figure (4.31, a) give highest intensity emission band at 570 nm, the band gap energy of this thin film electrode was 2.21 eV. The electrode of Cd/Zn 0.09:0.01 shown in Figure (4.31, b), and the band gap energy this film was 2.25 eV and the high intensity emission band at 532 nm. The thin film electrodes for Cd/Zn 0.07:0.03 illustrated in Figure (4.31,

c), the high intensity emission band at 570 nm, the exhibit emission with energy gap was 2.19 eV. The last slide for Cd/Zn 0.08:0.02, this give low intensity, the band peak emission at 533 nm, the band gap energy was 2.35 eV.

Figure (4.32), shows photo J-V plots for CdS/ZnS slowly cooled from 300 C, for different ratios of zinc and cadmium. The Figure shows that, for Cd/Zn 0.07:0.03 best J-V plot was observed. The film with Cd/Zn 0.09:0.01 was second, and the Cd/Zn 0.08:0.02 system, gave low of short circuit current.
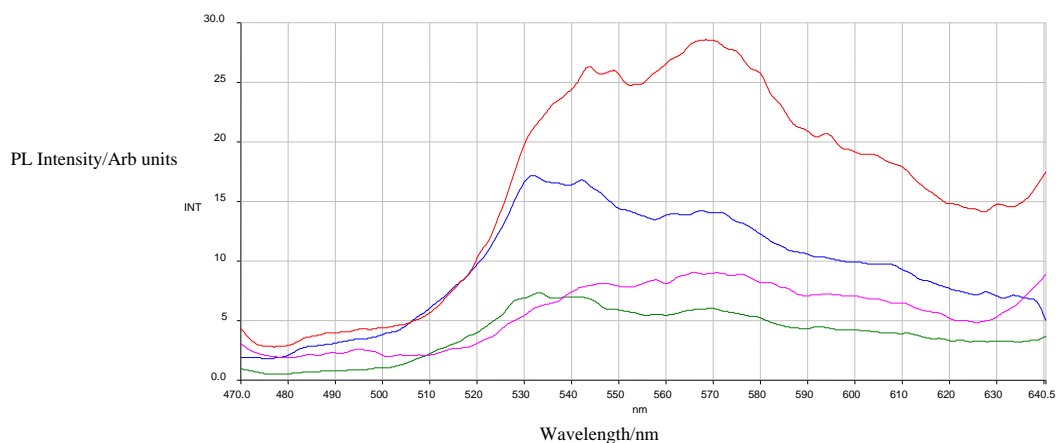
Figure (4.31): PL spectra of CdS thin films excited by λ_{exc}=220 nm at 27 C, three deposition steps prepared by CBD, slow cooling from 300 C a) red lion Cd/Zn 0.10:0.00 b) blue lion Cd/Zn 0.09:0.01 c) pink lion Cd/Zn 0.07:0.03 d) green lion Cd/Zn 0.08:0.02.
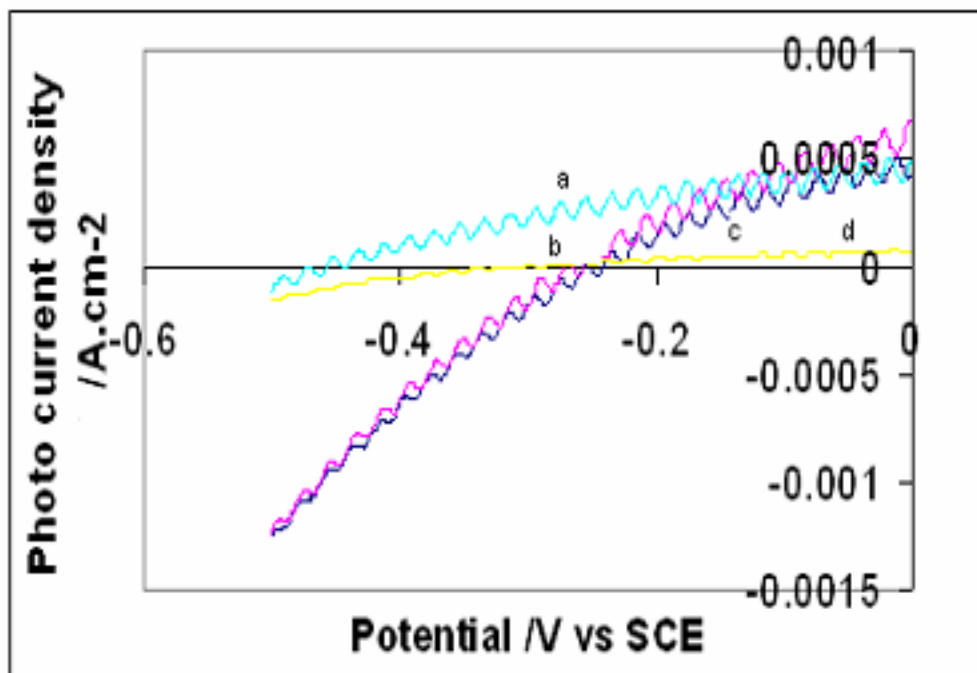
Figure (4.32): Photo J-V plots for CdS/ZnS slowly cooled from 300 C a)Cd/Zn 0.07:0.03 b) Cd/Zn 0.09:0.01 c) Cd/Zn 0.1:0.00 d) Cd/Zn 0.08:0.02. All measurements were conducted in aqueous LiClO$_4$/K$_4$Fe(CN)$_6$/K$_3$Fe(CN)$_6$ at 25 C.

Figure (4.33), shows photoluminescence (PL) spectra for CdS films with different ratios, slowly cooled from 400 C, prepared by CBD. A broad emission band peaking at 532 nm, with Cd/Zn 0.09:0.01. The band gap of this film was 2.3 eV. The electrodes withCd/Zn 0.07:0.03 showed emission band peaking at 554 nm, and band gap was 2.3 eV. The film with Cd/Zn 0.08:0.02 showed a band gap 2.1 eV, and the emission band peaking at 578 nm.
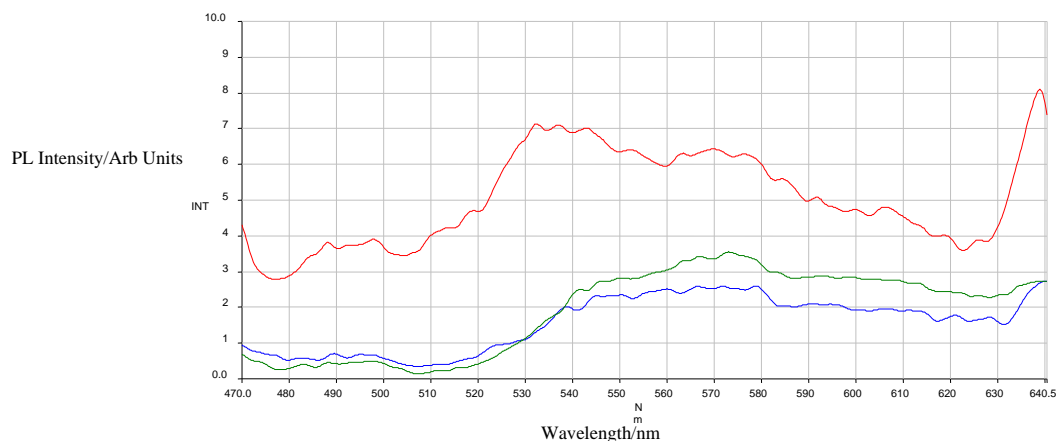
Figure (4.33): PL spectra of CdS/ZnS thin films excited by λexc=220 nm at 27 C, slow cooling from 400 C three deposition prepared by CBD a) red lion Cd/Zn 0.09:0.01 b) green lion Cd/Zn 0.07:0.03 c) blue lion Cd/Zn 0.10:0.00

Figure (4.34), shows photo J-V plots for Mn/polysiloxane modified CdS/ZnS electrodes, slowly cooled from 300 C, with different ratios of CdS/ZnS. The Figure shows that the Cd/Zn 0.07:0.03 ratio gives highest value for photo current density, followed by Cd/Zn 0.08:0.02 ratio and then by Cd/Zn 0.09:0.01 ratio. The least photo current was observed for Cd/Zn 0.10:0.00 ratio.

The Cd/Zn 0.07:0.03 gives highest dark current density followed by Cd/Zn 0.08:0.02 ratio. The lowest value was observed for Cd/Zn 0.09:0.01. Figure (4.35), shows dark J-V plots for Mn/polysiloxane modified CdS/ZnS film electrodes, slowly cooled from 300 C, using different ratio of CdS/ZnS.
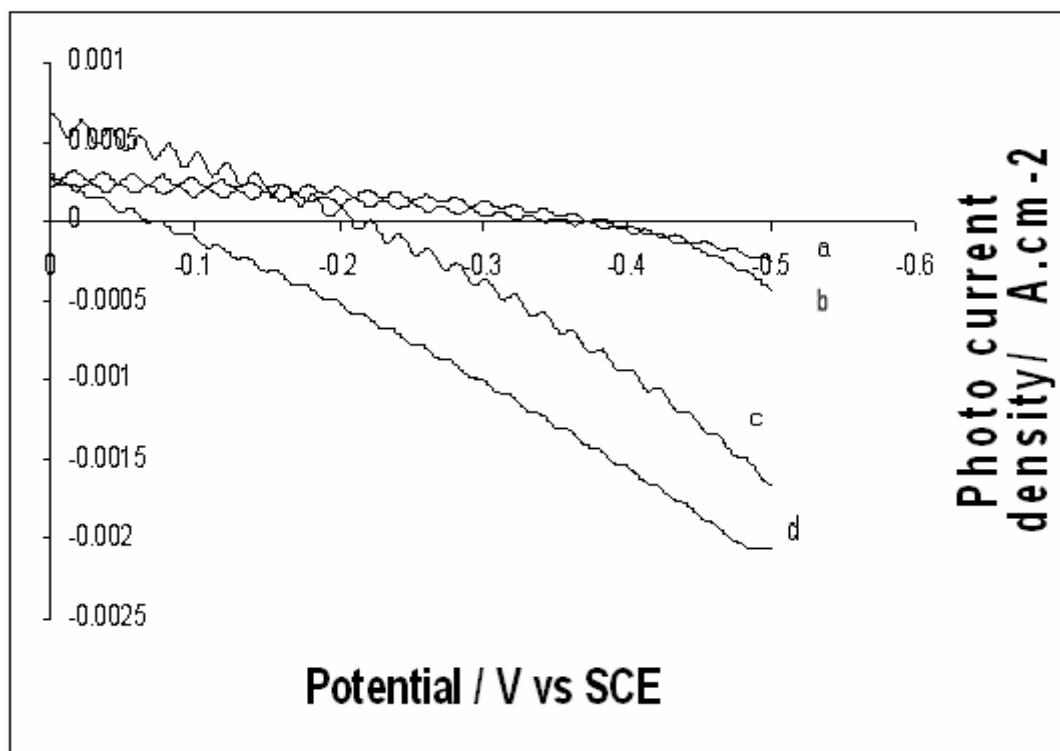
Figure (4.34): Photo J-V plots for CdS/ZnS modified electrodes slowly cooled from 300 C a) Cd/Zn 0.07:0.03 b) Cd/Zn 0.08:0.02 c) Cd/Zn 0.09:0.01 d) Cd/Zn 0.10:0.00. All measurements were conducted in aqueous LiClO$_4$/K$_4$Fe(CN)$_6$/K$_3$Fe(CN)$_6$ at 25 C.
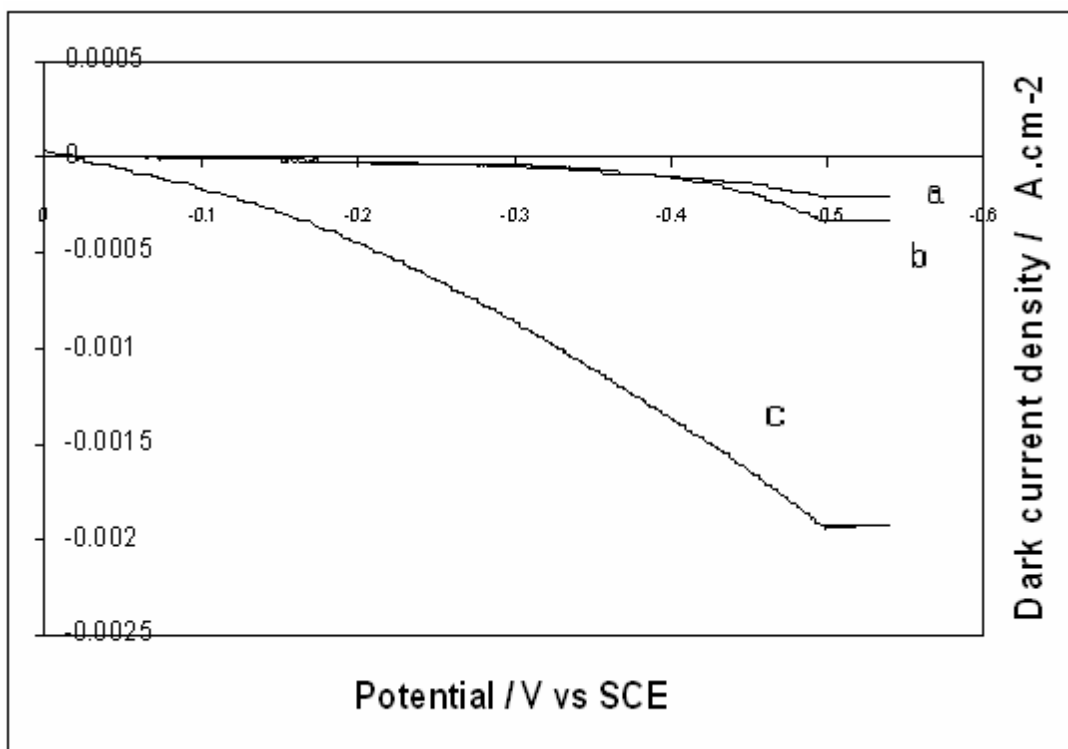
Figure (4.35): Dark J-V plots for CdS/ZnS modified electrodes, and slowly cooled from 300 C, a) Cd/Zn 0.07:0.03 b) Cd/Zn 0.08:0.02 c) Cd/Zn 0.10:0.00. All measurements were conducted in aqueous LiClO$_4$/K$_4$Fe(CN)$_6$/K$_3$Fe(CN)$_6$ at 25 C.

Table (4.3), shows values of J_{sc} and V_{oc} for different CdS/ZnS thin films prepared by three deposition steps with different ratio of CdS and ZnS using $LiClO_4$/$K_3Fe(CN)_6$/$K_4Fe(CN)_6$ as a redox couple. Among the different samples, the Cd/Zn 0.09:0.01 film electrode showed highest short circuit current density J_{sc} value. The Cd/Zn 0.07:0.03 film electrode has highest negative open circuit potential V_{oc} value.

Table (4.3): Values of J_{sc} and V_{oc} for CdS/ZnS film electrodes with different Cd/Zn ratios

Exp. #	[Zn]	[Cd]	Temperature (C)	Time of dep. min)	Number of depositions	J_{sc} (A)	V_{oc} (V)
1	0.00	0.1	70	45	Three	0.00043	-0.241
2	0.01	0.09	70	45	Three	0.00066	-0.256
3	0.02	0.08	70	45	Three	0.00008	-0.318
4	0.03	0.07	70	45	Three	0.0005	-0.445

4.7 Efficiency Studies

The light-to-electricity conversion efficiency of CdS/ZnS thin film electrodes have been enhanced by modification. Values of electrode percentage conversion efficiencies and fill factor values are calculated for different electrodes. Table (4.4), summarizes data on electrode conversion efficiency (μ), V_{oc}, J_{sc} and fill factor (FF). Table (4.4), shows that slow cooling CdS/ZnS thin film electrodes from 300 C gives higher efficiency than slow cooling from 400 C at different ratio of zinc and cadmium. Table (4.5), summarizes data on electrode conversion efficiency (μ), V_{oc}, J_{sc} and fill factor (FF), this table shows that slow cooling of CdS/ZnS electrodes from 300 C without covering with MnP gives higher efficiency than slow cooling of CdS/ZnS electrodes from 300 C covering with MnP.

Table (4.4): Values of μ Voc, Jsc and for FF of CdS/ZnS electrodes.*

Entry Number	Annealing Temp. (C)	[Cd]	[Zn]	Cooling Rate	Vo	Jsc	μ (%)**	FF (%) ***
1	300	0.1	0.00	Slow	-0.241	0.00043	4.722	45.35
2	400	0.1	0.00	Slow	0.00	0.00	0.00	0.00
3	300	0.09	0.01	Slow	-0.256	0.00066	6.11	35.16
4	400	0.09	0.01	Slow	-0.04	0.00024	2.407	24.37
5	300	0.08	0.02	Slow	-0.318	0.00008	0.716	27.36
6	400	0.08	0.02	Slow	-0.205	0.00022	1.403	30.24
7	300	0.07	0.03	Slow	-0.445	0.0005	7.926	34.62
8	400	0.07	0.03	Slow	-0.276	0.00004	0.5679	50.00

* All measurements were conducted in aqueous $LiClO_4/K_3Fe(CN)_6/K_3Fe(CN)_6$ at 25 C.

** μ (%)= [(maximum observed power density)/(reach-in power density)]×100%.

***FF = [(maximum observed power density)/Jsc×Voc] ×100%.

Table (4.5): Values of μ Voc, Jsc and for FF of CdS/ZnS electrodes.*

Entry Number	Annealing Temp. (C)	[Cd]	[Zn]	Cooling Rate	Vo	Jsc	μ (%)**	FF (%) ***
1	300	0.1	0.00	Slow	-0.241	0.00043	4.722	45.35
2	300(MnP)	0.1	0.00	Slow	-0.073	0.00028	0.571	27.15
3	300	0.09	0.01	Slow	-0.256	0.00066	6.110	35.16
4	300(MnP)	0.09	0.01	Slow	-0.220	0.00068	4.644	30.17
5	300	0.08	0.02	Slow	-0.318	0.00008	0.716	27.36
6	300(MnP)	0.08	0.02	Slow	-0.386	0.0003	4.480	37.65
7	300	0.07	0.03	Slow	-0.445	0.0005	7.926	34.62
8	300(MnP)	0.07	0.03	Slow	-0.371	0.00021	3.225	40.24

* All measurements were conducted in aqueous $LiClO_4/K_3Fe(CN)_6/K_3Fe(CN)_6$ at 25 C.

** μ (%)= [(maximum observed power density)/(reach-in power density)]×100%.

***FF = [(maximum observed power density)/Jsc×Voc] ×100%.

In general, pre-heating enhanced electrode efficiency. Annealing of CdS/ZnS thin films at 300 C shows better efficiency than annealing at 400 C. Table (4.4) indicates that electrodes annealed at 300 C give better conversion efficiency and fill factor than those annealed at 400 C. CdS/ZnS films' preheating improves the crystal in many ways. Film quality and performance will presumably be improved. Film resistance and crystal

defects are lowered by treatement. Such improvements in crystal quality would yield enhancement in electrode J-V plots and cell efficiency.

Consistent with earlier results, cooling rates of the preheated CdS/ZnS thin films also affected the CdS/ZnS electrode conversion efficiency. In general, preheating enhances electrode efficiency. However, slow cooling of CdS/ZnS thin films from temperatures 300 C show higher efficiency and higher fill factor values for Cd/Zn 0.07:0.03 than those slowly cooled from 400 C, as shown in Table (4.4). Slow cooling of heated CdS/ZnS thin films improves their crystallinity by affecting their dislocation density and structural defect concentration [73]. Slow cooling also improves composition uniformity and photo luminescence properties.

Conclusions

From the preceding presentation and analysis can be concluded that:

1. Enhancement of dark J-V plots of CdS/ZnS electrodes by annealing depends on the treatment temperature and on rate of cooling.

2. Slowly cooled CdS/ZnS thin film electrodes, heated at 300°C, show higher dark J-V plots than quenching, except for Cd/Zn 0.07:0.03.

3. Slowly cooled CdS/ZnS thin film electrodes, from 300 C with Cd/Zn 0.07:0.03 and 0.09:0.01 ratios, show better dark J-V plots than heated at slowly cooled electrodes from 400 C.

4. Slowly cooled CdS/ZnS thin film electrodes, from 400 C, with Cd/Zn 0.08:0.02 and 0.10:0.00 ratios, show better dark J-V plots than slowly cooled electrodes from 300 C.

5. The naked electrodes showed better dark J-V plots than MnP/polysiloxane modified electrodes with different Cd/Zn ratios except for Cd/Zn 0.08:0.02.

6. The highest PL intensity occurred for Cd/Zn 0.09:0.01 with slow cooling from 400 C. On the other hand, the highest PL intensity occurred for Cd/Zn 0.10:0.00 with slow cooling from 300 C.

7. Scanning electron microscopy (SEM) show enhancements on size and smooth surface with film pre –heating.

8. XRD show unheated and slowly cooled films of Cd/Zn 0.08:0.02 from 300 C have the cubic and hexagonal structures.

Suggestions for Farther Work

For further work, we recommend doing the following:

1) Use annealing at temperatures higher than 400°C and lower than 300°C.

2) Do more study on MnP/polymer film coating with more control of thickness and MnP concentration.

3) Study PH effect, during preparation of CdS/ZnS films, on electrode efficiency, stability and other characteristics.

References

(1) R. A.Serway, **"Physics for Scientists and Engineers with Modern Physics**", 4th ed., (1996), p.1305.

(2) K. Rajeshwar, P. Singh, and J. DuBow, "Energy Conversion in Photoelectrochemical Systems-a ReView", Electrochem. Acta, 23 (1978) 11-17.

(3) Masoud, Muayad Masoud Mahmaoud, "Surface Modification of n-GaAs Semiconductor with Metalloporphyrin/Polysiloxane Matrices, Effect of Modification on: Band-Edge Position, Shoet Circuit Current and Surface Stability in Aqueous Photoelectrochemistry" (Unpublished master's thesis), An-Najah National University, Nablus, Palestine, (2001) p.6.

(4) S. E. Shaheen, D. S. Ginley, and G. E. Jabbour, "Organic-Based Photovoltaics: Toward Low-Cost Power Generation", MRS Bulletin, **30**, (2005), p. 10 date sited, 15/8/2008.www.mrs.org/publications/bulletin

(5) A. J. Nozik, "Photoelectrochemistry: Application to Solar Energy Conversion", *Ann.ReV. Phys. Chem.*, **29** (1978) 189-222.

(6) B. Finnstr m, "Solar Energy-Photochemical Processes Available for Energy Convarsion", vol. 14,ed., S. Claesson and B. Holmstr m, National Swedish Board for Energy Source DeVelopment, (1982), pp. 56-64.

(7) R. de Boer, "Technologies and Prospects for Photochemical Conversion and Storage of Solar Energy: A survey of the state-of-the-art", ed., *ECN-C—01-029* (2001), P.15.

(www.ecn.nl/docs/library/report/2001/c01029.pdf) date sited,3/5/2008.

(8) H. O. Finklea, "Semiconductor Electrode", ed. H. O. Finklea, ElseVier, Amsterdam, (1988), pp.18-22.

(9) H. O. Finklea, "Semiconductor Electrode", ed. H. O. Finklea, ElseVier, Amsterdam, (1988), p.7.

(10) F. R. Fan, G. Keil, and A. J. Bard, *J. Am. Chem. Soc.*, **105** (1983) 220.

(11) T. Bergene, "Trapping of Minority Charge at Irradiated Semiconductor /Electrolyte Hetrojunctions', Int., *J. Hydrogen Energy*, **20** (1995) 785-788.

(12) W. A. Badawy, "Improved n-Si/Oxide Junctions for Environmentally Safe Solar Energy Conversion", *Sol. Energ. Mat. Sol. C*, **71** (2002) 281-294.

(13) H. S. Hilal, S. Shakhshir, and M.M. Masoud, "Metalloporphyrin/Polysiloxane Modified n-GaAs Surfaces: Effect on Photoelectrochemical Efficiency and Surface Stability", *J. Electronal. Chem.*, **527** (2002) 47-58.

(14) H. S. Hilal, W. M. Ateereh, T. Al-Tel, R. Shubeita, I. Saadeddin, and G. Campet, "Enhancement of n-GaAs Characteristics By

Combined Heating, Cooling Rate and Metalloporphyrin Modification Techniques", *Solid*. *State.Sci*, **6** (2004) 139-146.

(15) N. S, Lewis, "Frontier of Research In Electrochemical Solar Energy Conversion", *J. Electronal. Chem.*, **508** (2001) 1-10.

(16) J. Basu, K. K. Rontagi Mukherjee, and B. B. Bhowmick, "Modification of Electrode Surfaces for Improved Photoelectrochemical Characteristics", *Sol. Energ. Mat. Sol. C*, **39** (1995) 39-47.

(17) R. Tenne, and G. Hodes, "Improved Efficiency of CdSe Photoanodes by Photoelectrochemical Etching", *App. Phys. Let.,* **37** (1980) 428-430.

(18) N. Müller, and R. Tenne, "The Effect of Photoelectrochemical Etching on the Performance of CdTe Polysulfide Photoelectrochemical Cells", *Appl. Phys. Let.,* **39** (1981) 285-286.

(19) S. Licht, "Electrolyte Modified Photoelectrochemical Solar Cells", *Sol. Energ. Mat. Sol. C,* **38** (1995) 305-319.

(20) S. Chandra, "Photoelectrochemical Solar Cell", Gordon and Breach Science Publisher, New York, (1986), pp. 158-160.

(21) Rania M. A Ismail, "Enhancement of PhotoelectroChemical Characteristics of CdS Thin Film Electrodes Prepared by Chemical Bath Deposition: Effect of annealing and Rate of Cooling" (master thesis), An-Najah National University, Nablus, Palestine, (2008).

(22) V. D. Das, J. Sathyanarayanan, and L. Damodare, "Effect of Annealing and Surface Treatment on the Efficincy of Photoelectrochemical (PEC) Solar Cells with Vacuum-Deposited n-InSe Thin Film Electrode", *Surf. Coat. Technol.,* **94-95** (1997) 669-671.

(23) S. Chandra, "Photoelectrochemical Solar Cell", Gordon and Breach Science Publisher, New York, (1986), p. 140.

(24) L. I. Maissal, and R. Clang, "Handbook of Thin film Technology", ed McGraw-Hill, (1970) New York.

(25) J. L. Vossen, and W. Kern, "Thin Film Processes", ed. Academic Press, (1978) New York.

(26) R. F. Bunshah, "Deposition Technologies for Films and Coatings: deVelopments and Applications", Noyes Publications, Park Ridge, (1982) NJ.

(27) S. K. Ghandhi, "VLSI Fabrication Principles", John Wiley & Sons, (1983 New York.

(28) K. Seshan, "Handbook of Thin-film Deposition Processes and Techniques: Principles, Methods, Equipment and Applications", 2nd ed., Noyes Publications/William Andrew Publishing, (2002), pp. 15.

(29) S. Tiwaria, and S. Tiwaria, "DeVelopment of CdS Based Stable Thin Film Photoelectrochemical Solar Cells", *Sol. Energ. Mat. Sol. C* **90** (2006) 1621-1628.

(30) J. P. Enr quez, X. Mathew, "Influence of the Thickness on Structural, Optical and Electrical Properties of Chemical Bath Deposited CdS Thin Films", *Sol. Energ. Mat. Sol. C,* **76** (2003) 313-322.

(31) T. Pisarkiewicz, E. Schabowska-Osiowska, and E. Kusior, "Cadmium Sulfide Thin Films Manufactured By Chemical Bath Deposition Method", *Journal of Wide Bandgap Materials*, **9** (2001) 127-132.

(32) Isaiah, Oladeji, and LeeChow, "Optimization of Chemical Bath Deposited cadmium Sulfide Thin Films", *J. Electrochem. Soc.,* **144** (1997) 2343-2346.

(33) J. Aguilar-Hern ndez, J. Sastre- Hern ndez, N. Ximello-Quiebras, R. Mendoza-Pérez, O. Vigil-Gal n, G. Contreras-Puente, and M. C rdenas-Garc a, "Influence of the S/Cd ratio on the Luminescent Properties of Chemical Bath Deposited CdS Films, *Sol. Energ. Mat. Sol. C,* **90** (2006) 2305-2311.

(34) K. Zweibel, "Thin Films: Past, Present, Future", *National Renewable Energy Laboratory*, **3** (1995).

(35) S. Wagner and D. E. Carlson, 'Amorphous silicon solar cells', *10th E.C. Photovoltaic Solar Energy Conference*, pp. 1179-1183, Kluwer Academic, Dordrecht, 1991.

(36) H. Wiesman, A. K. Ghosh, T. McMahon and M. Strongin, 'a-Si: H produced by high temperature thermal decomposition of silane', *J. Appl. Phys.*, **50**(5), 3752-3754 (1979).

(37) H. Matsumura, 'Catalytic chemical vapor deposition (CTL-CVD) method producing higher quality hydrogenated amorphous silicon', *Jpn. J. Appl. Phys.*, **25**(2), L949-L951 (1986).

(38) J. Doyle, R. Robertson, G. H. Lin, M. Z.He and A. Gallagher, 'Production of high quality amorphous silicon films by eVaporative silane surface decomposition', *J. Appl. Phys.*, **64**(6), 3215-3223 (1988).

(39) E.A. Alsema and B.C.W. van Engelenburg, 'Environmental risks of CdTe and CIS solar cell modules', *11th European Solar Energy Conference*, Montreux, 12-16 1992.

(40) W.K. Tolley and G.R. Palmer, 'Recovering cadmium and tellurium from CdTe manufacturing scrap', *1991 AIME Annual Meeting*, New Orleans, LA, February 1991, Bureau of Mines, Salt Lake City, Utah, 1991.

date sited, 15/2/2009   www.nrel.gov/ncpv/documents/thinfilm.html

(41) O. Vigil-Gal n, A. Morales-AceVedo, F. Cruz-Gandarilla, and M.G. Jiménez-Escamilla, "Characterization of CBD-CdS Layers with Different S/Cd Ratios in the Chemical Bath and Their Relation with the Efficiency of CdS/CdTe Solar Cells", *Thin Solid Films*, **515** (2007) 6085-6088.

(42) J. N. Ximello-Quiebrasa, G. Contreras-Puentea, J. Aguilar-Hern!andeza, G. Santana-Rodriguezb, and A. Arias-Carbajal Readigosb, "Physical Properties of Chemical Bath Deposited CdS Thin Film, *Sol. Energ. Mat. Sol. C,* **82** (2004) 263-268.

(43) P. Roy, S. K. Srivastava, "A New Approach towards the Growth of Cadmium Sulphide Thin Film by CBD Method and Its Characterization", *Mat. Chem. Phys.,* **95** (2006) 235-241.

(44) K. V. ZinovieV, and O. Zelaya-Angel, "Influence of low temperature thermal annealing on the dark resistivity of chemical bath deposited CdS films", *Mat. Chem. Phys.,* **70** (2001) 100-102.

(45) B. J. Clar, T. frost, and M. A. Russell, "U.V. Spectroscopy", Chapman & Hall, London (1993) pp. 18-21.

(46) Van Vlack, L. H., "Elements of Material Science and Engineering", 4th ed. Addison-Wesley Publishing Company, Inc., Readig, (1980) p. 109.

(47) N. Gaewdang, T. Gaewdang and W. Lipar, "Some Characterization of Chemical Bath Co-Deposited CdS-ZnS Thin Films", Technical Digest of the International PVSEC-14, Bangkok, Thailand, 2004.

(48) Singh, R., Fakhruddin, M. and Poole, K.F. "Rapid Photothermal processing as a semiconductor manufacturing technology for 21st century" *Appl. Surf. Sci.*, **168** (2000) 198-203.

(49) J. Song, S.S. Li, S.Yoon, V. Craciun, W.K. Kim, T.J. Anderson, O.D. Crisalle, and F. Ren, "Groth and Characterization of $Zn_xCd_{1-x}S$ Buffer Layers by Chemical Bath Deposition", NCPV and Solar Program ReView Meeting 2004.

(50) H. El Malikia, J. C. Bernédea, S. Marsillaca, J. Pinelb, X. Castelb, and J. Pouzeta, "Study of the influence of annealing on the properties of CBD- CdS thin films", *Appl. Surf. Sci.*, **205** (2003) 65-79.

(51) R. Lozada-Morales, O. Zelaya-Angel, and G. Torres-Delgado, "Photoluminescence in cubic and hexagonal CdS films", *Appl. Surf. Sci*., **175-176** (2001) 562-566.

(52) K.V. ZinovieV, O. Zelaya-Angel,"Influence of low temperature thermal annealing on the dark resistivity of chemical bath deposited CdS films", *Mat. Chem. Phys.*, **70** (2001) 100-102.

(53) E. Cetin rgü, C. Gümüş, and R. Esen, "Effects of deposition time and temperature on the optical properties of air-annealed chemical bath deposited CdS films", *Thin Solid Films*, **515** (2006) 1688-1693.

(54) S. Mishra, A. Ingale, U.N. Roy, and A. Gupta, "Study of annealing-induced changes in CdS thin films using X-ray diffraction and Raman spectroscopy", *Thin Solid Films*, **516** (2007) 91-98.

(55) H. Metina, R. Esenb, "Annealing studies on CBD grown CdS thin films", *J. Cryst. Growth*, **258** (2003) 141-148.

(56) A. S. N. MURTHY and K. S. REDDY, "Photoelectrochemical Studies on Poly crystalline CdS (Chemical Bath Deposition) and CdSe (Chemical Bath and Electrodeposition) Thin Film Electrodes", *J. Power Sources*, **13** (1984) 159-167.

(57) Fumitaka Goto, Katsuonori Shirai, Masaya Ichimura, "Defect reduction in electrochemically deposited CdS thin films by annealing in O2", *Sol. Energ. Mat. Sol. C*, **50** (1998) 147-153.

(58) C. Guillén, M. A. Mart Anez, J. Herrero, "Accurate control of thin film CdS growth process by adjusting the chemical bath deposition parameters", *Thin Solid Films*, **335** (1998) 37-42.

(59) Huimin Jia, Yan Hu, Yiwen Tang, Lizhi Zhang,"Synthesis and photoelectrochemical behavior of nanocrystalline CdS film electrodes", *Electrochem. Commun.*, **8** (2006) 1381-1385.

(60) M. H. Christmann, G. H. Dierssen, O. N. Salmon, A.L. Taylor and W. H. Thom, "Native Defect Changes In CdS Single Crystal Platelets Induced By Vacuum Heat Treatments At Temperature up to 600°C", *J. Phys. Chem. Solids*, **36** (1975) 1371-1374.

(61) Y. Nishijmi, K. Makajima, K. Ostubo, and H Ishikama, "InGaAs Single Crystal with a Uniform Composition in the Growth Direction Method", *J. Cryst. Growth*, **208** (2000) 171-178.

(62) M. A. Kulakov, H. Hoster, Z. Zhang, and B. Bullemer, "Cooling Rate Determination of Si Samples in a Radiative Quench and Observation of an Apparent temperature Shift Of The 1x1-7x7 Surface Phase Transition", *Appl.Surf. Sci.*, **376** (1997) L414-L418.

(63) M. K. Lee, Y. C. Teseng, and C. H.Chu, "A High-Gain Porous Silicon Metal-Semiconductor-Metal Photodetector through Rapid Thermal Oxidation and Rapid Thermal Annealing", *Appl. Phys. A.*, **67** (1998) 541-543.

(64) T. Miyazaki and S. Yamasaki, "Effect of Rapid Sample Cooling on Efficincy of Multiple Impurity-Atom Doping", *Diam. Relat. Mater.,* **14** (2005) 2039-2042.

(65) T. Watanabe, A. Fujishima and K. Honda, "Energy Resources through Photochemistry and Catalysis", ed., M. Gratzel, Academic Press, N. Y., (1983), PP. 361-362.

(66) H. Gerischer "Photovoltaic and Photoelectrochemical Solar Energy Conversion", ed., F. Cardon, W.P. Gomes, and W. Dekeyser, Plenum Publishing Corporation, New York, (1980), pp. 246-253.

(67) J.M Dona, J. Herrero, "Chemical bath co-deposited CdS-ZnS film characterization", *Thin Solid Films*, 268 (1995) 5-12.

(68)   H. Gerischer, "The rule of semiconductor structure and surface properties in photoelectrochemical processes", *J. Electronal. Chem*., **150** (1983) 553-569.

(69) R. de Boer, "Technologies and Prospects for Photochemical Conversion and Storage of Solar Energy: A survey of the state-of-the-art", ed., *ECN-C—01-029* (2001), P.15.

 (www.ecn.nl/docs/library/report/2001/c01029.pdf) date sited, 3/5/2008.

(70) T. Watanabe, A. Fujishima and K. Honda, "Energy Resources through Photochemistry and Catalysis", ed., M. Gratzel, Academic Press, N. Y., (1983), PP. 361-362.

(71) Fujioka, H., Ohta, J., Katada, H., Ikida, T., Noguchi, Y. and Oshima, M. "Epitaxial growth of semiconductor on SrTiO3 Substrates" *J. Cryst. growth*, **229** (2001). 137-141.

(72) Claverie, A., Colombeau, B., Assayag, G. B., Bonafos, C., Cristiano, F., Omri, M. and Mauduit, B. Thermal eVolution of extended defects in implanted Si: Impact on dopant diffusion", *Mat. Sci. Semico. Proc.*, **3** (2000) 269-277.

(73) Wang, L., Huang, X., Ma, Z., Li, Z., Shi, J., Zhang, L., Bao, Y., Wang, X., Li, W., Xu, J. and Chen, K., "Thermal annealing of a- Si:H=a-SiNx:H multilayers" *Appl. Phys*. A.(2001).

(74) Kitatani, T., Kondow, M. and Tanaka, T., "Effect of thermal annealing procedure and a straind intermediate layer on a highly-strained GaInNAs=GaAs double-quantum-well structure", *J. Cryst. Growth*, **221** (2000) 491-495.

(75) Kitatani, T., Nakahara, K., Kondow, M., Uomi, K. and Tanaka, T., "Mechanism analysis of improved GaInNAs optical properties through thermal annealing", *J. Cryst. Growth*, **209** (2000) 345-349.

(76) S.K. Salih, H.S. Hilal, I. A. Sa`adeddin, E. Sellier, and G. Campet "modification of n-Si Characteristics by Annealing and cooling At Different Rates", *Active and Passive Elec. Comp*., **26** (2003) 213-230.

(77) K. Kita, C. Wen, J. Otomo, K. Yamada< H. Komiyama, and H. Takashashi, "Study on the Lateral Growth of Silicon Films from Metal

Solutions with Temperature Gradient", *J. Cryst. Growth*, **234** (2002) 153-158.

(78) H.S. Hilal, S.K. Salih, I. A. Sa`adeddin, and G. Campet, "Effect of Annealing and of Cooling Rates on n-GaAs Electrode Photoelectrochemical Characteristics", *Act. Pass. Electron. Comp.*, **25** (2003) 213-230.

(79) Technical Assessment Analysis Group (GCEP), "An Assessment of Solar Energy Conversion Technologies and Research Opportunities Technical Report", Stanford University, (2006), p.17.

(80) K. Seshan, "Handbook of Thin-Film Deposition Processes and Techniques: Principles, Methods, Equipment and Applications", 2nd ed., Noyes Publications/William Andrew Publishing, (2002), pp. 14-15.

(81) J. Basu, K. K. Ronatgi Mukherjee, B. B. Bhowmick, "Modification of electrode surfaces for improved photoelectrochemical characteristics, *Sol. Energ. Mat. Sol. C*, **39** (1995) 39-47.

(82) R. Tenne and G. Hodes, "Improved efficincy of CdSe photoanodes by photoelectrochemical etching", *Sol. Cells*, **1** (1979/80) 183-197.

(83) P. J. Sebastian, J. Campos and P. K. Nair, "The effect of post-deposition treatments on morphology, structure and opto-electronic properties of chemically deposited CdS thin films", *Thin Solid films*, **227** (1993) 190-195.

Appendix

A.1 XRD Powder Diffraction Data for Cubic CdS

Sys.CUBIC   P   Lambda= 1.541780
Lo 0/Lc 0 M 0=   .0 A= 174.72
a= 5.8320A. V=   198.36
Line   d-spacing A. Int.   Indices SinSqTheta*E4   2Theta Deg.
o. c. obs. calc. obs. wt. h k l obs. calc. obs. calc. diff.

Line	obs.			h k l	obs.	2Theta
1	5.8320			1 0 0	174.7	15.19
2	4.1238			1 1 0	349.4	21.55
3	3.3671			1 1 1	524.2	26.47
4	2.9160			2 0 0	698.9	30.66
5	2.6081			2 1 0	873.6	34.38
6	2.3809			2 1 1	1048.3	37.78
7	2.0619			2 2 0	1397.8	43.91
8	1.9440			3 0 0	1572.5	46.73
				2 2 1		
9	1.8442			3 1 0	1747.2	49.42
10	1.7584			3 1 1	1922.0	52.00
11	1.6836			2 2 2	2096.7	54.50
12	1.6175			3 2 0	2271.4	56.93
13	1.5587			3 2 1	2446.1	59.28
14	1.4580			4 0 0	2795.6	63.84
15	1.4145			4 1 0	2970.3	66.05
				3 2 2		
16	1.3746			4 1 1	3145.0	68.22
				3 3 0		
17	1.3380			3 3 1	3319.7	70.36
18	1.3041			4 2 0	3494.5	72.48
19	1.2726			4 2 1	3669.2	74.56
20	1.2434			3 3 2	3843.9	76.63
21	1.1905			4 2 2	4193.3	80.72
22	1.1664			4 3 0	4368.1	82.74
				5 0 0		
23	1.1437			5 1 0	4542.8	84.75
				4 3 1		
24	1.1224			3 3 3	4717.5	86.76
				5 1 1		
25	1.0830			5 2 0	5067.0	90.77
				4 3 2		
26	1.0648			5 2 1	5241.7	92.77
27	1.0310			4 4 0	5591.1	96.79
28	1.0152			5 2 2	5765.9	98.81
				4 4 1		
29	1.0002			5 3 0	5940.6	100.84
				4 3 3		
30	.9858			5 3 1	6115.3	102.89

31	.9720	4 4 2	6290.0	104.95
		6 0 0		
32	.9588	6 1 0	6464.7	107.03
33	.9461	6 1 1	6639.5	109.14
		5 3 2		
34	.9221	6 2 0	6988.9	113.44
35	.9108	5 4 0	7163.6	115.64
		6 2 1		
		4 4 3		
36	.8999	5 4 1	7338.4	117.88
37	.8894	5 3 3	7513.1	120.17
38	.8792	6 2 2	7687.8	122.52
39	.8694	5 4 2	7862.5	124.93
		6 3 0		
40	.8599	6 3 1	8037.3	127.41
41	.8418	4 4 4	8386.7	132.64
42	.8331	6 3 2	8561.4	135.42
		7 0 0		
43	.8248	5 5 0	8736.1	138.35
		5 4 3		
		7 1 0		
44	.8166	7 1 1	8910.9	141.46
		5 5 1		
45	.8088	6 4 0	9085.6	144.80
46	.8011	6 4 1	9260.3	148.44
		7 2 0		
47	.7936	5 5 2	9435.0	152.50
		6 3 3		
		7 2 1		
48	.7793	6 4 2	9784.5	163.12
49	.7725	7 2 2	9959.2	172.68
		5 4 4		

A.2 XRD Powder Diffraction Data for Hexagonal CdS

Sys.HEXA.   P   Lambda= 1.541780
Lo 0/Lc 0 M 0=   .0 A= 248.48 C= 47.00
a= 5.6470A. c=11.2450 c/a= 1.9913 V=   310.55

Line	d-spacing A.		Int.		Indices			SinSqTheta*E4		2Theta Deg.		
o. c.	obs.	calc.	obs.	wt.	h	k	l	obs.	calc.	obs.	calc.	diff.
1	11.2450				0	0	1	47.0		7.86		
2	5.6225				0	0	2	188.0		15.76		
3	4.8904				1	0	0	248.5		18.14		
4	4.4847				1	0	1	295.5		19.80		
5	3.7483				0	0	3	423.0		23.74		
6	3.6899				1	0	2	436.5		24.12		
7	2.9750				1	0	3	671.4		30.04		
8	2.8235				1	1	0	745.4		31.69		
9	2.8113				0	0	4	751.9		31.83		
10	2.7385				1	1	1	792.4		32.70		
11	2.5232				1	1	2	933.4		35.58		
12	2.4452				2	0	0	993.9		36.75		
13	2.4373				1	0	4	1000.4		36.88		
14	2.3894				2	0	1	1040.9		37.64		
15	2.2553				1	1	3	1168.4		39.98		
16	2.2490				0	0	5	1174.9		40.09		
17	2.2423				2	0	2	1181.9		40.22		
18	2.0480				2	0	3	1416.9		44.22		
19	2.0433				1	0	5	1423.4		44.33		
20	1.9922				1	1	4	1497.4		45.53		
21	1.8742				0	0	6	1691.9		48.58		
22	1.8484				2	1	0	1739.3		49.30		
23	1.8450				2	0	4	1745.9		49.40		
24	1.8239				2	1	1	1786.3		50.00		
25	1.7591				1	1	5	1920.3		51.98		
26	1.7560				2	1	2	1927.3		52.08		
27	1.7501				1	0	6	1940.4		52.27		
28	1.6578				2	1	3	2162.3		55.42		
29	1.6553				2	0	5	2168.8		55.51		
30	1.6301				3	0	0	2236.3		56.44		
31	1.6133				3	0	1	2283.3		57.09		
32	1.6064				0	0	7	2302.8		57.35		
33	1.5657				3	0	2	2424.3		58.99		
34	1.5615				1	1	6	2437.3		59.17		
35	1.5445				2	1	4	2491.3		59.88		
36	1.5262				1	0	7	2551.3		60.68		
37	1.4949				3	0	3	2659.3		62.09		
38	1.4875				2	0	6	2685.8		62.43		
39	1.4280				2	1	5	2914.3		65.35		
40	1.4118				2	2	0	2981.7		66.19		
41	1.4102				3	0	4	2988.2		66.27		

42	1.4056	0 0 8	3007.8	66.52
43	1.4008	2 2 1	3028.7	66.78
44	1.3963	1 1 7	3048.3	67.02
45	1.3692	2 2 2	3169.7	68.53
46	1.3564	3 1 0	3230.2	69.27
47	1.3509	1 0 8	3256.3	69.59
48	1.3466	3 1 1	3277.2	69.85
49	1.3426	2 0 7	3296.7	70.08
50	1.3212	2 2 3	3404.7	71.39
51	1.3199	3 0 5	3411.2	71.47
52	1.3185	3 1 2	3418.2	71.56
53	1.3160	2 1 6	3431.2	71.71
54	1.2754	3 1 3	3653.2	74.37
55	1.2616	2 2 4	3733.7	75.33
56	1.2583	1 1 8	3753.2	75.56
57	1.2494	0 0 9	3806.7	76.19
58	1.2300	3 0 6	3928.2	77.62
59	1.2226	4 0 0	3975.6	78.18
60	1.2216	3 1 4	3982.2	78.25
61	1.2186	2 0 8	4001.7	78.48
62	1.2154	4 0 1	4022.6	78.73
63	1.2125	2 1 7	4042.2	78.96
64	1.2106	1 0 9	4055.2	79.11
65	1.1957	2 2 5	4156.6	80.29
66	1.1947	4 0 2	4163.6	80.37
67	1.1623	4 0 3	4398.6	83.09
68	1.1615	3 1 5	4405.1	83.17
69	1.1442	3 0 7	4539.1	84.71
70	1.1426	1 1 9	4552.2	84.86
71	1.1276	2 2 6	4673.6	86.26
72	1.1245	0 0 10	4699.7	86.56
73	1.1219	3 2 0	4721.1	86.80
74	1.1212	4 0 4	4727.6	86.88
75	1.1189	2 1 8	4747.1	87.10
76	1.1164	3 2 1	4768.1	87.34
77	1.1126	2 0 9	4800.6	87.71
78	1.1003	3 2 2	4909.1	88.96
79	1.0988	3 1 6	4922.1	89.11
80	1.0959	1 0 10	4948.1	89.41
81	1.0748	3 2 3	5144.1	91.65
82	1.0742	4 0 5	5150.6	91.73
83	1.0672	4 1 0	5218.0	92.50
84	1.0645	3 0 8	5244.1	92.80
85	1.0624	4 1 1	5265.0	93.04
86	1.0604	2 2 7	5284.6	93.26
87	1.0485	4 1 2	5406.0	94.66
88	1.0447	1 1 10	5445.1	95.11
89	1.0420	3 2 4	5473.0	95.43
90	1.0364	3 1 7	5533.0	96.12
91	1.0351	2 1 9	5546.1	96.27

92	1.0264	4 1 3	5641.0	97.37
93	1.0240	4 0 6	5667.5	97.67
94	1.0223	0 0 11	5686.6	97.89
95	1.0216	2 0 10	5693.6	97.97
96	1.0040	3 2 5	5896.0	100.32
97	1.0006	1 0 11	5935.1	100.78
98	.9977	4 1 4	5970.0	101.19
99	.9961	2 2 8	5989.5	101.41
100	.9917	3 0 9	6043.0	102.04
101	.9781	5 0 0	6212.0	104.03
102	.9760	3 1 8	6238.0	104.34
103	.9744	5 0 1	6258.9	104.58
104	.9729	4 0 7	6278.5	104.81
105	.9641	4 1 5	6393.0	106.18
106	.9636	5 0 2	6399.9	106.26
107	.9626	3 2 6	6413.0	106.41
108	.9612	1 1 11	6432.0	106.64
109	.9607	2 1 10	6439.0	106.73
110	.9464	5 0 3	6634.9	109.09
111	.9432	2 0 11	6680.5	109.64
112	.9412	3 3 0	6708.9	109.99
113	.9379	3 3 1	6755.9	110.56
114	.9371	0 0 12	6767.5	110.70
115	.9356	2 2 9	6788.5	110.96
116	.9283	3 3 2	6896.9	112.30
117	.9274	4 1 6	6909.9	112.46
118	.9256	3 0 10	6936.0	112.78
119	.9242	4 2 0	6957.4	113.05
120	.9238	5 0 4	6963.9	113.13
121	.9225	4 0 8	6983.4	113.37
122	.9211	4 2 1	7004.4	113.63
123	.9203	1 0 12	7016.0	113.78
124	.9198	3 2 7	7023.9	113.88
125	.9190	3 1 9	7036.9	114.04
126	.9128	3 3 3	7131.9	115.24
127	.9120	4 2 2	7145.4	115.41
128	.8973	4 2 3	7380.4	118.43
129	.8969	5 0 5	7386.9	118.51
130	.8946	2 1 11	7425.9	119.02
131	.8925	3 3 4	7460.9	119.48
132	.8894	1 1 12	7512.9	120.17
133	.8889	4 1 7	7520.9	120.28
134	.8796	2 2 10	7681.4	122.43
135	.8783	5 1 0	7702.8	122.72
136	.8780	4 2 4	7709.3	122.81
137	.8769	3 2 8	7728.9	123.08
138	.8757	5 1 1	7749.8	123.36
139	.8750	2 0 12	7761.4	123.52
140	.8738	4 0 9	7782.4	123.81
141	.8682	3 3 5	7883.8	125.22

142	.8678	5 1 2	7890.8	125.32
143	.8671	5 0 6	7903.8	125.50
144	.8661	3 0 11	7922.9	125.77
145	.8657	3 1 10	7929.9	125.87
146	.8650	0 0 13	7942.4	126.05
147	.8552	5 1 3	8125.8	128.69
148	.8548	4 2 5	8132.3	128.79
149	.8518	1 0 13	8190.9	129.66
150	.8500	4 1 8	8225.8	130.18
151	.8411	3 3 6	8400.8	132.86
152	.8384	5 1 4	8454.8	133.71
153	.8358	2 1 12	8506.8	134.54
154	.8354	5 0 7	8514.8	134.66
155	.8348	3 2 9	8527.8	134.87
156	.8289	4 2 6	8649.3	136.87
157	.8280	2 2 11	8668.3	137.19
158	.8277	4 0 10	8675.3	137.31
159	.8271	1 1 13	8687.8	137.52
160	.8182	5 1 5	8877.7	140.85
161	.8164	3 1 11	8916.8	141.57
162	.8155	2 0 13	8936.3	141.93
163	.8151	6 0 0	8945.2	142.10
164	.8129	6 0 1	8992.2	142.98
165	.8124	3 0 12	9003.8	143.20
166	.8121	3 3 7	9011.7	143.35
167	.8115	4 1 9	9024.8	143.61
168	.8066	6 0 2	9133.2	145.76
169	.8040	4 3 0	9193.7	147.01
170	.8032	0 0 14	9211.3	147.38
171	.8028	5 0 8	9219.7	147.56
172	.8019	4 3 1	9240.7	148.01
173	.8011	4 2 7	9260.2	148.43
174	.7965	6 0 3	9368.2	150.88
175	.7959	4 3 2	9381.7	151.20
176	.7953	5 1 6	9394.7	151.51
177	.7942	3 2 10	9420.7	152.15
178	.7926	1 0 14	9459.8	153.12
179	.7861	4 3 3	9616.7	157.42
180	.7842	4 0 11	9662.2	158.82
181	.7835	2 1 13	9681.8	159.45
182	.7831	5 2 0	9690.6	159.74
183	.7828	6 0 4	9697.2	159.96
184	.7820	3 3 8	9716.7	160.62
185	.7812	5 2 1	9737.6	161.36
186	.7807	2 2 12	9749.2	161.78
187	.7756	5 2 2	9878.6	167.35
188	.7741	4 1 10	9917.7	169.59
189	.7730	4 3 4	9945.6	171.54
190	.7726	1 1 14	9956.8	172.46

A.3 XRD Powder Diffraction Data for Cubic ZnS

Sys.CUBIC   P   Lambda= 1.541780
Lo 0/Lc 0 M 0=   .0 A= 202.30
a= 5.4200A. V=   159.22

Line	d-spacing A.		Int.		Indices			SinSqTheta*E4		2Theta Deg.		
o. c.	obs.	calc.	obs.	wt.	h	k	l	obs.	calc.	obs.	calc.	diff.
1	5.4200				1	0	0	202.3		16.35		
2	3.8325				1	1	0	404.6		23.21		
3	3.1292				1	1	1	606.9		28.52		
4	2.7100				2	0	0	809.2		33.05		
5	2.4239				2	1	0	1011.5		37.09		
6	2.2127				2	1	1	1213.8		40.78		
7	1.9163				2	2	0	1618.4		47.44		
8	1.8067				3	0	0	1820.7		50.52		
					2	2	1					
9	1.7140				3	1	0	2023.0		53.46		
10	1.6342				3	1	1	2225.3		56.29		
11	1.5646				2	2	2	2427.5		59.04		
12	1.5032				3	2	0	2629.8		61.70		
13	1.4486				3	2	1	2832.1		64.31		
14	1.3550				4	0	0	3236.7		69.35		
15	1.3145				3	2	2	3439.0		71.81		
					4	1	0					
16	1.2775				3	3	0	3641.3		74.23		
					4	1	1					
17	1.2434				3	3	1	3843.6		76.63		
18	1.2119				4	2	0	4045.9		79.00		
19	1.1827				4	2	1	4248.2		81.35		
20	1.1555				3	3	2	4450.5		83.69		
21	1.1064				4	2	2	4855.1		88.34		
22	1.0840				5	0	0	5057.4		90.66		
					4	3	0					
23	1.0629				4	3	1	5259.7		92.98		
					5	1	0					
24	1.0431				3	3	3	5462.0		95.30		
					5	1	1					
25	1.0065				4	3	2	5866.6		99.98		
					5	2	0					
26	.9896				5	2	1	6068.9		102.34		
27	.9581				4	4	0	6473.5		107.14		
28	.9435				5	2	2	6675.8		109.58		
					4	4	1					
29	.9295				5	3	0	6878.0		112.06		
					4	3	3					
30	.9161				5	3	1	7080.3		114.59		
31	.9033				6	0	0	7282.6		117.16		
					4	4	2					

32	.8910	6 1 0	7484.9	119.80
33	.8792	6 1 1	7687.2	122.51
		5 3 2		
34	.8570	6 2 0	8091.8	128.20
35	.8465	4 4 3	8294.1	131.21
		6 2 1		
		5 4 0		
36	.8363	5 4 1	8496.4	134.37
37	.8265	5 3 3	8698.7	137.71
38	.8171	6 2 2	8901.0	141.28
39	.8080	6 3 0	9103.3	145.15
		5 4 2		
40	.7991	6 3 1	9305.6	149.44
41	.7823	4 4 4	9710.2	160.40
42	.7743	7 0 0	9912.5	169.26
		6 3 2		

A.4 XRD Powder Diffraction Data for Hexagonal ZnS

Sys.HEXA.   P   Lambda= 1.541780
Lo 0/Lc 0 M 0=   .0 A= 543.00 C= 151.65
a= 3.8200A. c= 6.2600 c/a= 1.6387 V=   79.11

Line	d-spacing A.		Int.		Indices			SinSqTheta*E4		2Theta Deg.		
o. c.	obs.	calc.	obs.	wt.	h	k	l	obs.	calc.	obs.	calc.	diff.
1	6.2600				0	0	1	151.6		14.15		
2	3.3082				1	0	0	543.0		26.95		
3	3.1300				0	0	2	606.6		28.52		
4	2.9249				1	0	1	694.6		30.56		
5	2.2736				1	0	2	1149.6		39.64		
6	2.0867				0	0	3	1364.8		43.36		
7	1.9100				1	1	0	1629.0		47.61		
8	1.8269				1	1	1	1780.6		49.92		
9	1.7649				1	0	3	1907.8		51.80		
10	1.6541				2	0	0	2172.0		55.56		
11	1.6304				1	1	2	2235.6		56.43		
12	1.5992				2	0	1	2323.6		57.64		
13	1.5650				0	0	4	2426.4		59.02		
14	1.4625				2	0	2	2778.6		63.62		
15	1.4147				1	0	4	2969.4		66.04		
16	1.4089				1	1	3	2993.8		66.34		
17	1.2962				2	0	3	3536.8		72.98		
18	1.2520				0	0	5	3791.2		76.01		
19	1.2504				2	1	0	3801.0		76.12		
20	1.2262				2	1	1	3952.6		77.91		
21	1.2105				1	1	4	4055.4		79.11		
22	1.1710				1	0	5	4334.2		82.35		
23	1.1612				2	1	2	4407.6		83.20		
24	1.1368				2	0	4	4598.3		85.39		
25	1.1027				3	0	0	4887.0		88.70		
26	1.0860				3	0	1	5038.6		90.44		
27	1.0726				2	1	3	5165.8		91.90		
28	1.0471				1	1	5	5420.2		94.82		
29	1.0433				0	0	6	5459.3		95.27		
30	1.0401				3	0	2	5493.6		95.66		
31	.9983				2	0	5	5963.2		101.11		
32	.9950				1	0	6	6002.3		101.56		
33	.9769				2	1	4	6227.3		104.21		
34	.9750				3	0	3	6251.8		104.50		
35	.9550				2	2	0	6516.0		107.65		
36	.9441				2	2	1	6667.6		109.48		
37	.9175				3	1	0	7059.0		114.32		
38	.9156				1	1	6	7088.3		114.69		
39	.9134				2	2	2	7122.5		115.12		
40	.9078				3	1	1	7210.6		116.24		
41	.9014				3	0	4	7313.3		117.56		

42	.8943	0 0 7	7430.7	119.09
43	.8847	2 1 5	7592.2	121.23
44	.8825	2 0 6	7631.3	121.75
45	.8805	3 1 2	7665.5	122.22
46	.8684	2 2 3	7880.8	125.18
47	.8633	1 0 7	7973.7	126.49
48	.8399	3 1 3	8423.8	133.22
49	.8275	3 0 5	8678.2	137.36
50	.8271	4 0 0	8687.9	137.53
51	.8199	4 0 1	8839.6	140.17
52	.8152	2 2 4	8942.3	142.04
53	.8099	1 1 7	9059.7	144.29
54	.8011	2 1 6	9260.3	148.44
55	.7996	4 0 2	9294.5	149.19
56	.7915	3 1 4	9485.3	153.77
57	.7867	2 0 7	9602.7	157.01
58	.7825	0 0 8	9705.5	160.24

جامعة النجاح الوطنية

كلية الدراسات العليا

تحضير الأفلام الرقيقة من سبائك (CdS/ZnS) تم تحسين فعاليتها في التحولات الفوتوكهروكيمياوية

إعداد

ميساء تيسير محمد عطاطرة

إشراف

د. موسى الحسن

أ.د حكمت هلال

قدمت هذه الرسالة استكمالا لمتطلبات درجة الماجستير في الفيزياء بكلية الدراسات العليا في جامعة النجاح الوطنية في نابلس، فلسطين.

2010م

تحضير الأفلام الرقيقة من سبائك (CdS/ZnS) تم تحسين فعاليتها في التحولات الفوتوكهروكيمياوية

إعداد

ميساء تيسير محمد عطاطرة

إشراف

د. موسى الحسن

أ.د حكمت هلال

الملخص

لقد تم تحضير أفلام كبريتيد الزنك والكادميوم الرقيقة شبه الموصلة باستخدام طريقة الترسيب الكيميائي على شرائح من الزجاج الموصل المطلي بفلم من أكسيد القصدير المطعم بالفلور (FTO) . وقد تم تحضير أفلام مختلفة من حيث نسبة الزنك والكادميوم بالإضافة إلى عدد مرات الترسيب على الشريحة الواحدة.

وقد تم دراسة خصائص الأفلام المحضرة في الأنظمة الفوتوكهروكيميائية حيث تم دراسة تأثير الشي (التسخين) عند دراجات حرارة معينة (300، 400 مئوية) ومعدل التبريد على خصائص هذه الأفلام، كما تم بحث خصائص هذه الأفلام بعد تغطيتها بمادة (metalloporphyrin). وقد بنيت هذه الدراسة على أساس قياس عدة عوامل مثل منحنيات كثافة تيار الظلمة (dark current density) مقابل الجهد، كثافة تيارات الدارة القصيرة (short circuit current) ، كفاءة الخلية في تحويل الضوء إلى كهرباء (conversion efficiency) بالإضافة إلى نتائج التصوير بواسطة الماسح الميكروسكوبي الالكتروني (SEM)، و (XRD) و (PL).

وقد وجد أن الشي قد حسن منحنيات تيار الظلمة ومنحنيات تيار الإضاءة مقابل الجهد لأفلام كبريتيد الزنك والكادميوم الرقيقة شبه الموصلة في الأنظمة الفوتوكهروكيميائية. كما حسن الشي نتائج التصوير بواسطة الماسح الميكروسكوبي الالكتروني. بالإضافة إلى ذلك حسن الشي كثافة تيارات الدارة القصيرة لدى قياسها بعد زمن التعرض للضوء مما أظهر ثباتا أكبر للأفلام

التي تمت معالجتها بالشي في مقاومة التحطم الضوئي مقارنة بالأفلام غير المعالجة. كمـــا أن كفاءة الخلية الفوتوكهروكيميائية تحسنت بشكل ملحوظ. ومن بين درجات الحرارة المســتخدمة كانت درجة 300 مئوية هي الأفضل حيث تحسنت منحنيات كثافة تيار الإضاءة وكثافة الخليـــة بدرجة ممتازة ثم هبطت الى مستويات أقل عند استخدام أفلام تم تبريدها من درجة 400 مئوية.

كما وجد أن التبريد البطيء للأفلام المشوية على درجة حــرارة 300 مئويـــة يعطـــي منحنيات أفضل لكثافة تيار الظلمة وتيار الإضاءة مقابل الجهد و يحسن كفاءة الخلية بدرجة أكبر مقارنة مع التبريد السريع لبعض التراكيز للمواد المتفاعلة. وقد جاءت نتائج التصوير بواسطة الماسح الميكروسكوبي الالكتروني منسجمة مع النتائج السابقة، وقد وجد أن أعلى كفاءة للخلية قد تحققت عن طريق استخدام أفلام تم تبريدها ببطء من درجة حرارة 300 مئوية من بين الدرجات المستخدمة.

أما بالنسبة إلى تغطية أفلام كبريتيد الكادميوم و الزنك الرقيقة شـــبه الموصــلة بمـــادة (metalloporphyrin) فقد وجد أنها تحسن ثبات سطح الفلم في مقاومـــة الـــتحطم الضــوئي بدرجة كبيرة، حيث يعطي منحنيات أفضل لكثافة تيار الإضاءة مقابل الجهد مقارنة مع الرقـــائق غير المغطاة بمادة (metalloporphyrin) عندما تكون النسبة Cd/Zn 0.08:0.02.